Universidad Autónoma de Madrid

Departamento de Bioquímica

Polycomb RING1B in neural stem cells proliferation

TESIS DOCTORAL

Fabio Nicolini

Madrid, 2017

Departamento de Bioquímica

Facultad de Medicina

Universidad Autónoma de Madrid

Polycomb RING1B in neural stem cells proliferation

Memoria presentada por Fabio Nicolini, licenciado en Biotecnologías farmacéuticas, para optar al grado de Doctor en Biociencias Moleculares por Universidad Autónoma de Madrid

Directores de Tesis:

Dr. Miguel Ángel Vidal Caballero

Centro de Investigaciones Biológicas (CIB-CSIC)

Dra. Carmela Calés Bourdet

Instituto de Investigaciones Biomédicas (IIB-UAM)

Tutor de Tesis:

Dr. Leandro Sastre Garzón

Instituto de Investigaciones Biomédicas (IIB-UAM)

La presente Tesis Doctoral con título: **Polycomb RING1B in neural stem cells proliferation** ha sido realizada por Fabio Nicolini bajo la dirección del Dr. Miguel Ángel Vidal Caballero y de la Dra. Carmela Calés Bourdet, pertenecientes el departamento de Biología Celular y Molecular del Centro de Investigaciones Biológicas (CSIC) y al departamento de Biología del Cáncer de Instituto de Investigaciones Biomédicas (CSIC-UAM), respectivamente.

El desarrollo del trabajo ha sido posible gracias a la financiación concedida por el Campus Excelencia Internacional-Universidad Autónoma de Madrid (CEI-UAM) a través de una beca de Formación de Personal Investigador (Resolución del Programa de Posgrado en Biociencias Moleculares de 26 de septiembre de 2012), así como a través de la Comunidad Autónoma de Madrid gracias al proyecto S2010/BMD-2470 del programa ONCOCYCLE y al proyecto SAF2013-47997-P (MINECO).

V°B° de los directores de la tesis:

Dr. Miguel Ángel Vidal Caballero

Dra. Carmela Calés Bourdet

V°B° del tutor académico:

Dr. Leandro Sastre Garzón

Acknowledgements

Alla mia famiglia…

Son muchas las personas a las que tengo que dar las gracias por haberme acompañado durante estos últimos cinco años que se concluyen, al menos en parte, con la realización de este trabajo. En primer lugar quiero dar las gracias a mis directores de tesis, el Dr. Miguel Ángel Vidal y la Dra. Carmela Cales Bourdet, por apoyarme, aconsejarme y confiar en mí y por hacer que mi pasión por la investigación crezca cada día más; espero ser, poco a poco, un mejor investigador y quizás una mejor persona.

We thank Dr. M. Serrano (CNIO) for sharing p21 and p53 KO mouse lines and Dr. M. Barbacid (CNIO) for RERT mouse line.

Gracias a mis amigas y compañeras del lab.106, Mónica, Kasia y Zairiñi, ha sido una suerte para mí haber encontrado personas como vosotras y haber compartido tanto buenos momentos juntos, dentro y fuera del laboratorio. En particular, gracias a ti, Moni, siempre has estado y siempre estás ahí, me has aportado muchísimo tanto a nivel científico como personal, aunque te cueste tanto darme la razón.
Gracias a las chicas del lab.1.4.2., Sandra y Lucía, y gracias a toda la gente que trabaja en cada uno de los servicios del CIB por ayudarme siempre. En especial gracias a Gema y Mayte del servicio de microscopia confocal por ayudarme a distinguir todos los bonitos colores (rojo y verde) que salían de la máquina. Gracias a las chicas del final del pasillo, Anita, Lore, Ester, Noe y a Patri ''bulbos'', sin ellas este trabajo no existiría. Gracias a todo el labo de Tere. Gracias a Sarah, mi francesa preferida, y a mi compañero de piso Lucho. Gracias a toda la gente del CEM, haberos encontrado ha sido una suerte para mí, sois muy buena gente. Gracias a Héctor y Barbarina, Álvaro y Emma, Pablo y Rosa.

Il grazie più grande di tutti lo devo dare ai miei genitori, che sempre mi hanno appoggiato, sostenuto, capito ed incoraggiato. Sono stati duri questi anni lontano da voi ma alla fine, grazie a voi, ce l'abbiamo fatta! Grazie a Dani e a Gioia, siete degli esempi per me, e grazie alla piccola Greta, manchi tanto al tuo zio spagnolo. Grazie a tutta la mia famiglia e in particolare alle mie nonne che ho dovuto salutare durante questi anni, siete sempre con me.

Infine, grazie ai miei amici: a tutti quelli di Rimini, che sono tanti e uno peggio dell'altro, che però sono sempre lí. E quelli di Madrid: Costa, Fra, Denis, Paolina e Silvana.
En fin, un grazie anche a quelle persone che c'erano e ora non ci sono più. Grazie mille a tutti voi.

Abstract

Abstract

Polycomb protein RING1B is part of the E3 ligase that makes the core component of Polycomb Repressive Complex 1 complexes responsible for monoubiquitination of histone H2A at lysine 119. RING1B has been described as transcriptional repressor and chromatin modifier, indispensable for a proper embryonic development and lineage specification in cellular differentiation. Previous work in our laboratory has revealed additional, non-transcriptional functions for RING1B i.e in S-phase progression.

Using unperturbed neural stem cells (NSCs) derived from a murine conditional model of loss-of-function of RING1B, we unveil roles of RING1B in cell proliferation, DNA damage and redox homeostasis, independently of its activity as transcriptional repressor. RING1B deficiency caused p21/CDKN1A upregulation, the principal mediator of the proliferative defect. This is mostly due to activation of DNA damage response (DDR). Upregulation of p21 followed the known ATM/P53/p21 DDR axis, as shown by restoration of proliferation rate in *p21/Cdkn1a* and *P53* knock out NSCs, or in the presence of ATM inhibitor. Concurrent with proliferation arrest of RING1B-depleted NSCs, accumulation of double-strand breaks (DSBs) originated, at least in part, by an increase in endogenous Reactive Oxygen Species (ROS). Consistently, treatment with antioxidant was able to decrease DNA damage and recover normal proliferation. This essential function, preventing accumulation of ROS in NSCs was fulfilled by RING1B, but not its paralog RING1A through stabilization of Polycomb cofactor BMI-1.

In summary, we have identified a novel function of RING1B promoting proliferation of multipotent progenitors through the maintenance of physiological levels of oxidative stress, avoiding and managing a response to DNA damage through mechanisms independent, at least partially, of its better known as transcriptional repressor and instead assuring the stability of its own cofactor in NSCs.

Resumen

Resumen

La proteína RING1B es el componente principal del Complejo Represor Polycomb 1 (Polycomb Repressive Complex , PRC1) y cataliza la monoubiquitinación de la lisina 119 de la histona H2A. RING1B se ha descrito como un represor transcripcional y modificador de la cromatina y se conoce para su papel clave en el correcto desarrollo del embrión y especificación celular en la diferenciación celular. Recientemente, en nuestro laboratorio se han descrito para RING1B funciones adicionales a las transcripcionales, tales como la correcta progresión por la fase S del ciclo celular.

En este trabajo hemos utilizado como modelo experimental células madre neurales crecidas en condiciones de proliferación, y hemos podido desvelar la participación de RING1B en la proliferación celular, daño al DNA y control de la homeostasis oxidativa. La deficiencia de RING1B causa una mayor expresión del inhibidor del ciclo celular p21/CDKN1A que ha resultado ser el principal mediador de la parada proliferativa. La expresión de p21/CDKN1A es consecuencia de la activación de una respuesta a daño al DNA y no simplemente de la ausencia de una represión transcripcional. En la respuesta a daño a DNA participan la quinasa ATM y la proteína P53, como demuestra la recuperación de la proliferación en ausencia de *p21/Cdkn1a* o *P53*, y también por tratamiento con un inhibidor de la actividad quinasa de ATM. En este trabajo se ha demostrado como RING1B es importante para prevenir la formación de rupturas dobles de cadena del DNA que se originan, principalmente, por el incremento de Especies Reactivas del Oxigeno (Reactive Oxygen Species, ROS) en las células mutantes, y que finalmente llevan a una parada de la proliferación. En consonancia, el tratamiento con el antioxidante *N*-acetil-cisteína previene la formación de daño a DNA y permite rescatar la proliferación. Los datos aquí presentados sugieren que el papel de RING1B, y no de RING1A, se desarrolla garantizando la estabilidad de su co-factor BMI-1, ya descrito como regulador de la homeostasis oxidativa.

En conjunto, en este trabajo se han identificado nuevas funciones de RING1B en prevenir el estrés oxidativo y la consecuente activación de una respuesta de daño al ADN de manera independiente de su función como represor transcripcional, y que implica la estabilización de su co-factor BMI-1 en células madre neurales.

Table of contents

Índice/Table of contents

Abbreviations

Abbreviations

4'-OHT: 4'-hydroxytamoxifen

53BP1: p53-binding protein 1

8-oxoG: 8-oxo-guanine

ATM: ataxia telangiectasia mutated

ATMi: ATM inhibitor

ATR: ataxia telangiectasia and Rad3-related protein

ATRi: ATR inhibitor

BER: Base Excision Repair

BMI-1: B lymphoma Mo-MLV insertion region 1 homolog

BRCA1: Breast cancer type 1 susceptibility protein homolog

BrdU: bromodeoxyuridine

CBX: chromobox protein

CDK: cyclin-dependent kinase

CDKI: cyclin-dependent kinase inhibitor

cDNA: complementary DNA

ChIP: chromatin immunoprecipitation

CHK1: serine/threonine-protein kinase 1

CHK2: serine/threonine-protein kinase 2

CreERT2: Cre recombinase - estrogen receptor T2

Ct: cycle threshold

DAPI: 4'-6-diamidino-2-phenylindole

DCF: 2', 7' –dichlorofluorescein

DCFDA: 2', 7' –dichlorofluorescin diacetate

DDR: DNA damage response

Dox: doxycycline

DSBs: double-strand breaks

d.p.c.: days post coitum

EdU: 5-ethynyl-2'-deoxyuridine

EED: embryonic ectoderm development

EtOH: ethanol

EZH: Enhancer of zeste homolog

FITC: Fluorescein isothiocyanate

H2AK119Ub: mono-ubiquitylated lysine 119 of histone H2A

H2AX: Variant X of histone H2A

H2Aub: mono-ubiquitylated histone H2A

H3K27me3: trimethylated lysine 27 of histone H3

HBSS: Hank's buffered salt solution

HCl: hydrochloric acid

HR: homologous recombination

IF: immunofluorescence

IP: immunoprecipitation

IPCs: intermediate progenitor cells

lncRNA: long non-coding RNA

mEFs: murine embryonic fibroblasts

MOI: multiplicity of infection

NAC: *N*-acetyl-L-cysteine

NBS1: Nijmegen breakage syndrome protein 1 homolog

NaCl: Sodium chloride

NER: nucleotide excision repair

NHEJ: non-homologous end joining

ns: not significant

NSCs: neural stem cells

OBSC: olfactory bulb stem cells

p38-MAPK: p38 mitogen-activated protein kinases

P38i: p38-MAPK inhibitor

PBS: phosphate buffered saline

PcG: polycomb-group proteins

PCGF: polycomb group RING finger

PCNA: proliferating cell nuclear antigen

PFA: paraformaldehyde

PHC: pericentromeric heterochromatin

Polr2a: RNA Polymerase II Subunit A

PRC: polycomb Repressive Complex

PRE: polycomb-responsive elements

p16-INK4a: cyclin-dependent kinase inhibitor 2a

p21/CDKN1A: cyclin-dependent kinase inhibitor 1a

p27/CDKN1B; cyclin-dependent kinase inhibitor 1b

p57/CDKN1C; cyclin-dependent kinase inhibitor 1c

RGC: radial glial cell

RING1A: Really interesting new gene 1A

RING1B: Really interesting new gene 1B

RIPA: Radioimmunoprecipitation assay buffer

RNasa: ribonuclease

RNF: ring finger protein

RNF8: RING finger protein 8

ROS: Reactive Oxygen Species

RPA32: Replication protein A (32 kDa subunit)

RYBP: RING1 and YY1-binding protein

SCE: Sex combs extra

SD: standard deviation

SDS: Sodium dodecyl sulfate

SSBs: single-strand breaks

ssDNA: single-stranded DNA

SUV12: suppressor of zeste 12 homolog

P53: Cellular tumor antigen p53 protein

$P53^{ser15}$: P53 protein phosphorylated at serine 15

TPBS: Phosphate-buffered saline and Tween 20

TTBS: Tris-Buffered Saline and Tween 20

Tuj-1: Neuron-specific class III beta-tubulin

Ub: ubiquitin

UTR: untranslated region

UV: Ultraviolet

vs: versus

WB: western blot

γH2AX: phosphorylated serine 139 of H2AX histone

Introduction

1. Polycomb system of chromatin regulators

The PcG of genes were discovered during the genetic analysis of development in the fly *Drosophila melanogaster* (Lewis, 1978; Duncan, 1982). Phenotypically, adults bearing Polycomb mutations shared morphological alterations interpreted as homeotic transformations, i.e. when a body part acquired structures from another body part. Generally, in PcG alterations, anterior body structures acquire features of a posterior part. Thus, in male flies, the presence of sex combs, a structure usually restricted to the last pair of legs, in the first and second pairs, as if these anterior legs became more like the posterior leg. It is, precisely, the presence of supplemental sex combs what determined the branding of the collection of mutations: the Polycomb group of genes, the founder member after the Polycomb (Pc) mutant. Other mutations were Posterior sex combs (Psc), Sex combs extra (Sce), Additional sex combs (Asx).

These mutations resembled those associated to the gain of function of the homeotic genes and thus, PcG genes were considered negative regulators of Hox genes. Characteristically, Polycomb larvae show expanded expression domains of Hox products, in contrast with the restricted patterns seen in wild type larvae (Lewis, 1978; Duncan, 1982; T. Sato & Denell, 1985; Schwartz & Pirrotta, 2007). This feature is consistent with a loss of gene silencing function and thus the association of PcG products with transcriptional repression (Isono et al., 2005).

Following the molecular cloning of Drosophila PcG genes, the conservation of their products was soon appreciated in mammalian cells (Aranda et al., 2015; Whitcomb et al., 2007). Given the notion that Polycomb products might act as protein complexes (supported by the phenotypic similarity of Polycomb mutations) a characterization of components of these complexes was initiated that led to the identification, among others, of RING1 proteins. Interestingly, no Drosophila Polycomb gene was known at the time that encoded a RING1 homolog. However, soon after molecular and genetic studies found that Drosophila Sex combs extra encoded a RING1 protein homolog. It was the case of a Polycomb gene identified in mammalian before than in Drosophila model (Fritsch et al., 2003; Gorfinkiel et al., 2004).

1.1. Polycomb Repressive Complexes (PRC)

1.1.1. PRC1 and PRC2 complexes

PcG proteins in both fly and mammalian cells are found as two major types of biochemical entities known as Polycomb Repressive Complexes 1 and 2 (PRC1, PRC2). PRC1 and PRC2 interact and modify chromatin in different ways.
These sets of complexes include a heterogeneous mix of assemblies, particularly that of PRC1 complexes (Aranda et al., 2015; Gao et al., 2012; Lanzuolo & Orlando, 2012).

PRC1 complexes contain a core composed by RING1 proteins (RING1A/B) that display E3 ligase activity monoubiquitinating histone H2A at lysine 119 (K119Ub, H2AUb in short). (Cao, Tsukada, & Zhang, 2005). Loss of these PRC1 components RING1A and RING1B results in a drastic reduction in basal levels of H2Aub (de Napoles et al., 2004), thereby demonstrating the exclusive requirement for these enzymes in catalyzing this particular modification. Core PRC1 complex also contains one of the six PCGF proteins defining the PRC1 complex (Gao et al., 2012). PRC1 complexes composed by PCGF2/MEL18 or PCGF4/BMI-1 are named PRC1.2 and PRC1.4, respectively, and are considered as ''canonical PRC1'' because they include, together with one Polyhomeotic subunit (PHC1, 2 or 3), a Chromobox (CBX2, 4, 6, 7 or 8) subunits. CBXs proteins have a chromodomain at the N-terminal that recognize histone mark deposited by PRC2 (Bernstein et al., 2006; Fischle et al., 2003). Non-canonical PRC1 complexes do not contain a CBX protein, but include instead RYBP or its homologue YAF1, that bind to core RING1-PCGF on its own or complexed with diverse subunits combinations (Gao et al., 2012; Tavares et al., 2012).

PRC2 complexes are composed by a methyltransferase called Enhancer of Zeste 1 or 2 (EZH1 or EZH2), that catalyzes the mono, di or tri-methylation of lysine 27 on histone H3 (H3K27me3), SUV12 and EED proteins (Margueron et al., 2008 and 2011; Shen et al., 2008).

PRC1 and PRC2 interact and mutually reinforce their activities. Thus, specific recognition of the histone modifications is the basis of the interdependent relationship between PRC1 and PRC2. On the one hand, some of the PRC1 complexes containing CBX subunits recognize H3K27me3 histone mark deposited by PRC2 (Bernstein et al., 2006; Fischle et al., 2003). On the other, PRC2 recognition of nucleosomes bearing H2AUb stimulates the lysine methyltransferase activity of EZH proteins. It is important

to note that PRC1 and PRC2 also associate and modify chromatin independently of each other (Blackledge et al., 2014; Kalb et al., 2014)

1.1.2. Recruitment mechanisms

How Polycomb complexes are recruited to their targets and the mechanisms through which Polycomb-modified chromatin is functionally altered are currently subject of intense research activity. Studies in *Drosophila melanogaster* determined the existence of hundreds-bases sequences able to recruit Polycomb proteins, called PRE (Polycomb Response Elements) (Chan et al., 1994; Mihaly et al., 1998; Tillib et al., 1999). These regions could localize kilobases far from target promoter or, in same cases, close to TTS (transcription starting site). In mammalians cells, there are no PRE elements on the genome, but PRC1 and PRC2 proteins have high affinity for CpG islands (un-methylated regions rich in cytosine and guanine bases) that could function as PRE elements in mammalian cells (Boyer et al., 2006; Ku et al., 2008; T. I. Lee et al., 2006; Mikkelsen et al., 2007). The recruitment of Polycomb proteins to CpG island is mediated by a DNA binding protein, KDM2B, that is part of the PRC1.1 (non-canonical) complex, through a ZF-CxxC binding domain with high affinity to CpG islands (Farcas et al., 2012; He et al., 2013; Wu et al., 2013). These observations suggest a more general recruitment model, called ''sampling'' where PRC1 and PRC2 or Trithorax group of proteins (antagonist of Polycomb's) (Ringrose & Paro, 2004) are stochastically bound to CpG islands (Klose et al., 2013). PRC1/2 complexes massive occupancy impedes transcriptional activation mediated by Trithorax proteins.

Another minor mechanism employed for the recruitment of Polycomb proteins to chromatin is mediated by long non-coding RNA (lncRNA), non-protein coding transcripts implicated in different processes as transcription, post-transcriptional and epigenetic regulation. X-chromosome inactivation during dosage compensation in mammals is mediated by the lncRNA *Xist* that allows the recruitment of PRC2 proteins and, consequently, deposition of H3K27me3 repressive mark (Kohlmaier et al., 2004; Leeb & Wutz, 2007).

PRC1 and PRC2 complexes are found in plants, animals and fungi (exceptionally, PRC1 is absent in the latter kingdom) suggesting an evolutionary conserved function (Lewis, 2017). Making the core of PRC1 complexes, RING1A, RING1B and their paralogs are the most conserved Polycomb products

1.2. RING1 proteins

1.2.1 Structure and H2A modifying activity

RING1B and its paralog RING1A were first identified in mammalian cells (Schoorlemmer et al., 1997). Named after the product of the original RING1 gene, one of the Really Interesting Genes (Lovering et al., 1993), they were found through their association with an homolog of one of the then well known in Drosophila PcG of proteins. RING1A and RING1B are proteins of 406 and 336 amino acids, respectively, and shared 67% of homology. (Fig.I1). They are metalloproteins with a N-terminal module that contains a RING finger motif (Lovering et al., 1993), and a C-terminal module contains a ubiquitin-like motif also known as RAWUL (from RING and WDR ubiquitin-like, (Sanchez-Pulido et al., 2008), important for the association with CBX and RYBP PcG subunits (Garcia et al., 1999; Schoorlemmer et al., 1997)

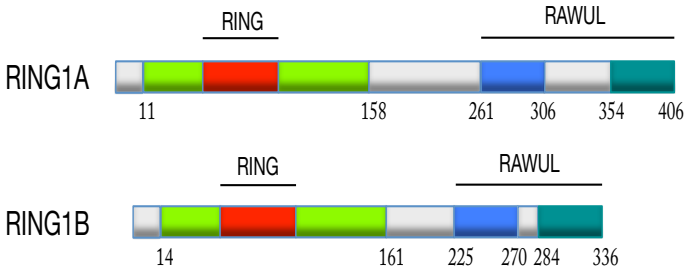

Figure I1. Schematic representation of RING1 proteins. Homology domains are represented with colors. Numbers indicate amino acids.

The only known substrate of E3 ligases containing RING1A and RING1B is histone H2A. *In vitro* studies with isolated or reconstituted PRC1 complexes indicate that the modification occurs only when histone H2A is in nucleosomal but not in free form. The demonstration that it is lysine 119 (and to a lesser extent 120 too) in the C-terminal tail of histone H2A the amino acid modified with monoubiquitin has come from mass-spectrometry analysis (McGinty et al., 2014). About 10-15% of histone H2A is mono-ubiquitylated in mammalian cells at a given time, comprising a large portion of the total pool of cellular ubiquitin. It is widely accepted that nucleosomes enriched in such a modified histone correlate with a transcriptionally silent state (Cao et al., 2005; Di Croce & Helin, 2013). The molecular structure needed for nucleosome binding and proper location at H2A residue to efficiently transfer the ubiquitin requires the

heterodimerization with the PCGF subunit, well documented for PCGF4/BMI-1(McGinty et al., 2014).

1.2.2. Mechanisms of gene repression

As members of Polycomb group, RING1A and RING1B act as transcriptional repressors through, at least, two well-know mechanisms: i) regulating RNA polymerase II activity; and ii) compacting the chromatin, making it inaccessible to others genome regulators. (Aranda et al., 2015; Di Croce & Helin, 2013).

At PRC1-binding regions CpG islands two histone marks can be present, H3K4me3 and H3K27me3, normally associated to an ''active'' and ''repressive'' transcriptional state, respectively. When both marks are present at the same time, the promoter is called ''bivalent'' and the RNA polymerase II is paused as it cannot start transcription. Bivalents promoters are normally repressed in pluripotent cells. Once differentiation stimulus occurs, only one of the two histone marks is maintained, determining the expression/repression of the gene (Azuara et al., 2006; Bernstein et al., 2006; Cui et al., 2009; Mikkelsen et al., 2007). For these reasons, inactivation of PRC1 or PRC2 proteins in ES cells may induce premature de-repression of genes that normally control the self-renewal process and pluripotency state (M Endoh et al., 2008; Pasini et al., 2007; Shen et al., 2008)

Presence of H2Aub affects the binding and transcriptional activity of RNA polymerase II. It has been demonstrated that loss of RING1 proteins and, consequently, of the H2Aub mark, allows an increased recruitment of RNA polymerase II to promoters and transcription initiation. Presence of H2Aub seems also to interfere with the elongation process during transcription (Endoh et al., 2012; Stock et al., 2007)

Chromatin compaction is another mechanism mediated for PRC1 and PRC2 proteins that regulates gene expression (King et al., 2005; R.Margueron et al., 2008). In ES cells lacking RING1B, FISH (fluorescent in situ hybridization) assays demonstrate that Hox genes are activated and physically separated from the rest of cluster, due to a diminished chromatin compaction (Eskeland et al., 2010). Surprisingly, the RING1B capacity to compact chromatin may well be independent from its E3 ligase activity (Eskeland et al., 2010; Illingworth et al., 2015).

Chromatin compaction has been proposed as a way to physically impede the access of other chromatin remodeler, such as SWI/SNF complex (Francis et al, 2001; Levine et al., 2002), necessary for transcription activation.

1.2.3. Transcriptional targets

PRC1 complexes are widely considered as chromatin regulators for negative modulation of transcription. However, recent, detailed studies in fly and mammalian cell systems describe the presence of PRC1 products on transcriptionally active loci. This asks for a re-evaluation of the accepted function of PRC1 complexes as transcriptional repressors (Kloet et al., 2016). Nevertheless, most work approaching PRC1 rol(es) in gene control has been a quest to understand the repressive mechanisms involved. Questions currently under investigation are those concerning recruitment of Polycomb complexes to their targets and how transcription is affected at Polycomb-modified chromatin. Location of PcG products on TSSs is predominant, but not exclusive and binding to gene bodies and enhancers, although less studied, is also found (Entrevan et al., 2016).

Original observations in *Drosophila* proposing PRC1 as transcriptional repressors, was corroborated in loss-of-function models in mammals and plants (Aranda et al., 2015; Lanzuolo & Orlando, 2012; N. Reynolds et al., 2013; Whitcomb et al., 2007). A seminal study, in murine embryonic stem cells (ESC), shows association of PRC1 and PRC2 products with regulatory sequences of hundreds of genes with roles in the major developmental pathways (Boyer et al., 2006). The data suggested that ESC pluripotency was maintained through the repression of these genes before they were called to direct commitment and specification processes of cell differentiation. In fact, the overall activity of Polycomb complexes is more important for actual differentiation than for the maintenance of the ESC state, and that only PRC1 but not PRC2 act as an efficient repressors of any relevance to the ESC state (Bracken et al., 2006, Boyer et al., 2006)).

In other genetic models, such as loss-of-function of Polycomb products in hematopoietic, neural or epidermal compartments, the outcomes have been rather modest, far from outright deviations from differentiation pathways as it might have been expected from initial hypothesis. Interestingly, a common observation in these models is that phenotypic alterations related more to deregulated proliferation than to cell identity gene expression changes, that prominently affect, although not exclusively, repression of cell cycle inhibitors (Bracken et al., 2007; Bravo et al., 2015; Calés et al., 2008; Fasano et al., 2007;

Iwama et al., 2004; Lessard & Sauvageau, 2003; Molofsky et al., 2003, 2005; Piunti et al., 2014; Román-Trufero et al., 2009).

2. PRC1 in cell proliferation

2.1. Cell cycle control through CDK inhibitors

For Polycomb proteins, somehow, the selective use of the coding potential of the genome, generating gene expression patterns specific to each cell type has attracted more attention than the control of genes important in cell proliferation. And yet, multicellular organisms can only result from the balanced generation of appropriate numbers of specialized cell types, both during development and during tissues maintenance in the adult. Thus, differentiation programs or responses to cellular stress include exquisite control of cellular proliferation.

Cell multiplication coordinates a myriad of processes, from sensing proliferative signals to the initiation of the replication of the genome and the segregation of duplicated chromosomes into daughter cells. These processes occur in sequential steps or phases, defining the so-called cell cycle or period between cell division events. DNA replication occurs in S-phase and actual division of the cell with duplicated genome takes place in mitosis. Between these steps is the G2 phase and the period following cell division and initiation of DNA replication is G1. Many chromatin regulators, besides Polycomb, participate decisively in the progression of the cell cycle (Fig.I2).

The successive phases of the cell cycle are regulated by the periodic accumulation (and destruction) of cyclins specific for each of the phases. For example, cyclins D are relevant in G1, cyclins E in the transit from G1 to S and cyclins A and B in S, G2 and mitosis (Bertoli et al., 2013). Oscillations in the levels of cyclins impacts the activity of kinases (cyclin-dependent kinases, CDKs) that determine the activity of genes required to enter the cell division and a plethora of other processes (Gérard & Goldbeter, 2012). Cells spend most of the time in G1, a period in which promoters of genes encoding products required for proliferation is silenced by recruitment of non-phosphorylated members of the retinoblastoma gene family. When the strength of proliferation signal builds up, cyclin D-CDK4/6 complexes gain kinase function and E2F transcription factors, released from inactivating retinoblastoma by phosphorylation-dependent eviction, engage transcription at cell proliferation-specific promoters (Giacinti & Giordano, 2006).

In addition to cyclins, the activity of G1-specific kinases is also controlled by the so-called CDK inhibitors (CDKIs), structurally unfolded small proteins that bind cyclin-CDK complexes inactivating their kinase function (Bruggeman & Van Lohuizen, 2006). These CDKIs are constitutively deficient in oncogenic conditions and are among the best-studied tumor suppressors.

Of these, the products of the *Cdkn2a* gene, p16-INK4a and p19-ARF in the mouse, two polypeptides generated by alternative use of promoters and partial differential splicing, inhibit CDK4/6 and are transcriptionally repressed by Polycomb products. In primary mouse embryonic fibroblasts deficient in BMI-1 a causal relationship between senescence (proliferative arrest) caused by upregulation of p16-INK4a and the absence of a Polycomb product was first observed (Jacobs et al., 1999). We also observed cell cycle arrest in differentiating hematopoietic precursors lacking RING1B which was reverted by a null mutation in the *Cdkn2a* gene (Calés et al., 2008). CDKN2B up regulation has also been reported in hematopoietic progenitors with decreased FBXL10/KDM2B (He et al., 2009). Effective control of genes in the *Cdkn2* cluster is considered important for the maintenance of adult pluripotent progenitors, the cells with the developmental potential required to replenish tissue compartments under physiological or pathological attrition.

Another decisive regulator of the cell cycle, p21/CDKN1A, inhibits cell cycle progression mainly by inhibiting cyclin E/CDK2 (Fig.I2). The activity of this kinase is strictly required to achieve irreversible commitment to proliferation and initiate DNA replication (licenses replication origins) (Porter, 2008). Transcriptional control of *p21/Cdkn1a* has been extensively studied. Best known pathway that leads to upregulation of this CDKI is the elicited by various cellular stresses, that leads to transcriptional activation of the gene by p53-dependent and p53-independent, Ras/Raf/MAPK/E2F-dependent, mechanisms (Abbas & Dutta, 2009). However, the control involves a plethora of diverse regulators that include not only transcription activators but also inhibitors that make the picture extremely complex and not fully understood. Inactivation of PRC1 subunits in some models of progenitor cells correlates with upregulation of p21/Cdkn1a at the mRNA and/or protein level (Fasano et al., 2007; Koike et al., 2014; Román-Trufero et al., 2009), but to date, no mechanism or function has been elucidated.
High levels of p21/CDKN1A are often associated to senescence pathways triggered by cellular stress like damaged DNA (Cazzalini et al., 2010; Ciccia & Elledge, 2010; Karimian, Ahmadi, & Yousefi, 2016).

2.2. p21 and G1/S checkpoint: DNA damage control

One of the essential functions of CDKIs, in particular p21/CDKN1A, is to stop cell cycle in response to various stimuli (stresses) that put at risk proper genetic duplication and cell division. This checkpoint function transiently delays the progress at specific junctions (G1/S, intra S, G2/M) to allow the cell to deal or repair whatever damage had been inflicted and ultimately assure genomic integrity (Abbas & Dutta, 2009; Karimian et al., 2016).

One of the most common and harmful damage for the cell is that affecting DNA. This occurs frequently after exposure to external agents such as irradiation (UV, XRays, radiochemicals) or chemicals (drugs, additives, cigarette smoke) that can provoke severe alterations of the DNA structure. Additionally, an important source of DNA damage also results from physiological metabolic processes, i.e. endogenous toxic accumulation of reactive oxygen species (ROS), products of cellular metabolism or alteration of redox homeostasis (Lombard et al., 2005;Wagner, 2013). Presence of high levels of ROS can cause several types of DNA lesions as breaks, adducts, and cross-links. The best known alteration is the 8-oxo-guanine (8-oxoG) base modification (Lindahl, 1993; Wagner, 2013). When this kind of lesions are not properly removed and replicative or transcriptional machinery encounter it, single-strand breaks (SSB) and double-strand breaks (DSBs) may be generated (Burhans & Weinberger, 2007; Woodbine et al., 2011). These can also occur through direct, potent genotoxic aggression.

When cells acquire DNA damage, a highly organized and coordinated cellular process, called DNA Damage Response (DDR) (Ciccia & Elledge, 2010), counteracts genotoxic stress, assuring that, if damage remains unrepaired or is not fixed within a reasonable time-frame, senescence or death by apoptosis or autophagy will take place (Sancar et al., 2004; Sherman et al., 2011)

DDR starts by sensoring the molecular alterations, then activating a signaling orchestrated by ATM/CHK2 and ATR/CHK1 kinases cascades, that may work together but with have non redundant functions (Maréchal & Zou, 2013). Ionizing radiations-induced DSBs are potent activators of ATM pathway, whereas stalled DNA replication forks and replicative stress elicit ATR branch (Adams, Golding, Rao, & Valerie, 2010; Smith, Mun Tho, Xu, & A. Gillespie, 2010). ATM/ATR kinases substrates comprise numerous proteins (e.g. nucleases) involved in repairing the DNA damage (Jazayeri et al., 2006), or favoring apoptosis, but also primarily factors that will

ensure checkpoint activation, thus cell cycle arrest. One of these is the tumor suppressor P53, with multiple targets such as p21/CDKN1A, that assures the temporary halt of phases progression (Shieh et al., 1997). But P53 has multiple other targets that include proteins involved in DNA repair, in cell apoptosis, autophagy or senescence. P53 is induced not only by DDR, but also to other stresses. Its accumulation and post-translational modifications determine cells outcome, e.g. cell cycle arrest or apoptosis (Kracikova et al., 2013; Sherman et al., 2011). P53 is phosphorylated by ATM at serine 18 (serine 15 in human) and further phosphorylated by CHK1 and CHK2 and that result in the stabilization of this protein with a basal rather high turnover (Lakin & Jackson, 1999; Mendrysa, Ghassemifar, & Malek, 2011; Smith et al., 2010).

2.3. PRC1 non-transcriptional functions

2.3.1. RING1B role in DNA replication

As already mentioned, recent evidences support a non-transcriptional, direct role of PRC1 proteins in controlling cell proliferation.

RING1B on nascent DNA and, the presence of RING1A on the maturing chromatin following the formation of nascent DNA (Alabert & Groth, 2012; Lee et al., 2014; Piunti et al., 2014), suggests that RING1 proteins have a role in DNA replication. Work in our laboratory has shown that RING1-deficient mouse embryonic fibroblasts (mEFs) display sign of replicative stress due to the presence of slower or stalled replication forks (Bravo et al., 2015), in particular in sensible regions as PCH (Branzei & Foiani, 2010). The presence of H2Aub at PHC is essential to assure a correct DNA replication. Replicative stress could culminate with the presence of signs of double-strand breaks affecting genome integrity (Bravo et al., 2015). In this context, concurrent inactivation of RING1 proteins and knock-down of *p21/Cdkn1a* could only temporally restore the p21-mediated proliferative defect (Bravo et al., 2015).

Others groups reports have also contributed to unveil the presence of RING1 proteins on nascent DNA suggesting a critical role of PRC1 proteins in avoiding replicative stress-derived activation of DNA damage response that could affect cell cycle progression. Immortalized fibroblasts with oncogenic overexpression were used for the study, and this may have added exogenous, non-physiological, replicative stress (Piunti et al., 2014). Also, Nascent Chromatin Capture (NCC) technique coupled with quantitative

proteomics performed in human cells also allowed to identified RING1A and RING1B on biotin-dUTP labeled nascent DNA (Alabert & Groth, 2012).

2.3.2. Other PRC1 functions affecting DNA biology

Collectively, the data above are telling about the limited view of RING1B role as transcriptional repressor and thus, that PRC1 functions may affect other aspects of DNA-related processes not only the described direct role in DNA replication, but also in DNA damage, DNA repair and/or some of the pathways that lead to DDR such as oxidative stress, as it has already been explored (Liu et al., 2009; Vissers Joseph H. A., 2012).

For instance, BMI-1 has been reported to be involved in redox homeostasis in different cell types (Banerjee Mustafi et al., 2016; Chatoo et al., 2009; Liu et al., 2009). Also, the presence of PRC1 components has been detected at site of ionizing radiation (IR)- and laser-induced double-strand breaks (Chou et al., 2010; Facchino et al., 2010; Ginjala et al., 2011; Ismail et al., 2010). The protein recruitment kinetics was similar to that of other proteins involved in DNA damage response as NBS1 and RNF8 (H. Ismail et al., 2010). That involved PCR1 proteins in the earliest signaling and amplification steps of DDR (Lukas et al., 2011). Also recently, it was described that ATM-dependent phosphorylation of the elongation factor ENL allows the recruitment of PRC1 proteins (BMI-1 and RING1B) to the site of DSBs. This induced transcriptional repression (H2Aub) and allowed DNA repair proteins access to DSBs (Ui et al., 2015).

Ubiquitination of histone H2A has also been suggested to be implicated in DNA damage signaling and transcriptional silencing of surrounded regions close to DSBs (Bergink et al., 2006; Vissers et al., 2012) suggesting that E3 ligase activity of RING1 proteins could be playing an important role.

All these evidences point at functions of PRC1 related to DNA that could define a much broader task for these proteins.

3. Cell models of PRC1 role in cell proliferation

3.1. Hematopoietic cells

Loss of function studies in the hematopoietic system shown as PcG products act as positive regulators of cell proliferation. In particular, hematopoietic stem cells proliferation and self-renewal capacities are linked to the activity of PRC1 proteins to repress the *Ink4a/Arf* locus (Fig.I2). De-repression of this locus in BMI-1 deficient cells induced a higher expression of p16-INK4a and p19-ARF that interfere with cell cycle progression, in particular at G1 to S phase transition (Iwama et al., 2004; Lessard & Sauvageau, 2003; Park et al., 2003). As mentioned before, our laboratory described as loss of RING1B differentially affected immature and mature hematopoietic compartments. In lineage negative cells, RING1B loss induces a transient hyperproliferation effect, but in more mature cells upregulation of p16-INK4a is the principal mediator of proliferative arrest, as *Cdkn2a* null mutation is able to rescue the phenotype (Cales et al., 2008)

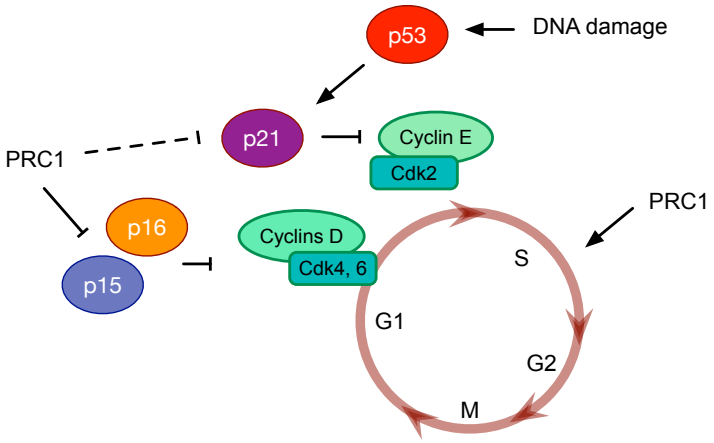

Figure I2. Schematic representation of cell cycle and PRC1 control on some CDK inhibitors.

3.2. Neural stem/progenitor cells and PRC1 proteins role on proliferation

The central nervous system originates in neural stem cells (NSCs), progenitor cells located in the neuroectoderm, an epithelial structure in the early embryo. Its expansion, through symmetric divisions of NSCs, and closure gives rise to a neural tube whose inside is lined by NSCs. By the onset of neurogenesis, day 9-10 of development in the mouse, NSCs transform in another pluripotent cell type with fewer epithelial feature, the radial glial cells (RGCs) (Götz & Huttner, 2005; Guillemot, 2007; Temple, 2001). From this pool of progenitors, asymmetrically, a RGC and an intermediate progenitor cell are generated. Subsequently, during neurogenesis (days 14 to 16) symmetric and asymmetric divisions of intermediate progenitor cells (IPCs) located in more basal positions, away from ventricular surfaces, give rise to neurons. The population of progenitors evolves with time and at a later time, by day 18, no neurons are formed and, instead, astrocytes, a type of glial cells, are produced (see review by Pinto & Götz, 2007). Cultures of NSCs and pluripotent progenitors can be established from dissociated explants of select portions (subventricular zone of adult mice or olfactory bulb) (W. Guo et al., 2012; Vicario-Abejon et al., 2003) of the developing nervous system. Cells in these cultures grow as spheroid structures known as neurospheres and contain a mixture of NSCs and other progenitors with a high self-renewal potential and, when provided appropriate signals, able to differentiate into neuronal and glial cell types (Reynolds & Rietze, 2005; Reynolds & Weiss, 1996) Previous work in the lab showed that upon deletion of *Ring1B*, spontaneous neuronal differentiation occurs in a fraction of the progenitors, which becomes more noticeable when RING1A redundancy is eliminated in double mutant cells (Román-Trufero et al., 2009).

Similar to the hematopoietic system, the PcG products act as positive regulators of proliferation also in NSCs. RING1B-deficiency induces upregulation of different CDK inhibitors, among that p16-INK4a and p21/CDKN1A, and other genes correlated with P53 function. ChIP-on-ChIP analysis shows that RING1B does not directly bind p21/CDKN1A promoter, suggesting additional, unexplored, mechanism that induced p21 upregulation and proliferation defect (Román-Trufero et al., 2009). BMI-1 knock-out also induced a proliferative defect *in vivo* as *in vitro*, more accentuated in adult mice or post-natal derived neurospheres respect to embryonic phase (Molofsky et al., 2003). *Bmi-1* and *Ink4a* double inactivation only partially restore number, self-renewal and proliferation capacities of NSCs (Bruggeman et al., 2005; Molofsky et al., 2003, 2005), suggesting the implication of p16-INK4a but that others mechanisms could be

participate. In 2007, Fasano and colleagues demonstrated as p21/CDKN1A is the mediator of the proliferative defect after knock-down of *Bmi-1* in fetal and adult NSCs (Fasano et al., 2007). Curiously, it was not observed an upregulation of *Ink4a/Arf* products. Probably, p21/CDKN1A upregulation was interpreted as removal of repressing influence (BMI-1) but not clear evidences supported this hypothesis.

We intend that the role of RING1B on cell proliferation have been only partially clarified. The involvement of PRC1 proteins in fundamental processes as redox homeostasis, DNA damage and DNA replication suggests that RING1B could positively control cell proliferation independently of its well-known role as transcriptional repressor or its E3 ligase activity. Using NSCs as cellular model derived from *Ring1B* conditional knock-out mouse strain, we want to explorer additional functions of RING1B that indirectly control cell proliferation, if there is a possible functional collaboration with others PRC1 components and determine a dual role of RING1B in control cell cycle progression and differentiation.

However, to date the mechanisms by which PRC1 exerts its positive control on NSCs self-renewal and proliferation have not been clarified**.**

Objectives

Objectives

We aimed at investigating the mechanism(s) involved in RING1B promotion of proliferation using a cellular model of murine embryonic NSCs, pursuing the following objectives:

1. To study the relationship between RING1B as a proliferation activator and CDK inhibitors

2. To determine the putative implication of RING1B in endogenous triggering of p53-dependent DNA damage response.

3. To explore possible mechanisms involving other PRC1 subunits.

Materials and methods

1. Mouse strains

Ring1B conditional knockout (Fig.M1) and genotyping were described previously (Cales et al., 2008). Inducible Cre-expressing mouse lines were *Polr2a::CreERT2* (Mijimolle et al., 2005) and *Rosa26::CreERT2* (Seibler et al., 2003). Compound *Ring1B$^{f/f}$;P53$^{-/-}$*, *Ring1B$^{f/f}$;Ink4a$^{-/-}$* and *Ring1B$^{f/f}$;Cdkn1A/p21$^{-/-}$* were obtained crossing *Ring1B$^{f/f}$; Polr2a::CreERT2* or *Ring1B$^{f/f}$;Rosa26::CreERT2* mice with *P53$^{-/-}$* (Jacks et al., 1994), *Ink4a$^{-/-}$* (Serrano et al., 1996) and *Cdkn1A/p21$^{-/-}$* (Brugarolas et al., 1995) mouse lines, respectively. Mouse embryonic fibroblasts (mEFs) were obtained from *Bmi-1$^{-/-}$* (Jacobs, et al, 1999), *Ring1A$^{-/-}$* (del Mar Lorente et al., 2000) and *Ring1B$^{f/f}$; Polr2a::CreERT2* (Cales et al., 2008).

Translocation of Cre-ERT2 to cell nuclei and *loxP* recombination were achieved by adding to the cultures 4'-hydroxytamoxifentamoxifen (4'-OHT, 1µM final concentration; Sigma-Aldrich) or vehicle (+4'-OHT or -4'-OHT, respectively).

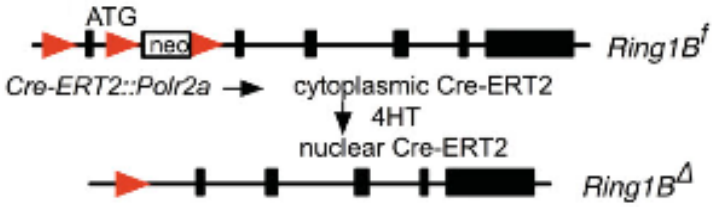

Figure M1: Strategy for generation of *Ring1B$^{\Delta/\Delta}$* cells. ATG denotes the initiation codon of *Ring1B*, red triangles loxP sequences and filled boxes *Ring1B* exons (Román-Trufero et al., 2009).

2. Cell culture:

2.1. Primary cells

2.1.1. Neural Stem/Progenitor Cell Culture

Neural stem cells were prepared from mouse embryonic olfactory bulbs (OBs) on the gestational days E13.5, considering E0.5 the day on which a vaginal plug was found in the pregnant female. After taking the brain out of the skull, the OBs (Fig.M2) were dissected using a sterile razor blade. Cells of dissected OBs were obtained by combining mechanical

dissociation (pipetting with sterile 100µL tips) and treatment with Hank's buffered salt solution (HBSS) supplemented with 0.025% of EDTA (HBSS+EDTA) for 20 minutes at 37°C in a 5% CO_2 atmosphere. After washing with Hank's buffered salt solution (HBSS) (without EDTA), cells were resuspended in DMEM/F-12 (1:1) (Life Technologies) including HEPES buffer (5 mM), glucose (0.6%), sodium bicarbonate (3 mM), and glutamine (2 mM). A defined hormone and salt mixture composed of insulin (25 mg/ml) apo-transferrin (100 mg/ml), progesterone (20 nM), putrescine (60 mM), and sodium selenite (30 nM) (all from Sigma-Aldrich) was used instead of serum. During NSCs viral transduction, B27 serum supplement (Gibco) was added to the medium to improve cell survival and proliferation.

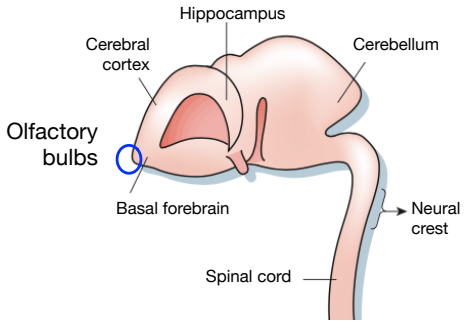

adapted from Temple 2001

Figure M2. The principal regions of the embryonic nervous system. NSCs have been isolated from the OBs.

Freshly derived OB stem cells (OBSCs) were plated on uncoated tissue culture dishes at a density of 35,000 cells per square centimeter, and incubated at 37°C in a 5% CO_2 atmosphere. FGF-2 and EGF (20 ng/ml each) were added daily to expand the proliferative precursor cell population (Vergaño-Vera et al., 2006) Once neural stem/progenitor cells culture was established, cells were seeded at 5000 cells per square centimeter and grown as floating aggregates or "spheres" (B. A. Reynolds & Weiss, 1996) and passaged every 3–5 days. At this point, the neurospheres should be passaged to prevent the cell clusters from growing too large, which can lead to necrosis as a result of a lack of oxygen and nutrient exchange at the neurospheres center. During passages, cells were dissociated using HBSS+EDTA buffer as described previously.

For immunofluorescence and ROS detection assay, NSCs were grown as monolayer culture. 6-wells plates (ROS detection) or glass coverslips (Thermo Scientific) were treated with 15µg/ml of poly-L-ornithine hydrobromide (Invitrogen) for 16 hours, washed with 1X PBS (3x) and treated with 1µg/ml bovine plasma fibronectin (FN) (Sigma-Aldrich) for at least 4 hours. Poly-L-ornithine is a synthetic amino acid chain that is positively charged and widely used as a coating to enhance cell attachment and adhesion to both plasticware and glass surfaces. FN is a multifunctional extracellular matrix glycoprotein used as cell adhesion molecule. Neurospheres were dissociated after a conventional passage as described before and seeded at a density of 10.000 cells/cm^2 directly on treated-coverslips or wells. Mitogens were added daily to avoid cells differentiation.

For clonal analysis, neurospheres were dissociated into a single-cell suspension and diluted to eight cells/ml in a mixture 1:1 of DMEM/F12/N12 and OBSC-conditioned medium (OBSC-CM, medium where the neurospheres were grown for 4 days). Neurospheres were centrifuged and supernatant (conditioned medium) was filtered through with 0.2μm filter. Two hundred microliters of the 8 cells /ml suspension was plated into each well of 96-well plates (1.6 cells/well). One day after seeding, wells containing a single cell were marked and induced to proliferate for 9 days, when the wells were screened for the presence of clonal neurospheres.

Phase contrast neurospheres photographs were acquired with DM IL LED microscope (Leica). Neurospheres diameters were calculated using ImageJ software.

2.1.2. Mouse embryonic fibroblasts (mEFs)

Mouse embryonic fibroblasts (MEFs, passage +2) were established from *Ring1B*$^{f/f}$, *Polr2a:Cre-ER*^{T2} , *Bmi-1*$^{-/-}$ *or Ring1A*$^{-/-}$ E13.5 embryos. After dissect head and red organs, embryos were washed in PBS and finely minced using a sterile razor blade until it becomes possible to pipette. mEFs were seeded at a density of 300.000 cells/10cm-plate or 100.000 cells/6cm-plate at day 0 and grown in Dulbecco's modified Eagle's medium (DMEM; Biowest) supplemented with 10% fetal bovine serum (heat-inactivated FBS, Sigma-Aldrich-Aldrich) and 100U/ml of antibiotics (Pen-Strep, Thermo Fisher) at 37°C, in a 5% of CO_2 atmosphere. To induce *Ring1B* recombination, 4'OHT (1 μM, Sigma-Aldrich-Aldrich) was added to the culture for 16 h. Control cells were treated with same amount of vehicle (Ethanol=-4-'OHT). Analysis was performed 96 hours after treatment initiation.

2.2. Established cell lines

Murine NIH-3T3 cell lines were grown in DMEM medium (Biowest) supplied with 10% Fetal Calf Serum (heat-inactivate, Sigma-Aldrich) and 100U/ml of penicillin/streptomycin antibiotics (Thermo Fisher).

293T cell line is a highly transfectable derivative of human embryonic kidney 293 cells, and contains the SV40 T-antigen. 293T cells were cultured in high glucose DMEM (Biowest) with 10% heat-inactivated Fetal Bovine Serum (FBS, Sigma-Aldrich) and 100U/ml of penicillin/streptomycin antibiotics (Thermo Fisher).

3. Cell immunostaining

NSCs, seeded at 10.000 cells/cm^2 at day 0 of the experiment, were grown as monolayer culture as described in section 2.1.1. on sterile glass coverslips for four days in presence of EGF and FGF-2.
mEFs were seeded at 100.000 cells/6cm-plate on sterile glass coverslips. At day +4 after 4'-OHT treatment, cells were pulse-labelled with EdU (10 μM) and fixed in 4% paraformaldehyde (PFA, Pierce) for 11 minutes, permeabilized with 0.5% Triton X-100 in PBS and blocked for 30 min in TPBS (0.1% Tween-20-containing PBS) containing 1% gelatin from cold water fish skin (Sigma-Aldrich) and 10% goat serum (blocking buffer). Incubation with primary antibodies (diluted in blocking buffer, see Table M1) was for 1 h at room temperature or at 4°C overnight. After washes, coverslips were incubated with 1μg/ml of Alexa-Fluor-conjugated goat antibodies (Alexa Fluor 488 or 568, Life Technologies), for 1 h at room temperature. After three washes in TPBS, DNA was stained for five minutes with 2 μg/ml 4',6-diamino-2-phenylindole (DAPI) diluted in TPBS.

Cell proliferation was assessed by 5-ethynyl-2'-deoxyuridine (EdU) incorporation (ten minutes pulse-labelling at 10μM final concentration directly in culture medium) with Click-it EdU Alexa Fluor 488 or 647 imaging kit (Life Technologies) according to the manufacturer's instructions. Detection is based on a click reaction, a copper-catalyzed covalent reaction between an azide and an alkyne. In this application, the EdU contains the alkyne and the Alexa Fluor dye contains the azide. The advantages of the Click-iT EdU labeling are that the small size of the dye azide allows for efficient detection of the incorporated EdU using mild conditions. Standard aldehyde-based fixation (4% PFA for eleven minutes) and detergent permeabilization (0.5% Triton X-100/PBS during 20 minutes) are sufficient for the Click-iT detection reagent to gain access to the DNA.
Coverslips were mounted using Mowiol (Calbiochem). Confocal images (confocal z-planes acquired every 0.5μm) were acquired using a LEICA TCS-SP5-AOBS microscope with an oil immersion 63× or 40x HCX PL APO objective lens. The nuclei were outlined using DAPI staining as a template and copied to the appropriate fluorophore channel. Nuclei were then counted and measurements of the mean fluorescent intensity or number of foci were recorded using ImageJ software. Background was determined in images from incubations without primary antibody and was subtracted so that only the 'true signal' was analyzed with the Find maxima tool from the ImageJ software.
A list of antibodies used for immunostaining is presented in Table M1.

4. Apoptosis assays

Apoptotic cells were scored using Annexin-V–FITC apoptotis detection kit (Bender MedSystems). Neurospheres cultured for 4 days after EtOH/4'-OHT treatment were dissociated into a single-cells suspension, washed once in PBS followed by a wash with the provided 1x binding buffer. Then cells (1×10^6/ml, 0.1 ml) in binding buffer containing 5µl of FITC-conjugated Annexin V and incubated for 10 minutes at room temperature. After washes with the provided 1x binding buffer, 10 µl of Propidium Iodide (20 µg/ml) staining solution were added and cells were acquired with DIVA software in a FACS Canto cytometer (both from Becton Dickinson) and analyzed using FlowLogic software (Inivai Technologies). Apoptosis was also assessed by conventional immunofluorescence (as above) using an anti-active caspase-3 (Promega).

5. Western Blot Analysis

Cells were lysed in Radioimmunoprecipitation assay buffer (RIPA, 10 mM Tris-HCl, pH 7.2; 150 mM NaCl; 1% Triton-100; 0.1% sodium dodecyl sulfate; 1% sodium deoxycholate; 5 mM EDTA, 1x PhosSTOP (Roche) and 1x Protease inhibitor cocktail (Biotools) for 15 minutes on ice, followed by 3 cycles (30 seconds ON/OFF) of sonicator (Diagenode) and additional 15 minutes incubation on ice. Protein extracts were quantified using BCA protein assay kit (Thermo Scientific) following the manufacturer's instructions. 15-30 µg of protein extract was subjected to SDS-PAGE electrophoresis (12% acrylamide in SDS PAGE gel) for 55 minutes at 180V. Separated proteins were transferred to a nitrocellulose blotting membrane (GE Healthcare) for one hour at 100V. Membranes were blocked with 5% non-fat dry milk (Chem Cruz) solubilized in 0.1% of tween-20 in PBS (blocking solution) and incubated with antibodies indicated in table 1 diluted in 1% Bovine Serum Albumin (BSA, Chem Cruz) in TTBS for two hours at room temperature or overnight at 4°C. After 3 washes in TTBS, membranes were incubated with the corresponding mouse (Dako) or rabbit (Life technologies) HRP secondary antibodies diluted in blocking solution at a final concentration of 0.2µg/ml for one hour at room temperature. Chemiluminescent reactions were performed using ECL Prime reagent (GE Healthcare) and luminescent signals were acquired on curix medical X-ray film (AGFA) or with ChemiDoc Touch Imaging System (Bio Rad).

6. Intracellular ROS analysis

For analysis of intracellular ROS, NSCs and mEFs were grown as monolayer in P60mm plates. At day +4, DCFDA (Sigma-Aldrich) was added directly in cell culture medium to a final concentration of 10 μM, and left at 37 °C for 30 min. DCFDA is a fluorogenic dye that measures hydroxyl, peroxyl and other reactive oxygen species (ROS) activity within the cell. After diffusion in to the cell, DCFDA is deacetylated by cellular esterases to a non-fluorescent compound, which is later oxidized by ROS into 2', 7'–dichlorofluorescein (DCF). NSCs monolayer cultures were detached with StemPro Accutase (0.5ml/6cm-plate, Thermo Scientific) at 37 °C for 5 minutes. mEFs were detached with 0.05% Trypsin-EDTA (1ml/10cm-plate, Gibco) at 37 °C for 5 minutes. Both NSCs and mEFs were immediately analyzed by Flow Cytometry using a EPICS XL (Beckman-coulter). Where indicated, *N*-acetyl-L-cysteine (NAC, Sigma-Aldrich) was added directly in culture medium at a final concentration of 0.5mM in H_20.

7. Quantitative RT-PCR

Total RNA was isolated lysing $5x10^6$ NSCs using 1ml of TRI reagent (Sigma-Aldrich) for 5 minutes at room temperature. Phases separation were performed adding 0.2ml/ml of TRI reagent of chloroform and centrifugation at 12.000x for 15 minutes at 4°C. Total RNA containing-aqueous phase was separated and RNA was precipitated adding 0.5ml of 2-propanol and centrifugation at 12.000g for 10 minutes at 4°C. RNA was resuspended in RNase-free water and quantified with Nanodrop. 1μg of RNA was used to setup reverse transcription (RT) reaction, carried out using the iScript cDNA Synthesis Kit (Bio-Rad) according to the manufacturer's guidelines. A quantitative polymerase chain reaction (qPCR) analysis was performed in duplicate using 1:10 or 1:100 diluted cDNA per reaction in a LightCycler 96 (Roche) with Bio-Rad SYBR-Green (Bio-Rad). β-Actin was the reference gene used for normalization. Relative gene expression was calculated using the comparative Ct method also referred to as the $2^{-\Delta\Delta CT}$ method. Sequences of primer pairs for the qRT-PCR are indicated in table M2.

8. Vector Production and Viral Packaging

Lentiviral particles were obtained upon co-transfection of 10µg of pFUGW-H1 (Fasano et al., 2007) or pTRIPZ (Thermo Scientific) plasmid into 293T cells with 4.8µg psPAX2 packaging and 2.6µg pMD2G envelope plasmids (Addgene plasmids# 12260 and 1259, respectively). Viral containing media were collected, filtered, and 100-fold concentrated (only for NSCs transduction) by ultracentrifugation at 23000rpm for two hours at 4° C degrees using a Beckman Coulter ultracentrifuge and SW28 rotor. Viral titers were measured by serial dilution on NIH-3T3 cells. For viral transduction, 10^7 fresh viral particles were used to infect 10^6 single cell suspension of NSCs (MOI=10) in presence of 8 µg/mL of Polybrene (Sigma-Aldrich), 1x B27 serum supplement (Gibco), EGF and FGF2 (20 ng/ml each) and medium up to 1ml seeded in a well of 6 wells-plate. To improve transduction efficiency, 6 wells-plate was centrifuged for 1 hour at 1500rpm (rotor A-4-63, Eppendorf 5810 R) at 4° C degrees.

For viral transduction of mEFs, non-ultracentrifuged lentiviral vectors were diluted 1:2 with complete medium and incubated overnight with 100.000 cells/6cm-plate in presence of 8µg/mL of polybrene (Sigma-Aldrich).

A third-generation lentiviral vector pFUGW-H1 was used to express a shRNA to target the p21 ORF (TTAGGACTCAACCGTAATA and AGTAGCAGTTGTACAAGGA) (Fasano et al., 2007). The pTRIPZ lentiviral doxycyclin-inducible vector (Tet-On system, Thermo Scientific) was used to overexpressed a wild type or a E3 ligase mutant (IL53,55A,A; ΔE3) form of RING1B, or BMI-1 ORF. NSCs and mEFs transduced with pTRIPZ lentiviruses were grown in presence of 1.1µg/mL of puromycin (Toku E) for 3 days to select only transduced cells. After antibiotic selection, cells were treated, or not (as control) with 2 µg/mL of doxycycline (Sigma-Aldrich) during the 96 hours of the experiment to induce the expression of cDNA cloned in the pTRIPZ lentiviral doxycyclin-inducible vector.

9. Statistical analysis

Data were processed in Prism 6 (GraphPad software) using an unpaired, two-tailed Student's t-test, or Mann–Whitney U test, as indicated.

Table M1: Antibodies used in this work

Protein	Species	Source	Use (dilution)	Clone
53BP1	Rabbit	Novus Biological	IF (1:500)	Polyclonal
CDKN1A/p21	Mouse	BD Pharmingen	IF (1:200)	SX119
CDKN1A/p21	Mouse	Santa Cruz Biotechnology	WB (1:200)	F-5
CDKN2A/p16^{Ink4a}	Rabbit	Santa Cruz Biotechnology	WB (1:1000	M-156
H2A	Rabbit	Millipore	WB (1:2000	Polyclonal
H2AK119Ub1	Rabbit	Cell Signaling	WB (1:5000	D2754
RING1A	Rabbit	(Schoorlemmer et al., 1997)	WB (1:500)	
RING1B	Rabbit	(Garcia et al., 1999)	IF (1:1000), WB (1:1000)	
BMI-1	Rabbit	Cell Signaling	WB (1:1000)	D42B3
RPA32	Rat	Cell Signaling	IF (1:100)	4E+04
α-tubulin	Mouse	Sigma-Aldrich	WB (1:50.000)	B-5-1-2
γH2AX (Ser139)	Rabbit	Cell Signaling	IF (1:400)	20E3
γH2AX (Ser139)	Mouse	Biolegend	IF (1:400), WB (1:750)	2F3
p53	Mouse	Cell Signaling	WB (1:1000)	1C12
Phospho-p53 (ser15)	Rabbit	Cell Signaling	WB (1:500)	Polyclonal
p57	Rabbit	Santa Cruz Biotechnology	WB (1:500)	H-91
Phospho-p38-MAPK	Rabbit	Cell Signaling	WB (1:1000)	Polyclonal
p38-MAPK	Rabbit	Cell Signaling	WB (1:1000)	Polyclonal
Phospho-AKT (Ser473/474/472)	Rabbit	GeneTex	WB (1:200)	Polyclonal
p27	Rabbit	Santa Cruz Biotechnology	WB (1:300)	C-19
Active Caspase-3	Rabbit	Promega	IF (1:50)	polyclonal
Tuj-1 (β-tubulin III)	Rabbit	Covance	IF (1:1000), WB (1:1000)	MRB-435P

Table M2: qRT-PCR primers

Gene (cDNA)	Oligonucleotide	Primer sequence
β-actin	sense	GGCTTGTATTCCCCTCCATCG
	antisence	CCAGTTGGTAACAATGCCATGT
NeuroD1	sense	ATGACCAAATCATACAGCGAGAG
	antisence	TCTGCCTCGTGTTCCTCGT
Eomes	sense	GGCCCCTATGGCTCAAATTCC
	antisence	CCTGCCCTGTTTGGTGATG

Results

1. RING1B role in proliferation and viability of neural stem cells

To gain insight into the mechanisms by which RING1B could be controlling neural stem cells (NSCs) proliferation and/or viability, we explored best readouts to determine whether major cell cycle regulators were involved in this process.

1.1. Proliferation and apoptosis in RING1B-deficient neural stem cells

We first quantified the effect of RING1B deletion in NSCs proliferation by culturing NSCs under conditions that allow neurospheres generation (Reynolds & Weiss, 1996). We then measured their diameters and total number of derived cells. RING1B deficiency induced a proliferative defect and, as a result, less and smaller neurospheres were obtained at day +4 after EtOH (*Ring1B$^{f/f}$*) or 4'-OHT (*Ring1B$^{\Delta/\Delta}$*) treatment (Fig.R1A). Thus, RING1B-mutant neurospheres contained around half the cells than control and their diameters were also around half those of wild type spheres (Fig.R1B).

We then aimed to determine if the decrease in cells number and neurospheres sizes was due to a proliferation defect or an increase of apoptosis. We first performed EdU incorporation assay. Similarly to BrdU, EdU (5-ethynyl-2'-deoxyuridine) is a nucleotide analog incorporated in replicative cells. At day +3 and +4 after EtOH and 4'-OHT treatment, we pulse-labeled *Ring1B$^{f/f}$* and *Ring1B$^{\Delta/\Delta}$* monolayer cultures with EdU (10μM) for ten minutes (Fig.R1C). Immunofluorescence analysis showed that the percentage of cells that had incorporated EdU was significantly lower in RING1B-mutant than in control cells, 38 vs 28% or 25%, at days +3 and +4 respectively.

This was consistent with our already reported poorer expansion of RING1B-deficient, compared to wild-type neurosphere cultures at day+4 after EtOH/4'-OHT treatment (Román-Trufero et al., 2009)

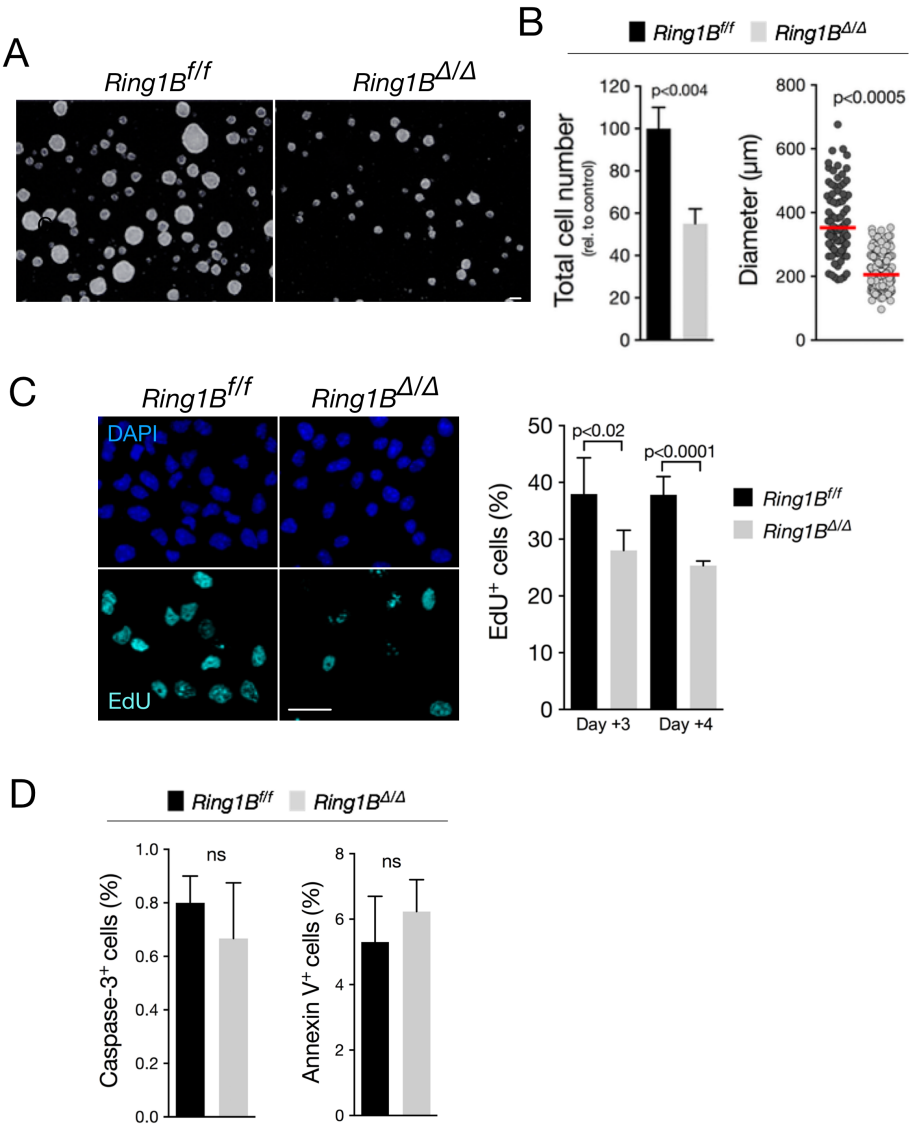

Figure R1. **Impaired proliferation of RING1B-deficient neural stem cells**. (**A**) Representative micrographs of neurospheres at day+4 after EtOH or 4'-OHT treatment (*Ring1B*$^{f/f}$ and *Ring1B*$^{\Delta/\Delta}$, respectively). (**B**) Left: total cell number in *Ring1B*$^{f/f}$ and *Ring1B*$^{\Delta/\Delta}$ cultures (n=3). Right: scatter plot showing neurosphere diameters. At least 100 neurospheres diameters were measured in each experiment (n=7). Red bar shows median value. (**C**) Cell proliferation rates (n=7) measured as percentage of EdU-positive cells (10 minutes pulse labeling) at day +3 and day +4 after 4'-OHT addition, as assessed by immunofluorescence analysis. (**D**) Caspase-3 and Annexin V-staining labeling showed infrequent apoptosis signals in control and RING1B mutant cells. At least 300 cells were analyzed in each experiment (n=3). Bar charts represent mean±s.d. (B left, C and D) and p values were calculated using unpaired, two-tailed Student's t- (B left, C and D), or Mann–Whitney U (B, right) tests. Scale bar=200 microns (A), 50 microns (C).

Next we performed Annexin V and Caspase-3 immunostaining to test if reduced cell number

and neurosphere sizes of mutant cells were associated with cell death due to increased apoptosis. Annexin V staining (Fig.R1D, right chart) was similar in both mutant and control cells: 5% and 6% Annexin V$^+$ cells respect to total cells in *Ring1B$^{f/f}$* and *Ring1B$^{\Delta/\Delta}$*, respectively. In addition, caspase-3 analysis (Fig.R1D, left chart) also showed very similar labeling in mutant and control cells, with almost no apoptotic cells in either culture (0.8% and 0.6% of caspase-3$^+$ cells respect to total cells in *Ring1B$^{f/f}$* and *Ring1B$^{\Delta/\Delta}$* cultures, respectively).

Collectively, these results show that defective expansion of RING1B-mutant NSCs is due to a decrease in the proliferative rate with no increase in apoptosis. It also allowed us to choose quantification of neurospheres diameters and EdU incorporation as main readout of RING1B deficiency-associated phenotype in NSC cultures.

1.2. Cyclin-dependent kinase inhibitors expression in the absence of RING1B

RING1 and other PcG proteins are responsible for *Cdkn2a* locus repression (Bracken et al., 2007; Bruggeman et al., 2005; Calés et al., 2008; Jacobs et al., 1999; Maertens et al., 2009). Other Cdk inhibitors have also been associated with RING1B and Polycomb activity (Calés et al., 2008; Fasano et al., 2007; Pateras et al., 2009; Román-Trufero et al., 2009; Bravo et al. 2015). We thus decided to look at the expression of some of these proliferation inhibitors.

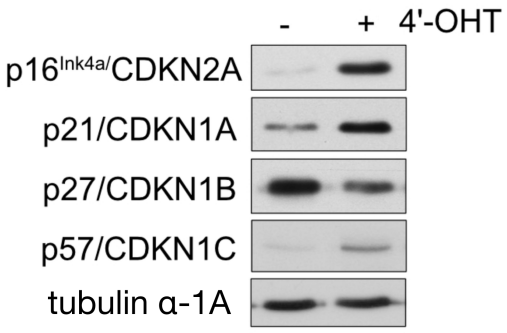

Figure R2. Cyclin-dependent kinases inhibitors protein levels in control and RING1B-mutant neural stem cells

Western blotting analysis of total protein extracts (20μg of protein/lane) of control (-4'-OHT, control) and mutant (+4'-OHT, KO) neurospheres. Alpha-Tubulin was used as loading control.

We performed Western Blotting analysis with *Ring1B*$^{f/f}$ and *Ring1B*$^{\Delta/\Delta}$ neurosphere cultures protein extracts. As expected, RING1B depletion induced p16-INK4a upregulation as already described in other cell types (Fig.R2). Equally, p57/CDKN1C and p21/CDKN1A were both upregulated whereas p27/CDKN1B levels seemed to be lower in RING1B-mutant than in control cultures.

It can thus be hypothesized that proliferation defects in RING1B deficient NSCs may be due to increased cell cycle inhibitors. To determine whether all or only some of them was responsible for the antiproliferative phenotype we decided to first concentrate into p16-INK4a, as paradigmatic PcG target, and into p21/CDKN1A, recently shown to be upregulated after *Ring1B* inactivation in different cell types (Bravo et al., 2015; Koike et al., 2014).

1.3. RING1B deficiency-driven proliferation defect and p16-INK4a upregulation

We first derived OBSCs from *Ring1B*$^{f/f}$*, ER-Cre, Cdkn2a*$^{-/-}$ 13.5 d.c.p. embryos and cultured them in the presence or absence of 4'-OHT. Western blotting analysis performed with neurospheres protein extracts (day+4 after EtOH/4`-OHT treatment) to confirm *Ring1B* recombination in 4'-OHT-treated extracts, as well as absence of p16-INK4a expression in *Cdkn2a*$^{-/-}$ cells. We also confirmed the increase of p16-INK4a levels in RING1B-mutant cells (Fig.R3A). Although no apparent increase in neurosphere size was detected (Fig.R3B), we measured their diameters as well as EdU incorporation to test proliferation ability of single or double mutant cells. The combined inactivation of *Ring1B* and of *Cdkn2a* resulted only in a modest, non-significant, effect on cell proliferation. Thus, the size of the neurospheres increased only marginally (Fig.R3C) and the proportion of double mutant cells that incorporated EdU was also augmented modestly (Fig.R3D).
In any case, double mutant cells produced significantly smaller neurospheres compared to their control values, but not much different form RING1B-deficient cultures.

We conclude that p16-INK4a does not play a crucial role in the early antiproliferative effect of RING1B loss.

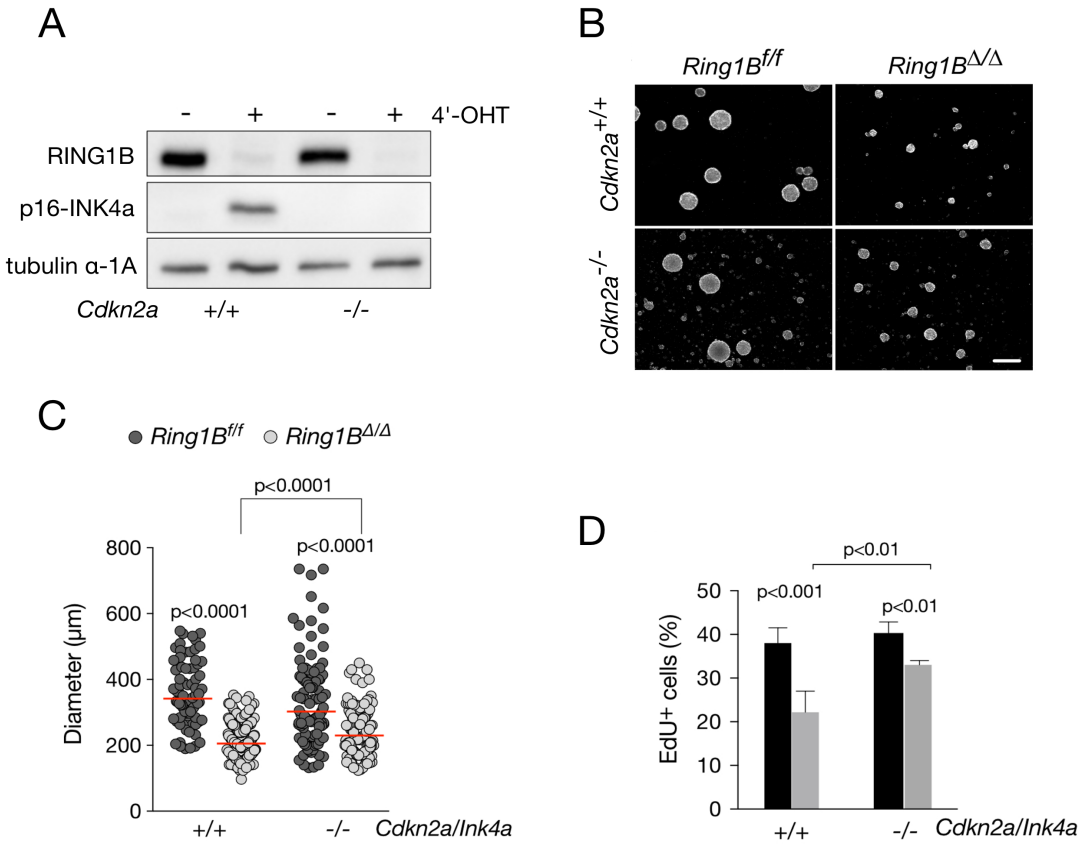

Figure R3. *Cdkn2a* locus knock-out did not rescue the proliferative defect of RING1B-mutant cells. **(A)** Western Blotting showing RING1B and p16-INK4a expression in neurosphere extracts from *Cdkn2a* WT and KO mice, untreated or treated with 4'-hydroxytamoxifen to induce *Ring1B* recombination. **(B)** Representative photographs of cultured neurospheres. Scale bar=400 microns **(C)** Scatter plot (n=3) of neurospheres diameters showing that, in *Cdkn2a*$^{-/-}$ cultures, most RING1B-mutant spheres remained smaller in size compared with RING1B-expressing cultures. At least 100 neurosphere diameters were analyzed in each experiment. Red bars show median values. (**D**) Proliferation rates (n=3) measured as % of EdU-positive cells (10 minutes pulse labeling), as assessed by immunofluorescence analysis of *Ring1B*$^{f/f}$ or *Ring1B*$^{\Delta/\Delta}$ cells bearing a wild type or a mutant *Cdkn2a* allele. Bar charts show mean±s.d. p values were calculated using unpaired, two-tailed Student's t- (D), or Mann–Whitney U (C) tests.

1.4. RING1B absence-induced p21/CDKN1A upregulation and NSCs proliferation inhibition.

1.4.1. Knockdown of *p21/Cdkn1a* effect on RING1B-mutant neurosphere size

We asked whether p21/CDKN1A upregulation was responsible for proliferation inhibition in RING1B-deficient NSCs. We knocked down *p21/Cdkn1a* by lentiviral transduction of a small hairpin RNA (shRNA) or of an empty vector (EV-control) as a control. The cells were then treated with EtOH or 4'-OHT to induce *Ring1B* recombination. After 4 days, we photographed neurospheres to measure diameters and we obtained a protein extract from the same neurospheres. Western blotting assay (Fig.R4A) showed a clear downregulation of p21/CDKN1A in *p21* shRNA-transduced NSCs. RING1B-deficient neurospheres transduced with *p21* shRNA presented similar sizes to control cells (Fig.R4B), and the calculated diameters (Fig.R4B, right) confirmed the rescue of RING1B-deficiency phenotype, suggesting a critical role of p21/CDKN1A in proliferation of mutant cells

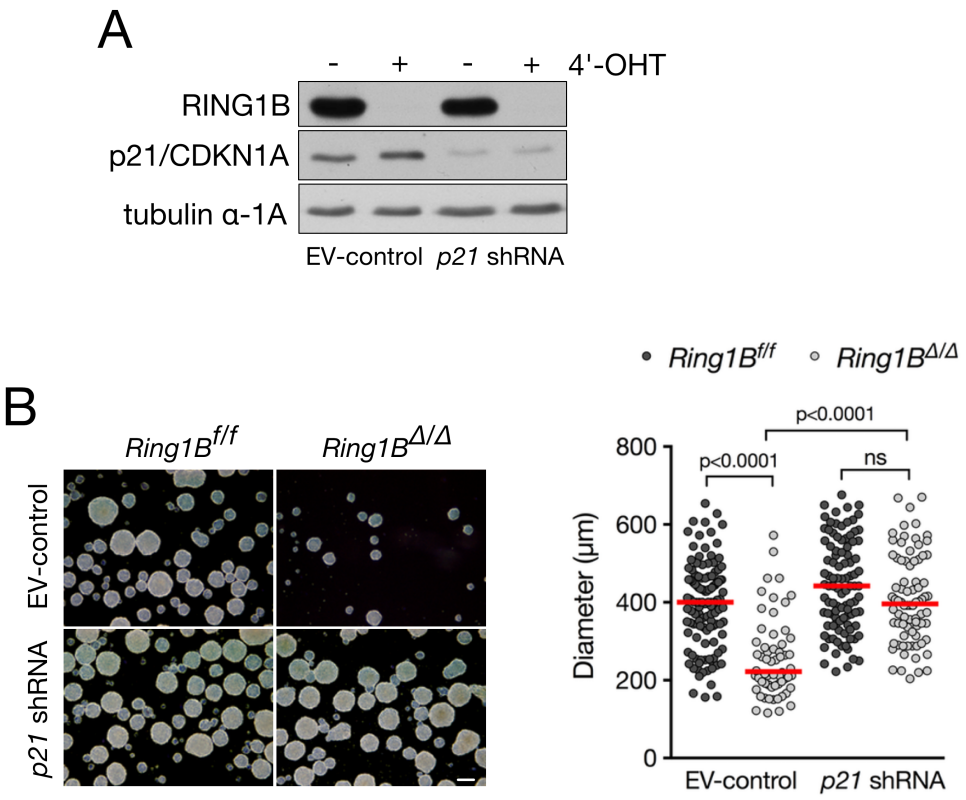

Figure R4. Proliferation defect in RING1B-deficient NSCs is mediated by p21/CDKN1A. **(A)** Western blot showing p21/CDKN1A levels in *Ring1B$^{f/f}$* (-4'-OHT) or *Ring1B$^{\Delta/\Delta}$* (+4'-OHT) cells transduced with a lentivirus expressing *p21* shRNA or an empty vector (EV-control). **(B)** Left: Representative photographs of *Ring1B$^{f/f}$* or *Ring1B$^{\Delta/\Delta}$* neurosphere cultures, transduced with *p21* shRNA or an empty vector (EV-control). Right: Scatter plot of neurospheres diameters showing that RING1B-mutant spheres transduced with *p21* shRNA have a similar size compared with controls. At least 100 neurosphere diameters were analyzed in each experiment (n=3). Red bars show median values. Scale bar=400 microns (B). p values were calculated using unpaired Mann–Whitney U (B) tests; ns, not significant (P≥ 0.05).

1.4.2. *p21/Cdkn1a* knock-out interference with proliferation defect of RING1B mutant neural stem cells

We then decided to analyze NSCs primary cultures from embryos that combined the conditional *Ring1B* allele and a null allele for *Cdkn1a*, encoding p21/CDKN1A. Western blotting analysis showed the absence of p21 expression in *p21/Cdkn1a* knock-out NSCs and RING1B deletion at day+4 after EtOH/4'-OHT treatment (Fig.R5A).

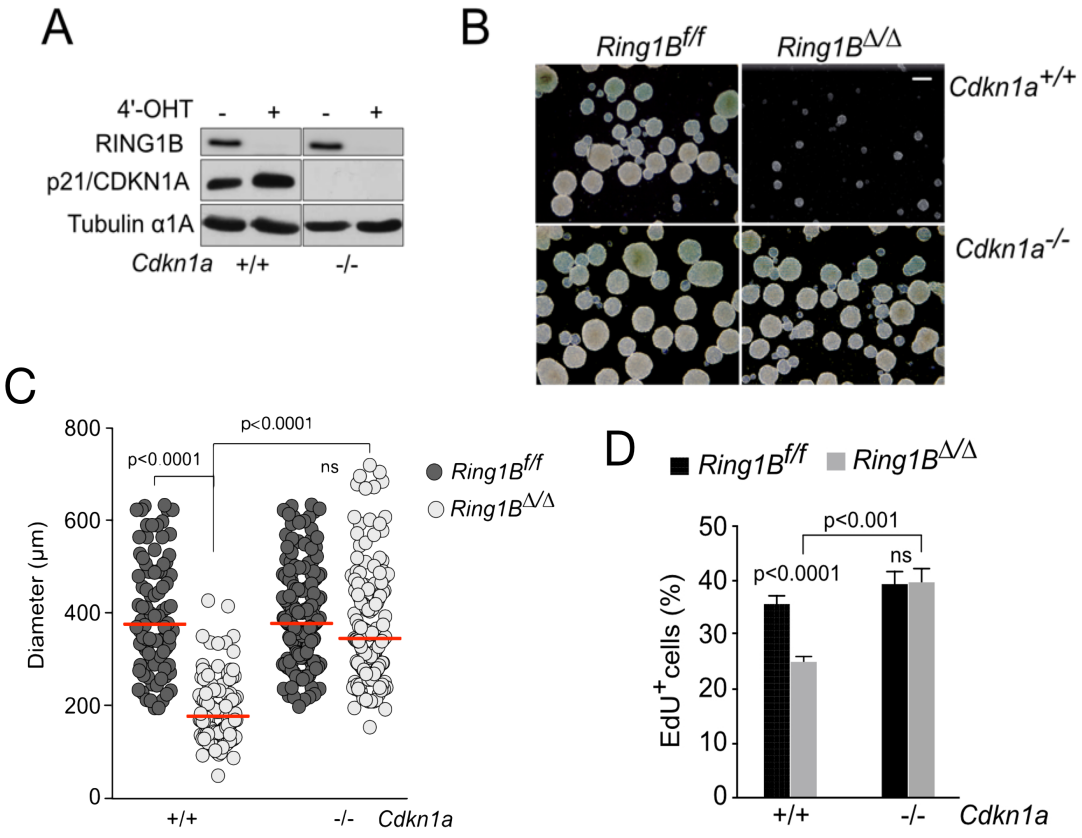

Figure R5. ***p21/Cdkn1a*** **knock-out rescued the proliferative defect in RING1B-mutant neural stem cells. (A)** Western blot showing RING1B and p21/CDKN1A levels in *Ring1B$^{f/f}$* (-4'-OHT) or *Ring1B$^{Δ/Δ}$* (+4'-OHT) cells and absence of p21/CDKN1A in *Cdkn1a$^{-/-}$* NSCs. Tubulin Alpha-1A chain was used as loading control. **(B)** Representative phase-contrast images of *Ring1B$^{f/f}$* or *Ring1B$^{Δ/Δ}$* neurosphere cultures bearing a wild type (+/+) or a mutant (-/-) *p21/Cdkn1a* allele, at day+4 after 4'-OHT or EtOH treatment. Scale bar=400 microns. **(C)** Scatter plot of neurosphere diameters showing that *Ring1B$^{Δ/Δ}$, Cdkn1a$^{-/-}$* double mutant spheres have a similar size compared to controls. At least 100 neurosphere diameters were measured in each experiment (n=3). Red bars show median values. **(D)** Proliferation rates (n=3) measured as % of EdU-positive cells (10 minutes pulse labeling), as assessed by immunofluorescence analysis of *Ring1B$^{f/f}$* or *Ring1B$^{Δ/Δ}$* cells bearing a wild type (+/+) or a mutant (-/-) *Cdkn1a* allele. Bar charts show mean±s.d. p values were calculated using unpaired, two-tailed Student's t (D), or Mann–Whitney U (C) tests. ns, not significant (P≥ 0.05).

Ring1B$^{Δ/Δ}$, Cdkn1a$^{-/-}$ culture displayed noticeable recovery of neurospheres size (Fig.R5B), further assessed by measuring their diameter (Fig.R5C).

When *Ring1B$^{f/f}$ or Ring1B$^{Δ/Δ}$, Cdkn1a$^{-/-}$* NSCs were pulse-labeled with EdU, they showed a similar proliferation rate respect to RING1B proficient cells (Fig.R5D).

These results further demonstrate that the RING1B deficiency-driven proliferative defect is mediated by p21/CDKN1A levels increase.

2. RING1B role in the response to DNA Damage

It has been described that, on top of the well-known role in transcriptional silencing (Di Croce & Helin, 2013; Lanzuolo & Orlando, 2012; Simon & Kingston, 2009), H2AK119 ubiquitylation and localization of RING1B and BMI-1 at sites of DNA Damage might be related to DNA damage response (Chou et al., 2010; Ginjala et al., 2011; Ismail et al., 2010)

We aimed at determining whether RING1B deficiency provoked DNA damage in NSCs, with no external sources of induced-DNA damage, UV or IR-laser treatment. We checked for the presence of two very-well known DNA damage markers, phosphorylation of H2AX at Serine 139 (hereafter γH2AX) and detection of 53BP1 at site of DNA damage (Balajee & Geard, 2004; Fernandez-Capetillo et al., 2004; Wang, Matsuoka, Carpenter, & Elledge, 2002).

2.1. Phosphorylation of H2Ax and presence of RPA foci in proliferating RING1B-mutant neural stem cells

We first performed a Western Blotting analysis with control and mutant proliferating neurosphere protein extracts to determine phosphorylation of H2AX at serine 139. As shown in Fig.R6A, γH2AX levels increased in RING1B-mutant cells, compared to control cells. We then performed immunostaining analysis to determine the extent of DNA damage at single cell level. Co-immunostaining of γH2AX and EdU (Fig.R6B) allowed identification of γH2AX fluorescence intensity in non-proliferating (EdU^-) and proliferating (EdU^+) cells. As seen in Fig.R6C, γH2AX labeling was more intense in EdU^+ cells respect to non-proliferating cells, and significantly increased in RING1B-mutant neural stem compared to control cells ($p<0.0005$). No differences were observed between RING1B-mutant and control non-proliferating (EdU^-) cells. However, γH2AX foci appeared at higher frequencies in mutant than in control proliferating cells (Fig.R6C, panel right). From then on, we decided to score fluorescent intensity of γH2AX in EdU^+ cells only.

The evidence of DNA damage only in proliferative mutant cells could be related to replicative stress. We decided to check for the presence of RPA32, a ssDNA-binding protein that protects DNA from the nuclease activity, and can be considered a replicative stress read-out (Zou & Elledge, 2003). To detect insoluble replication-associated RPA, EdU-pulsed cultures were treated with detergent, prior to fixation (Fig.R6D). We found almost a twofold increase of scored double $EdU^{+}/RPA32^{+}$cells with signs of replicative stress among mutant compared to control cultured cells (Fig.R6D, right charts).

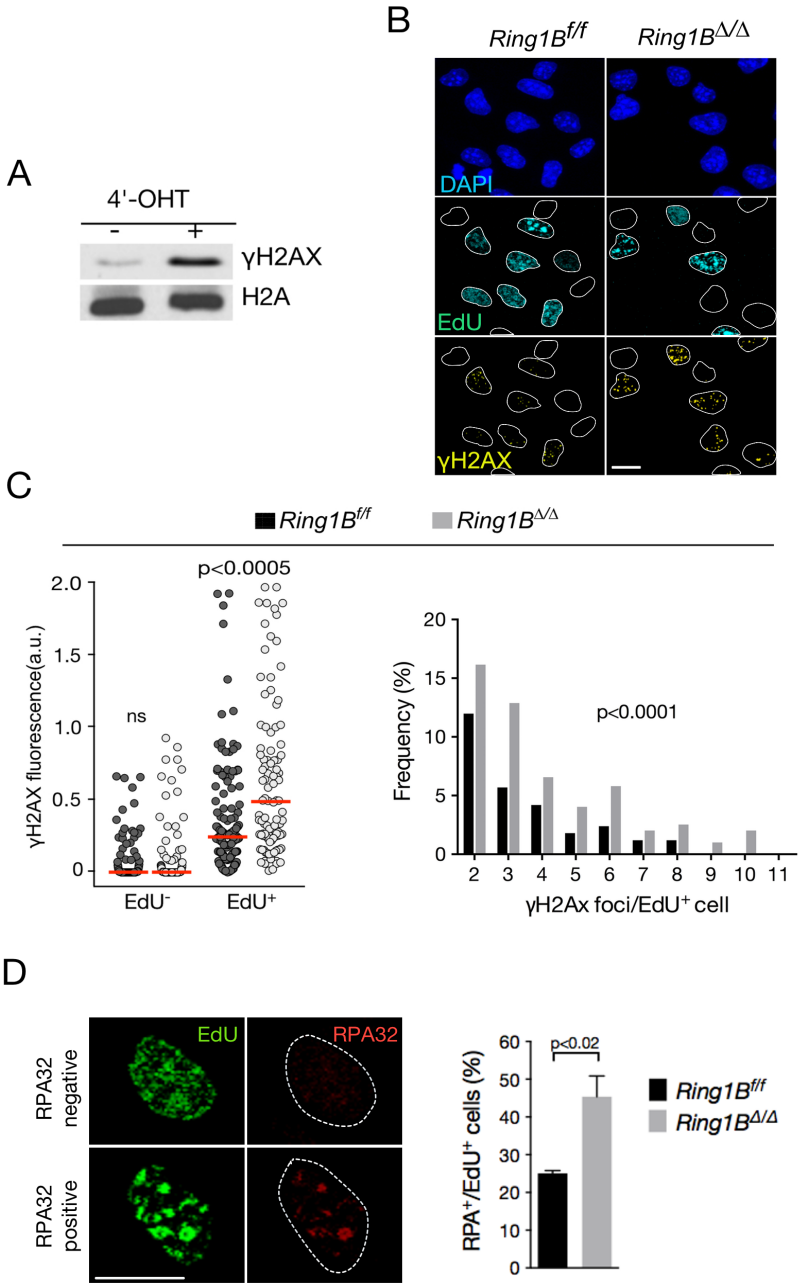

Figure R6. DNA damage foci are detected in RING1B deficient NSC cultures. (**A**) Western blotting showing an increase of H2AX phosphorylation in mutant culture. H2A histone was used as loading control (**B**) Immunostaining of γH2AX, EdU and DAPI in *Ring1B$^{f/f}$* or *Ring1B$^{Δ/Δ}$* neural stem cells monolayer cultures at day +4 after EtOH/4'-OHT treatment, showing presence of γH2Ax foci in proliferating (EdU^{+}) RING1B-mutant cells. Scale bar=10 microns. (**C**) Left: Scatter plot of γH2AX fluorescence intensity in proliferating (EdU^{+}), or non-proliferating (EdU^{-}) cells, showing an increase of γH2AX signal in proliferating RING1B-mutant culture. Red bars show median values. Right: Relative frequency of γH2AX foci/EdU^{+} cells in control and RING1B-mutant neural stem cells. At least 100 EdU^{-} and EdU^{+} cells were analyzed for each condition and experiments (n=3). (**D**) Left: Representative immunostaining of RPA32^{-}/EdU^{+} and RPA32^{+}/EdU^{+} NSCs. Cells were pre-extracted with detergent before fixation in order to detect insoluble RPA32 only. Scale bar=20 microns. Bar chart (right) indicates % of RPA^{+}/EdU^{+} cells in *Ring1B$^{f/f}$* or *Ring1B$^{Δ/Δ}$* cultures (n=2). p values were calculated using unpaired, two-tailed Student's t-(D), or Mann–Whitney U test (C). ns, not significant (P≥

2.2. Accumulated double-strand breaks in RING1B-deficient cells

To further assess the number of double-strand breaks foci, we aimed at determining 53BP1 foci, as it accumulates at site of double-strand breaks and plays an active role in DNA damage response and repair (Wang et al., 2002). Immunostaining of 53BP1 and EdU showed that double-strand breaks foci accumulated in proliferating EdU$^+$ cells (Fig.R7A), as observed for γH2AX. The percentage of 53BP1$^+$/EdU$^+$ cells (more than 3 foci per cell) was higher in RING1B-mutant than in control cells (3.9% vs 24.2%, p<0.0005) (Fig.R7B, left chart).

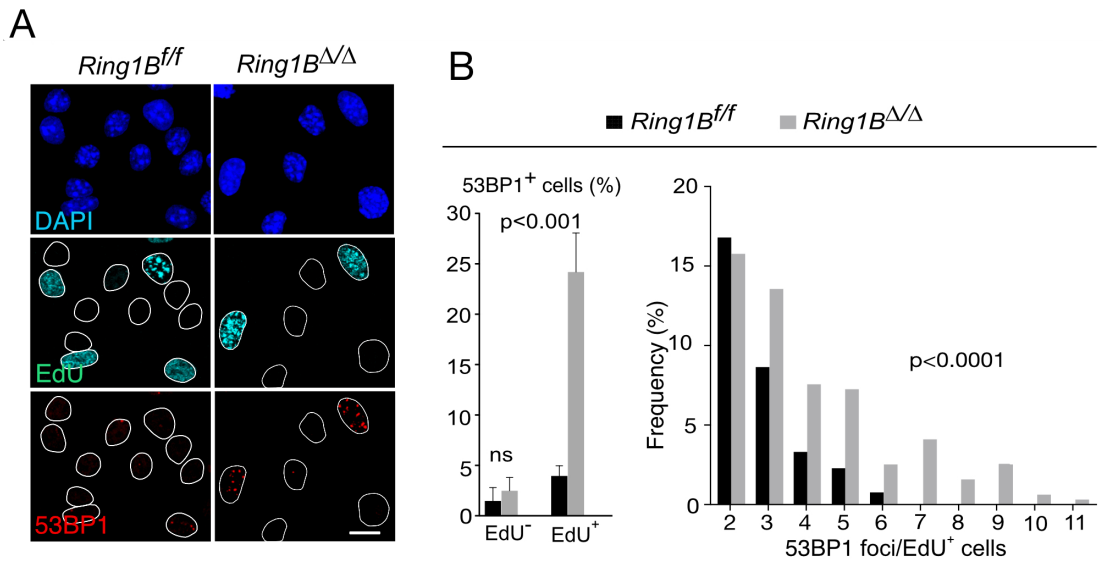

Figure R7. 53BP1 double-strand breaks foci are detected in RING1B deficient NSC cultures. **(A)** Immunostaining of 53BP1, EdU and DAPI in *Ring1B$^{f/f}$* or *Ring1B$^{Δ/Δ}$* neural stem cells monolayer cultures at day +4 after EtOH or 4'-OHT treatment, respectively, showing the presence of 53BP1 foci in proliferating (EdU$^+$) RING1B-mutant cells. Scale bar=10 microns. **(B)** Left: percentage of 53BP1$^+$/EdU$^-$ or 53BP1$^+$EdU$^+$ cells (3 or more foci/cell were considered as positive). At least 100 EdU$^-$ and EdU$^+$ cells were analyzed for each condition and experiment (n=3). Bar charts show mean±s.d. Right: Relative frequency of 53BP1 foci/EdU$^+$ cells in control and RING1B-mutant neural stem cells. p values were calculated using unpaired, two-tailed Student's t-(B left), or Mann–Whitney U test (B right). ns, not significant (P≥ 0.05).

In addition, we scored 53BP1 foci at single cell level, analyzing proliferating cells (EdU^+) only (Fig.R7B, right histogram). The relative frequency of 53BP1 foci in EdU^+ cells appeared at higher frequencies in RING1B-mutant cells.

These results indicate that RING1B is essential to assure that DNA damage does not accumulate in proliferating NSCs, thus may be essential to maintain genomic stability.

3. RING1B and the ATM/ATR-P53 DNA damage checkpoints

As DNA damage results in the activation of ATM, responsible for the phosphorylation of H2AX and of activating the p53/p21 checkpoint axis (Abraham, 2001; Shiloh & Ziv, 2013; Smith et al., 2010), we wanted to evaluate whether the upregulation of p21/CDKN1A in RING1B-deficient cells was due to an activation of DNA Damage Response (DDR) through ATM and P53 activation.

3.1. *P53* knockout interference with proliferation defect of RING1B-deficient neural stem cells

We first evaluated whether P53 was mediating RING1B deficiency effect on neurospheres proliferation. For this, we derived NSCs from mice bearing a wild type or a mutant *Tp53* allele and the floxed *Ring1B* allele.

Western Blotting analysis confirmed the absence of P53 and recombination of *Ring1B* (Fig.R8A). We could also observe that no significant changes in P53 expression were detected in the absence of RING1B in $Tp53^{+/+}$ cells, whereas p21/CDKN1A levels increased, as already described for RING1B-mutant NSCs, probably due to P53 phosphorylation that results in its activation (Fig.R9A). However, p21/CDKN1A was undetectable in the absence of P53, regardless of the presence or absence of RING1B (Fig.R8A), indicating that, at least in these cells, *p21/Cdkn1a* expression is exclusively controlled by the transcriptional activity of P53.

In agreement to what had been observed in *p21/Cdkn1a*$^{-/-}$ NSCs, no differences in neurospheres size (Fig.R8B) or EdU incorporation (Fig.8C) were observed between RING1B control and mutant cells in *Tp53* knock-out background.

Thus, the absence of P53 completely rescued proliferation defects of RING1B-mutant NSCs by impeding *p21/Cdkn1a* expression, in a similar way that we observed in *p21/Cdkn1a*$^{-/-}$ cells or knocking-down *p21/Cdkn1a*.

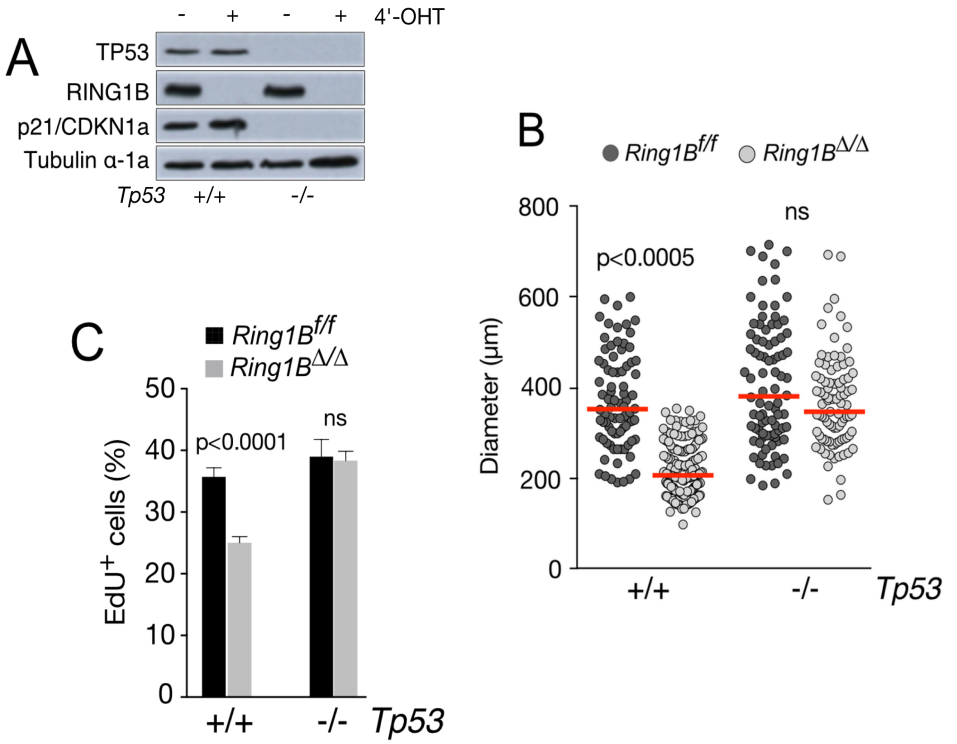

Figure R8. *Tp53* knock-out rescued the proliferative defect in RING1B-mutant neural stem cells (A) Western blotting assay performed with RIPA total protein extract showing absence of P53 and p21 expression in *Ring1B*$^{f/f}$ or *Ring1B*$^{Δ/Δ}$ cells bearing a wild type (+/+) or a mutant (-/-) *Tp53* allele. Tubulin Alpha-1A chain was used as loading control. **(B)** Scatter plot of neurospheres diameters showing that *Ring1B*$^{Δ/Δ}$, *Tp53*$^{-/-}$ double mutant spheres have a similar size respect to controls. At least 100 neurospheres diameters were measured in each experiment (n=3). Red bars show median values. **(C)** Proliferation rates: % of EdU-positive cells after a pulse of 10 minutes at day +4 after addition of EtOH or 4'-OHT (n=3) of *Ring1B*$^{f/f}$ or *Ring1B*$^{Δ/Δ}$ cells bearing a wild type (+/+) or a mutant (-/-) *Tp53* allele. Bar charts show mean±s.d (n=3). p values were calculated using unpaired, two-tailed Student's t (C) or Mann–Whitney U (B) tests. ns, not significant (P≥ 0.05).

3.2. DNA damage and ATM/P53/p21 pathway activation in RING1B-deficient NSCs

It is known that DSB formation predominantly signals through Ataxia Telangiectasia Mutated (ATM) kinase which modifies a large number of substrates, including H2AX, P53, CHK2, NBS1, and BRCA1 (Abraham, 2001; Shiloh & Ziv, 2013; Smith et al., 2010). To determine if the p21-dependent proliferative arrest seen in RING1B-deficient NSCs was a consequence of ATM-DNA damage signaling activation, we used a commercial, specific and very potent small molecule inhibitor of ATM, 2-morpholin-4-yl-6-thianthren-1-yl-pyran-4-one, termed KU-55933 (Hickson et al., 2004) to inhibit ATM kinase activity and to block the ATM-P53-p21 pathway.

We treated RING1B-deficient cells for two hours with 10μM of KU55933 (+ATMi), or DMSO as control (-ATMi). Western blotting analysis of RING1B-mutant NSCs exposed to ATM inhibitor showed a decrease in $P53^{ser15}$ and H2AX phosphorylation (pP53 and γH2AX, respectively) together with the abrogation of p21/CDKN1A accumulation in mutant NSC (Fig.R9A). Control and RING1B-mutant cells were pulse-labeled with EdU just after ATM inhibitor treatment. A rescue of the proliferation rate could be observed in ATMi-treated RING1B-depleted cells, showing comparable values of EdU incorporation than control cells (Fig.R9B). γH2AX and p21/CDKN1A expression was also evaluated in immunofluorescence assay that confirmed a decrease of γH2AX signal in EdU^+ cells and of p21/CDKN1A labeling in mutant cells with an inhibited ATM (Fig.R9C and D).

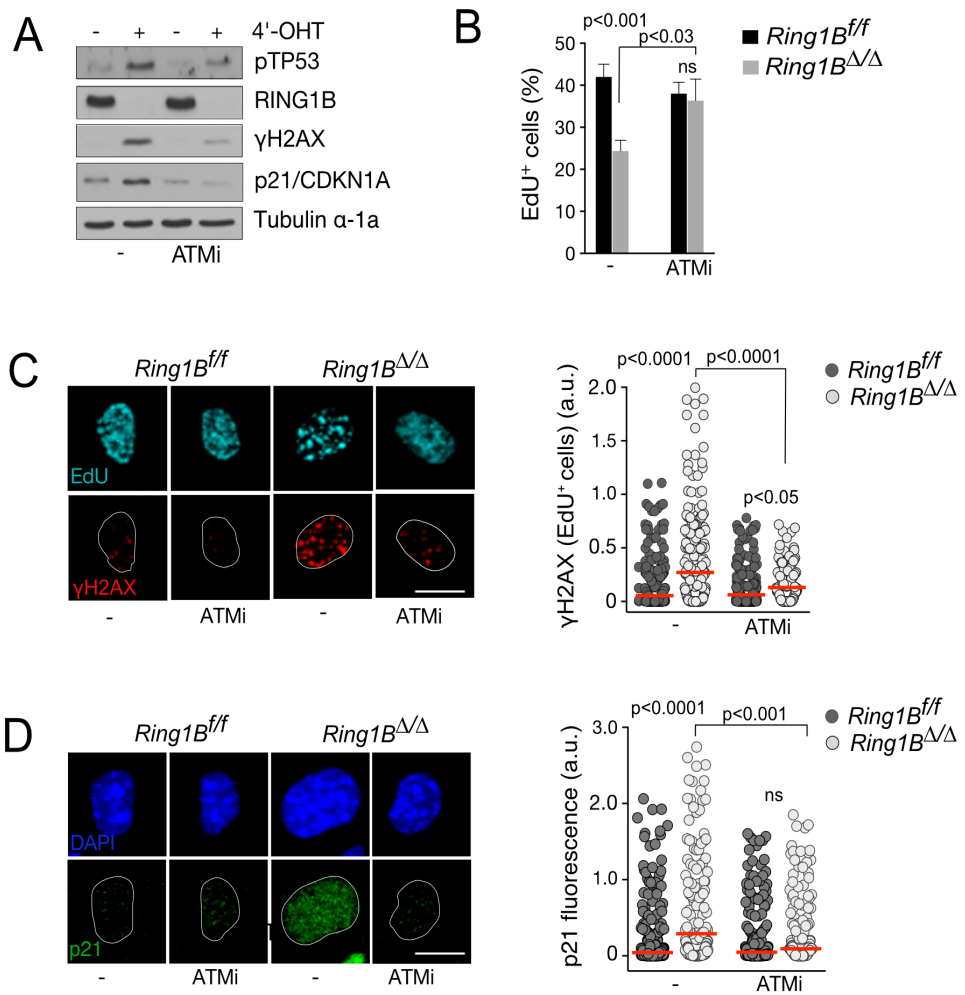

Figure R9. DNA damage activated ATM-P53-p21 DNA damage response (DDR) in RING1B-deficient NSCs (A) Western blotting showing phosphorylation of P53 (Serine15), H2Ax and increase in p21 levels in mutant culture. Treatment with ATM inhibitor (ATMi, KU55933 10μM, 2 hours) reduced phosphorylation of P53 and of H2Ax and levels of p21. Tubulin Alpha-1A chain was used as loading control **(B)** Proliferation rates: % of EdU-positive cells after a pulse of 10 minutes at day +4 after addition of EtOH or 4'-OHT (n=3) of *Ring1B$^{f/f}$* or *Ring1B$^{Δ/Δ}$* cells treated (ATMi), or not (-), with ATMi added just before EdU pulse. Bar charts show mean±s.d (n=3). **(C)** Left: Immunostaining of γH2AX in EdU+ nuclei of *Ring1B$^{f/f}$* and *Ring1B$^{Δ/Δ}$* NSCs treated or not with ATMi. Right: Scatter plot of γH2AX fluorescent intensity of EdU$^+$ cells treated, or not, with ATMi, showing a reduction of fluorescent intensity after ATMi treatment in mutant cells. **(D)** Left: Immunostaining of P21 of *Ring1B$^{f/f}$* and *Ring1B$^{Δ/Δ}$* NSCs treated or not with ATMi. Right: Scatter plot of p21 fluorescent intensity in control or mutant cells treated, or not, with ATMi. Scale bar=10 microns (C and D). Red bars show median values (C and D). At least 100 EdU$^+$ cells were analyzed in each experiment (C and D, n=3). p values were calculated using unpaired, two-tailed Student's t- (B), or Mann–Whitney U (C and D) tests. ns, not significant (P≥ 0.05).

3.3. ATR-dependent H2AX phosphorylation and RING1B-deficient NSCs proliferation

H2AX and P53 are common substrates of ATM and ATR kinase activity (Abraham, 2001; Adams et al., 2010). We thus look for a possible ATR activation in response to replication stress. We used a specific ATR inhibitor (ETP-46464) (Toledo et al., 2011) to verify the possible activation of ATR-P53-p21 pathway. As shown in Fig.R10 (left plot), fluorescent intensity of γH2Ax was clearly reduced in *Ring1B*$^{\Delta/\Delta}$, and also in control cells treated for two hours with the ETP-46464 (+ATRi) respect to DMSO (vehicle, -ATRi) treated cells. These data sustain a high basal level of γH2Ax in these cells due to ATR activity. Then we determined p21 levels in control and RING1B-deficient cells treated, or not, with ATRi. As shown in Fig.R10 (right plot), although to a lesser extent than without inhibiting ATR, p21 upregulation was still seen in mutant cells, suggesting a differential role of ATM and ATR in the DNA damage response in these cells. These results demonstrate that RING1B deficiency provokes DNA damage accumulation and subsequent DNA damage response involving ATM, P53 and p21 that results in a proliferative defect.

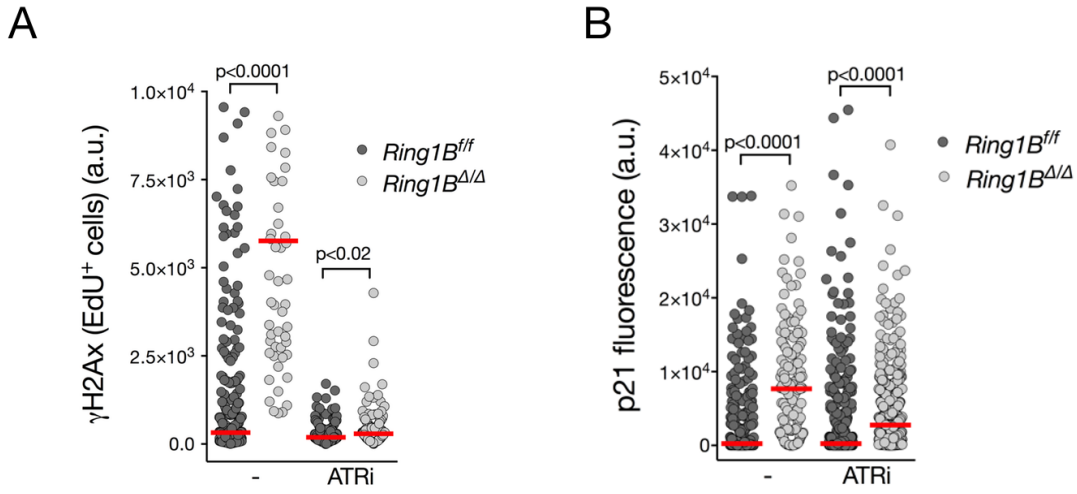

Figure R10. ATR kinase affects H2AX phosphorylation but not p21 expression (A) Scatter plot of γH2AX fluorescent intensity/EdU$^+$ of *Ring1B*$^{f/f}$ and *Ring1B*$^{\Delta/\Delta}$ NSCs treated, or not, with 10μM of ATR inhibitor (ATRi, ETP-46464) showing a reduction of fluorescent intensity of γH2AX of RING1B-deficient cells. **(B)** Scatter plot of p21 fluorescent intensity in control or mutant cells treated, or not, with ATRi. Red bars show median values. p values were calculated using unpaired Mann–Whitney U test.

4. RING1B and oxidative stress in neural stem cells

DNA damage response occurs during normal proliferation due to replication stress provoked by various endogenous and exogenous factors. RING1A and RING1B-mediated ubiquitylation of H2A is essential to deal with replication of pericentric heterochromatin, a source of potential endogenous replication stress, at least in fibroblasts (Bravo et al., 2015).
Among the sources of replication stress and DNA damage is the increase of reactive oxygen species (ROS) due to alterations of redox homeostasis mechanisms or external factors that facilitate their formation, such as ionizing radiations (i.e. UV exposure) or chemicals that increase the formation of free radicals (i.e carcinogens). (Ciccia & Elledge, 2010; Hoeijmakers, 2009; RichardWagner, 2013)

We asked whether RING1B could also be contributing to maintain a proper redox homeostasis to avoid a DNA damage response due to ROS-induced DNA damage

4.1. RING1B and Reactive Oxygen Species (ROS) accumulation

We asked if RING1B was related to ROS homeostasis that could contribute to set off DNA damage and DDR. We first analyzed accumulated ROS levels in control and RING1B-mutant NSCs using the cell permeant reagent 2',7'–dichlorofluorescin diacetate (DCFDA), a fluorogenic dye that measures hydroxyl, peroxyl and other reactive oxygen species (ROS) activity within the cell. As shown in Fig.R11, absence of RING1B resulted in 1.6 fold increase levels of ROS. We used *N*-acetyl-cysteine (NAC), a ROS scavenger, to reduce ROS levels. Treatment with 0.5mM of NAC during 3 days significantly reduced ROS levels in RING1B-deficient NSCs (Fig.R11, right charts).

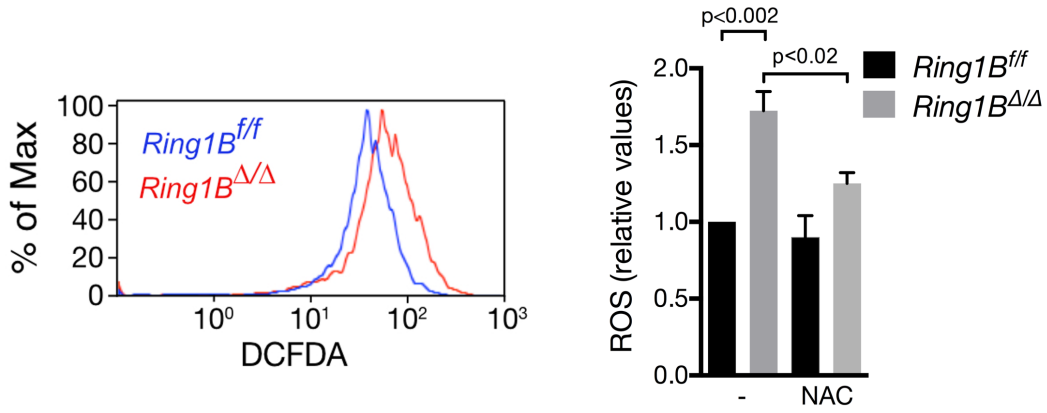

Figure R11. ROS levels increase in the absence of RING1B. Left: Representative flow cytometry histogram of ROS levels as assessed by DCFDA fluorescence in control and RING1B-deficient neural stem/progenitor cells. Right: DCFDA fluorescence intensity quantified as fluorescence intensity of *Ring1B$^{f/f}$* and *Ring1B$^{\Delta/\Delta}$* NSCs treated, or not, with *N*-acetyl-L-cysteine (NAC). Bar charts show mean±s.d (n=2) p values were calculated using unpaired, two-tailed Student's t test

These results indicate that ROS accumulate in the absence of RING1B.

4.2. Oxidative stress-related DNA Damage in RING1B-deficient NSCs.

One of the biggest hazards posed by oxidative stress is the generation of DNA damage and, in particular, DNA double-strand breaks (DSBs) (Hoeijmakers, 2009; Lombard et al., 2005) To determine if oxidative stress was the source of DNA damage accumulation in RING1B mutant NSCs we performed Western Blotting analysis to check phosphorylation of H2AX before and after treatment with antioxidant. The increase in γH2AX levels occurring in mutant cells was clearly reduced with antioxidant NAC treatment, with no changes in total H2A protein levels (Fig.R12A). Similarly, 53BP1 labeling at DSBs foci was dramatically reduced in NAC-treated RING1B-deficient culture (Fig.R12B and C). Number of 53BP1 foci per cell and percentage of 53BP1^{+} cells (i.e., with more than 3 foci per cell) were restored to levels similar to control cells.

These results reinforce the idea that it is the accumulation of ROS that drive DNA damage in RING1B-deficient NSCs.

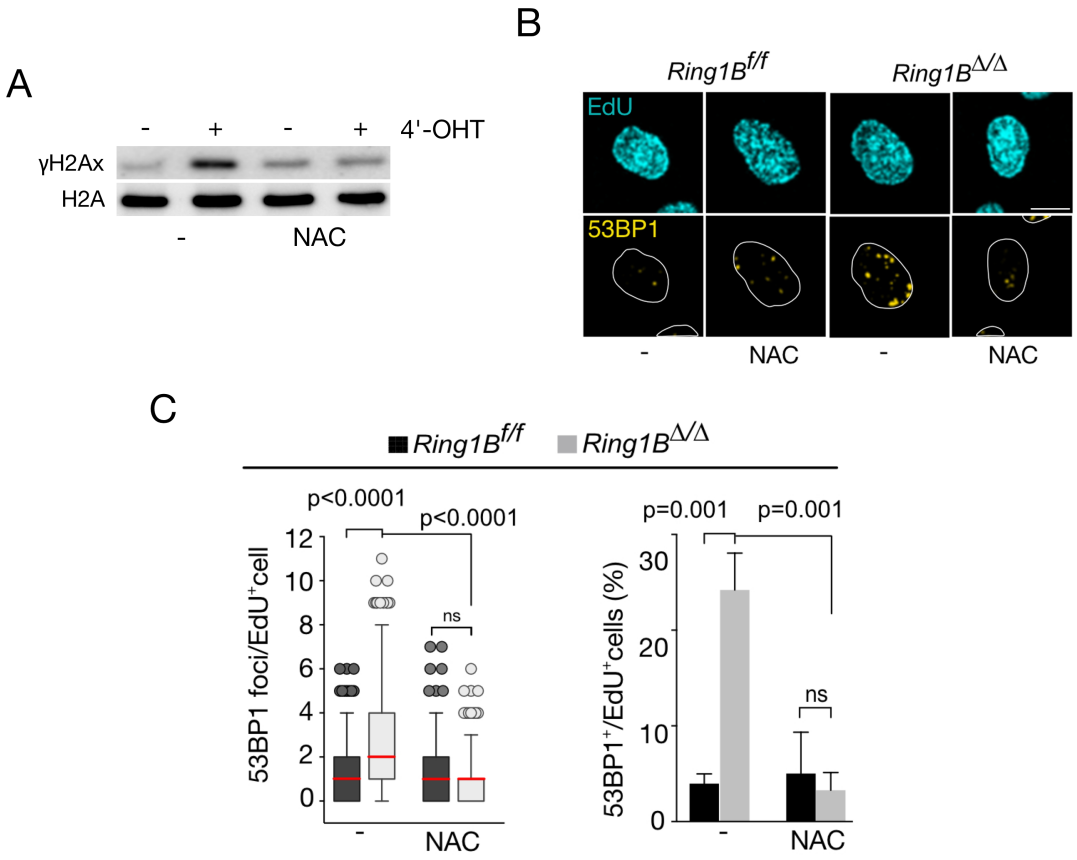

Figure R12. Antioxidant treatment reduced DNA damage accumulation in RING1B-mutant NSCs. (A) Western blotting showing phosphorylation of H2AX. Treatment with NAC reduced phosphorylation of H2AX. H2A was used as loading control **(B)** Immunostaining of 53BP1 in EdU$^+$ nuclei of *Ring1B$^{f/f}$* and *Ring1B$^{\Delta/\Delta}$* NSCs treated, or not, with NAC. Scale bar=100 microns **(C)** Left: Box plot (5-95 percentile) of number of 53BP1 foci/EdU$^+$ cell treated, or not, with NAC showing a reduction of DSBs (53BP1) in RING1B-deficient cells treated with NAC. Right: Bar charts showing the percentage of 53BP1 positive cells in mutant culture treated, or not, with antioxidant. Bar charts show mean±s.d (n=3). and red bars show median values. p values were calculated using unpaired, two-tailed Student's t-test (C, right), or Mann–Whitney U test (C, left). ns, not significant (P≥ 0.05).

4.3. Antioxidant treatment rescued proliferation defect of RING1B mutant neural stem cells

ROS-derived DSBs induces activation of ATM to active DNA repair, DNA damage response and cell cycle regulation. (Ditch & Paull, 2012; Z. Guo et al., 2010; Meter et al., 2016)

To determine if presence of ROS was linked to DNA damage response and the subsequent proliferative defect observed in RING1B mutant cells, we analyzed p21/CDKN1A fluorescent intensity in control and mutant cells treated (or not) with antioxidant for a period of 3 days. p21/CDKN1A expression was clearly reduced close to control levels (Fig.R13A). However, the increase in p16-INK4a levels that occurred as a consequence of RING1B deletion was still observed, despite NAC treatment of mutant cells (Fig.R13B). In these conditions of upregulation of p16-INK4a but normal levels of p21/CDKN1A the proliferative capacity of RING1B-deficient NSC was not compromised in the presence of NAC. Thus, EdU-incorporating rates of NAC-treated mutant cells equaled to those of control cells (Fig.R13C) and cultured RING1B-derived neurospheres achieved sizes comparable to control cells (Fig.R13D).

This results point at the increased levels of ROS as the first cause of impaired proliferation in RING1B-deficient NSCs.

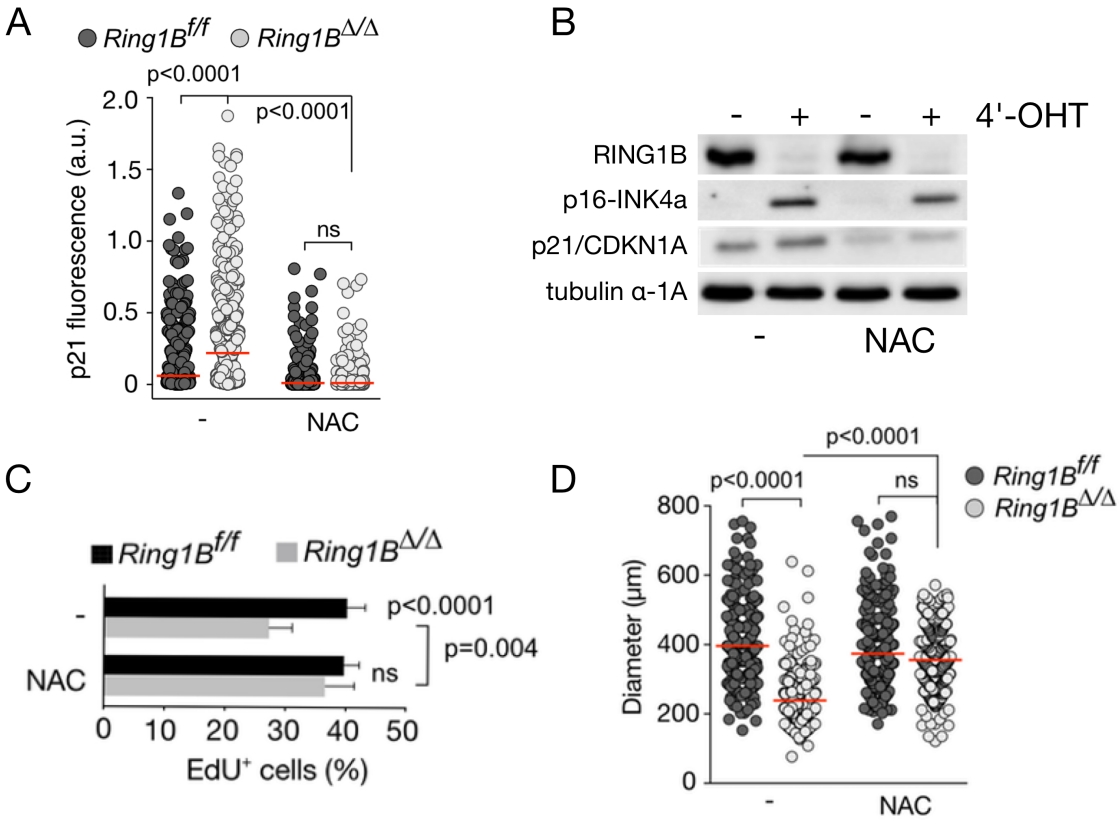

Figure R13. Proliferation of RING1B-deficient NSCs is restored with antioxidant treatment. **(A)** Scatter plot of p21/CDKN1A fluorescent intensity in control or mutant cells treated, or not, with NAC. **(B)** Western blotting showing that NAC treatment reduces p21/CDKN1A, but not the amount of p16-INK4a, in mutant cells. **(C)** Proliferation rates: percentage of EdU-positive cells after a pulse of 10 minutes, 96 hours after addition of 4'-OHT (n=3) of *Ring1B$^{f/f}$*, Cre-ER cells treated, or not, with 0.5mM NAC for 4 days. Bar charts show mean±s.d.. **(D)** Scatter plot (n=3) of neurospheres diameters showing that *Ring1B$^{Δ/Δ}$* spheres treated with antioxidants had a similar size respect to controls. Red bars show median values. p values were calculated using unpaired, two-tailed Student's t-test (C), or Mann–Whitney U test (A and D). ns, not significant (P≥ 0.05).

4.4. P38-MAPK pathway involvement in proliferation defect of RING1B deficient neural stem cells

p38-MAPK has been implicated in cell proliferation, differentiation, and survival of neural cells and is one of the signaling proteins induced in response to ROS (K. Sato, Hamanoue, & Takamatsu, 2008). We thus analyzed whether p38-MAPK would be an indirect manifestation of ROS accumulation in mutant cells. Western Blotting analysis showed no changes in p38-MAPK total levels, however its phosphorylated, active form increased in RING1B-mutant compared to normal cells. Such increase in p38-MAPK activation was clearly reduced by NAC treatment (Fig.R14A).

We wondered whether p38-MAPK pathway would be involved in determining the inhibition of RING1B-deficient NSCs proliferation.

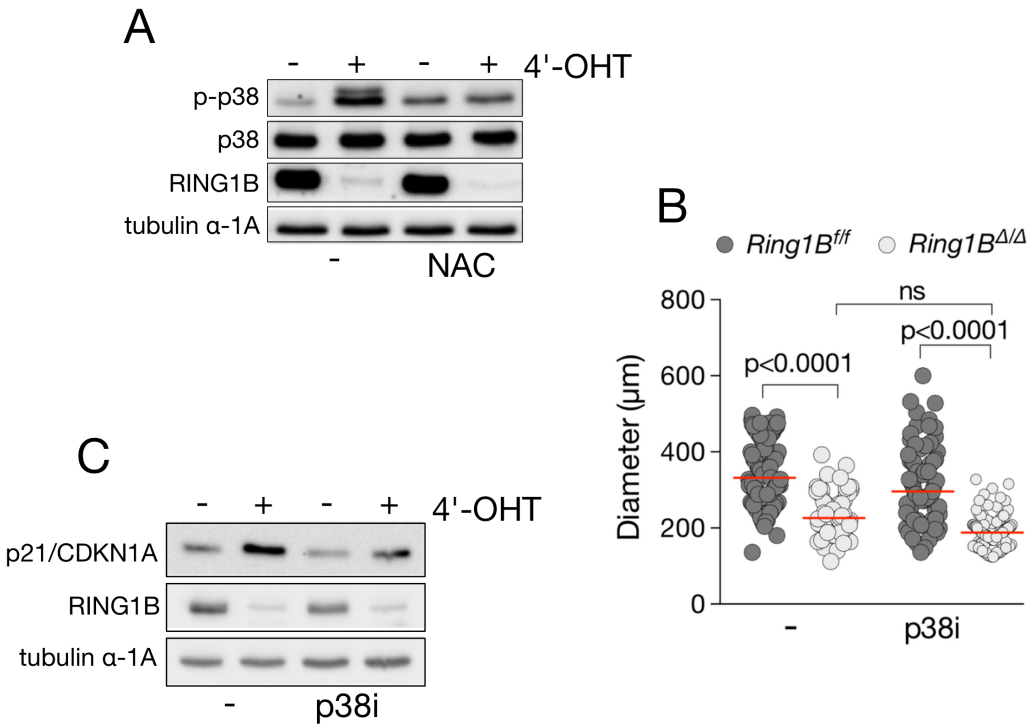

Figure R14. P38-MAPK inhibition does not restore proliferation of RING1B-deficient NSCs **(A)** Western blotting showing phosphorylation of p38-MAPK in mutant cells. Treatment with antioxidant reduced p38-MAPK phosphorylation **(B)** Scatter plot (n=3) of neurospheres diameters showing that RING1B-deficient spheres treated with p38 inhibitors were not able to restore proliferation. Red bars show median values. **(C)** Western blotting showing that p38 inhibitor treatment did not reduce p21/CDKN1A levels in mutant cells. p values were calculated using unpaired Mann–Whitney U test (B).

We cultured *Ring1B*$^{f/f}$ and *Ring1B*$^{\Delta/\Delta}$ neurospheres in the presence (+ p38i) or absence (-p38i) of SB203580, a selective inhibitor of p38-MAPK, previously described to improve neurospheres numbers and proliferation rate in primary cultures from mouse embryonic brain (K. Sato et al., 2008). Western blotting analysis performed with total protein extracts of neurosphere showed that p21 levels were still higher in *Ring1B*$^{\Delta/\Delta}$ cells respect *Ring1B*$^{f/f}$ when treated with p38 inhibitor (Fig.R14B, right blot). We then measured the neurospheres diameters but were unable to detect a rescue of proliferation in p38 inh.-treated RING1B-deficient NSCs (Fig.R14F). It thus seems that p38-MAPK kinase activity is not involved in the pathway leading to p21/CDKN1A upregulation and RING1B-deficient NSCs proliferation inhibition.

Altogether, these results show that increased oxidative stress is at the basis of the effect of RING1B loss in NSCs proliferation, as a consequence of induced DNA damage and activated DNA damage response via ATM/P53/p21 pathway but independently of p38-MAPK signaling.

5. RING1B role in self-renewal/differentiation balance of neural stem cells and its relation to oxidative stress.

Previous work in our laboratory had shown that inactivation of RING1B impaired proliferation and self-renewal and induced a premature differentiation toward neuronal (Román-Trufero et al., 2009). As shown up to this point, we had evidenced that RING1B was assuring NSCs proliferation through control of oxidative stress and of subsequent ATM/P53/p21 response to DNA damage, we asked whether these mechanisms were also at the base of RING1B control of NSCs self-renewal and differentiation.

5.1. ROS influence(s) on RING1B-depleted NSCs

We wished to determine the possible contribution of the increased oxidative stress of mutant NSCs on its reduced self-renewal capacity (Román-Trufero et al., 2009). To this end we used a well-established clonal analysis assay in which self-renewal is assessed as the frequency of cells that are able to form a neurosphere from a single cell. Two types of experiments were carried out (Fig.R15A). In the first one, *Ring1B$^{f/f}$* neurospheres received 4'-OHT or EtOH and the day after were dissociated into a single-cell suspension and seeded into 96-well plates. Duplicate cultures were set up with/without NAC. Wells that received a single cell were marked and followed during 10 days with daily additions of FGF-2 and EGF. In the second type of experiments (Fig.R15A), after 4'-OHT/EtOH treatment, cells received fresh medium and were let to grow neurospheres for four days. After desegregation into single cells, a clonal assay was performed as described above.

At the end of day 10, 96-well cultures were photographed to measure the diameter of neurospheres and wells containing neurospheres larger than 40μm scored as cultures derived from a self-renewing single cells. Panels B and C of figure R15 evidence how the addition of NAC rescues the size of primary mutant neurospheres and the frequency of cells with clonogenic capacity, both of which were reduced, compared to controls, after RING1B-depletion. Recovery, however, was far from total, although the differences did not score as statistically significant. On the contrary, mutant cultures seeded with cells grown for four days after RING1B-deletion, showed neurospheres of a severely diminished diameter whether in the absence/presence of NAC (Fig. R15E, left). In agreement with impaired

proliferation that resulted in small neurospheres, the proportion of wells containing single-cell derived neurospheres was also very much reduced (Fig.15D, right).

The results of both types of experiments then appear as contradictory. In the first case, cells seeded while reducing their levels of RING1B, if their levels of ROS are maintained in check with NAC acted almost as cells that express RING1B. In the second type of experiment, cultures rid of most cells containing any RING1B act as if few of them initiate clonal cultures but the small neurospheres soon arrest growth. The results, at a first glance, appear contradictory because NAC-quenching of ROS in single cells seeded at the beginning of RING1B depletion has an effect not seen with single cells already lacking RING1B. In other words, in the latter case, proliferation arrest may be taking place by other mechanisms than those induced by oxidative stress.

In summary, prevention of DNA-damage triggered breaks on proliferation of mutant cells can maintain their self-renewal capacity but only transiently.

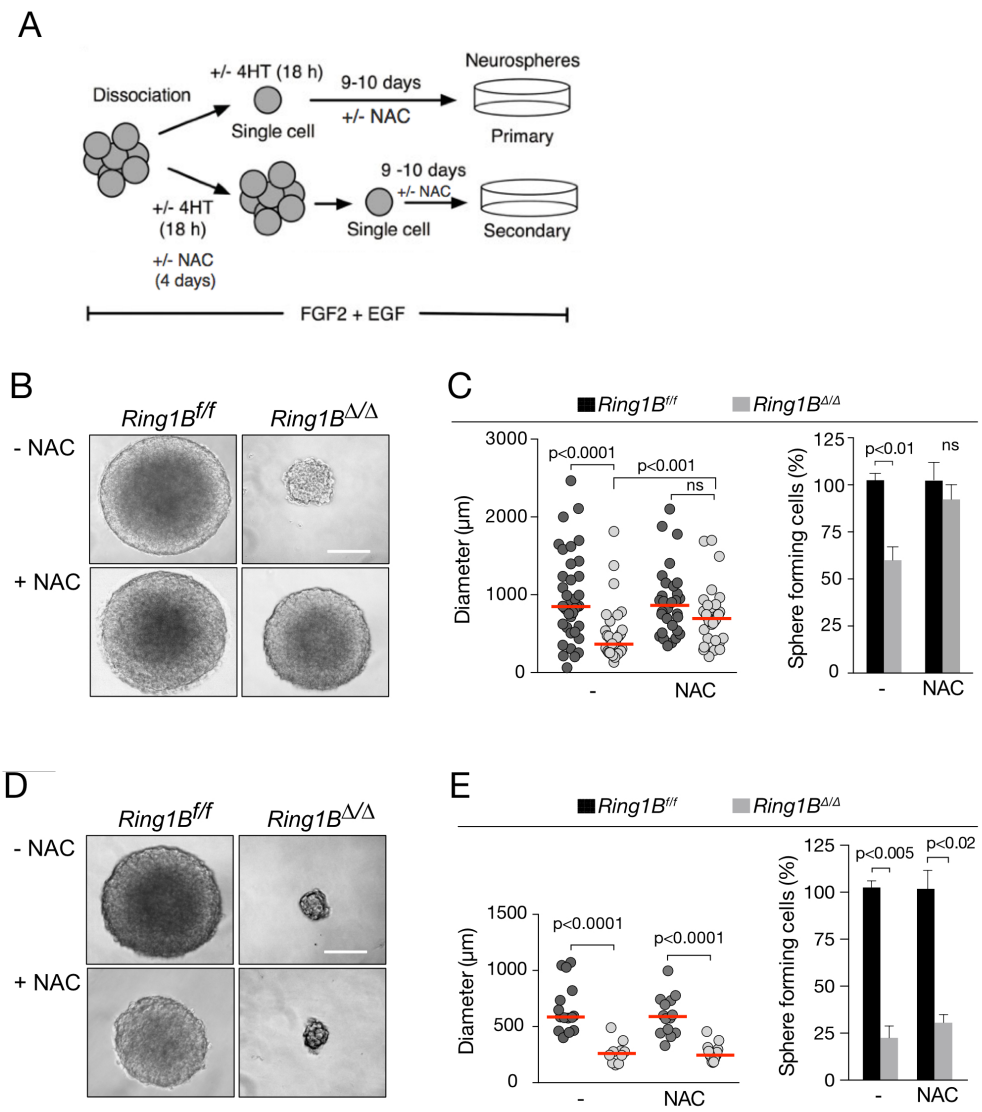

Figure R15. Transient rescue of decreased self-renewal of RING1B-deficient NSCs by antioxidant treatment. (A):Schematic diagram of clonal analysis protocols to obtain primary and secondary *Ring1B*$^{\Delta/\Delta}$ spheres. In the first protocol (upper), 4-hydroxy-tamoxifen (4HT) was added to the cultures 18 hours before plating single cells and sphere formation was scored after 9 days in culture in presence/absence of NAC (+/-NAC). In the second protocol (bottom), 4HT was added at the time of plating cells at a density of 5,000 cells/cm^2, to allow the formation of *Ring1B*$^{\Delta/\Delta}$ primary spheres growth in presence or absence of NAC (+/-NAC) for 4 days. At this point, mutant spheres cultured in presence of NAC displayed a restored proliferation as showed in fig. R13D. Then, primary spheres were disaggregated and plated as single cells in presence/absence of NAC. *Ring1B*$^{\Delta/\Delta}$ secondary sphere formation was also scored after 9 days in culture. (**B and D):** Phase-contrast images of representative primary **(B)** and secondary **(D)** single cell-derived neurospheres, at day+9 after cell seeding. Scale bar= 500 microns. (**C and E):** Left: Scatter plot of primary **(C)** and secondary **(E)** neurospheres diameters showing that NAC treatment significantly rescued primary *Ring1B*$^{\Delta/\Delta}$ spheres diameters (measure of proliferation) (n=2), but not rescue secondary *Ring1B*$^{\Delta/\Delta}$ neurosphere proliferation (n=2). Right: Relative values (% of respective control) of single cells forming primary (C) or secondary (E) spheres. Antioxidant treatment increased self-renewal ability of primary RING1B-mutant cells. Bar charts (C and E, right) show mean±s.d.. Red bars (C and E, left) show median values. p values were calculated using unpaired, two-tailed Student's t- (C and E, right), or Mann–Whitney U test (C and E, left) tests. ns, not significant (P> 0.05).

These data indicate that, despite a temporary beneficial effect of NAC on primary clonal and non-clonal RING1B-mutant neurospheres proliferation, RING1B role in maintained an undifferentiated state and self-renewal ability is dominant respect to ROS homeostasis, DNA damage and proliferation control. Probably, the poor expansion of secondary mutant neurospheres is due to the differentiation of a part of culture.

5.2. ROS-independent differentiation of *Ring1B*-mutant NSCs

We also tested whether premature, unscheduled neural differentiation of NSCs associated to the loss of RING1B (Román-Trufero et al., 2009) was influenced by ROS accumulation. We chose a couple of loci encoding two transcription factors involved in neurogenesis and neural identity, Eomes and NeuroD1, respectively, known to be derepressed in the absence of RING1B (Arnold et al., 2008; Boutin et al., 2010; Román-Trufero et al., 2009). Expression analysis, through Real time PCR of cDNAs derived from control and mutant cultures, grown with/without NAC during four days after beginning of inactivation, showed that derepression occurred to a similar extent for both of them (Fig. R16A). Thus, activation of differentiation program(s) in mutant cells seems independent of the concurrent accumulation of ROS. Further confirmation of this notion was the detection, in mutant cultures, of a neuronal-specific component of cytoskeleton (tubulin beta III) recognised by Tuj1 antibody. Figure R16B shows increased frequencies of Tuj1 +ve cells in mutant cultures, compared to controls, whether NAC is or not present in the medium.

We conclude that the altered balance of ROS in RING1B-deficient cells does not stimulate or slow down, within the period studied, the associated neuronal differentiation.

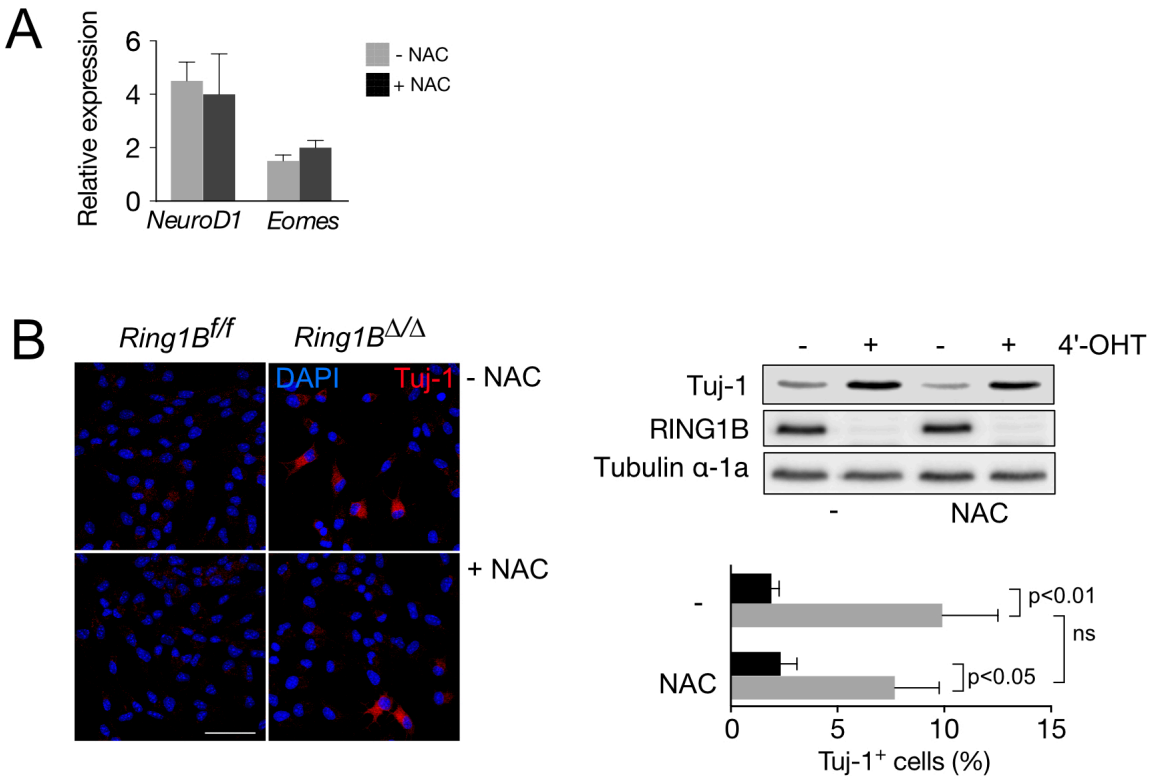

Figure R16. RING1B inhibited premature differentiation of neural stem cells independently of ROS. **(A)** qRT-PCR analysis for *Eomes* and *NeuroD1*. Changes in expression levels are displayed as the ratio between normalized (for β-actin expression) levels of select transcripts in RING1B-deficient and wild-type neurosphere cultures cultured with (+NAC) or without (-NAC) antioxidant. **(B)** Left: Immunostaining of neuronal differentiation marker Tuj-1 and DAPI in control and mutant neural stem cells grown in the presence of mitogens, treated, or not (-), with NAC. Scale bar=100 microns. Right: quantification (bottom, n=3) of Tuj-1$^+$ cells showing only partial decrease of neuronal differentiated (Tuj-1$^+$) mutant cells when cultured in presence of NAC. Bar charts show mean±s.d. Western blotting showing as antioxidant treatment does not impede differentiation of mutant cells p values were calculated using unpaired, two-tailed Student's t. ns, not significant (p>0.05).

.

6. BMI-1 stability is compromised in RING1B-deficient cells

As shown above, RING1B deficiency resulted in accumulated ROS levels and activation of DDR mainly via ATM/P53/p21 axis. BMI-1, another component of PRC1 complex and cofactor of RING1B E3 ligase activity, plays a crucial role in regulating cell cycle entry and self-renewal capacity, and has been described to control redox homeostasis and DNA damage repair in different cell types (Chatoo et al., 2009; Liu et al., 2009; Vissers Joseph H. A., 2012).

We asked whether these functions described for BMI-1 were related to those we had seen in NSCs as a result of RING1B loss.

We performed Western Blotting analysis to determine BMI-1 expression in NSCs. Surprisingly, BMI-1 was considerably downregulated in RING1B-mutant NSCs (Fig.R17A). However, RING1B paralog RING1A was upregulated. This indicated that RING1A was only able to partially compensate the effect of RING1B loss on BMI-1 levels.
To determine if this RING1B-elicited regulation of BMI-1 levels was cell-type specific or a more general phenotype, we performed similar analysis with mouse embryonic fibroblasts (mEFs) derived from the same floxed-RING1B; creERT mouse model from which we derived NSCs. Although to a lesser extent than in NSCs, BMI-1 was also downregulated in *Ring1B*$^{\Delta/\Delta}$ mEFs, and RING1A levels were higher than in control fibroblasts (Fig.R17A, right). This suggested that RING1B plays a role in the homeostasis not only of its paralog, but also of its cofactor. Moreover, this effect on BMI-1 levels seems RING1B specific, since RING1A knock-out did not determine BMI-1 downregulation, but on the contrary, resulted in a robust increase of its levels (Fig.R17A, right blots). However, similarly as RING1A levels increased in the absence of RING1B, RING1B levels increased in the absence of RING1A (Fig.R17A, right blot), suggesting a reciprocal, compensating effect on each other paralog, but a distinct, opposite effect on their cofactor accumulation, i.e. on BMI-1 bulk.

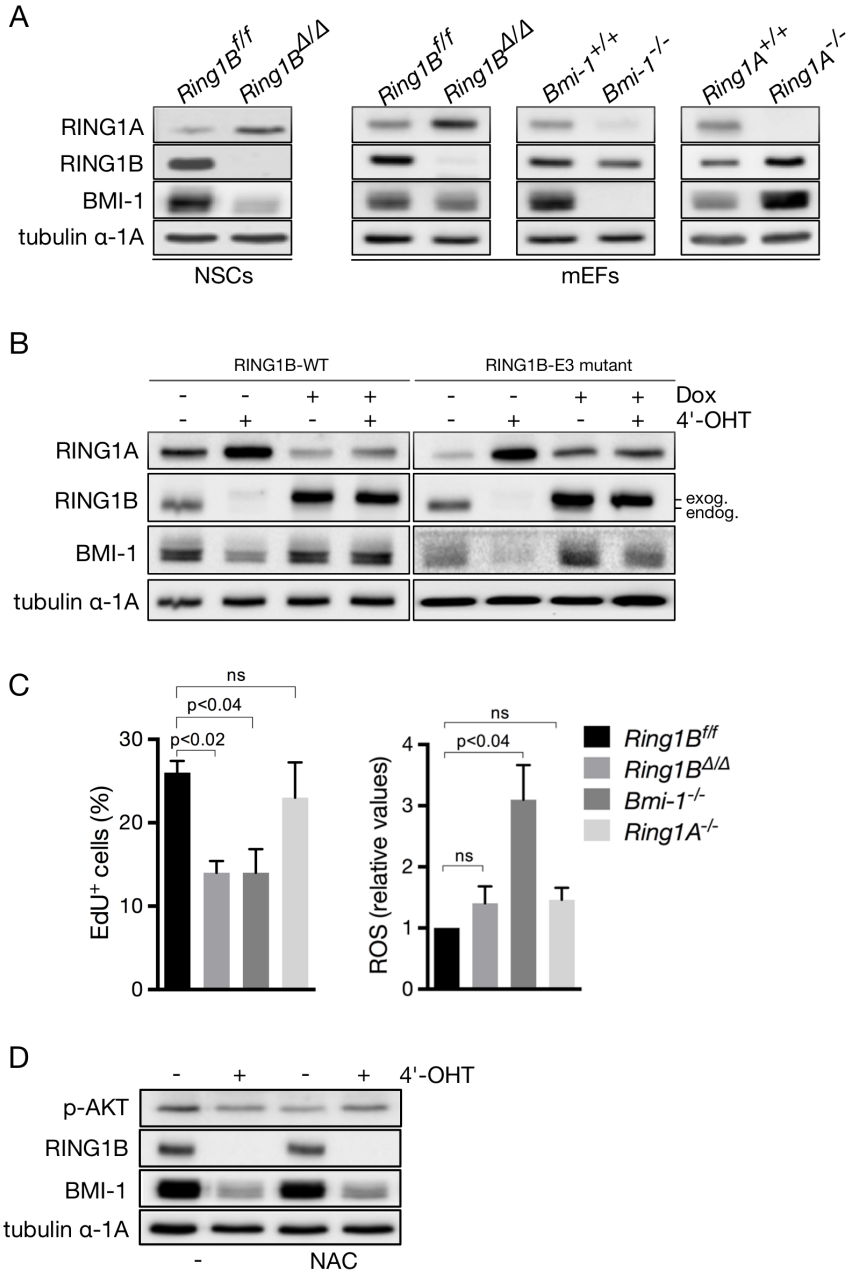

Figure R17. RING1B assures BMI-1 stability. (**A**) Western blotting analysis performed with neural stem cells (left, NSCs) or mouse embryonic fibroblasts (right, mEFs) with the indicated genotypes. (**B**) Western blotting of mEFs transduced with a doxycyclin-inducible lentiviral vector expressing a WT (RING1B-WT) or a E3 ligase mutant (RING1B-E3-mutant) performed at day+4 after treatment with EtOH/4'-OHT. Exogenous (Exog.) or endogenous (Endog.) forms of RING1B are indicated. (**C**) Left: Proliferation rates: % of EdU-positive cells after a pulse of 30 minutes at 96 hours after addition of 4'-OHT (n=2) of RING1B, BMI-1 or RING1A-deficient mEFs compared to *Ring1B$^{f/f}$* as control. Right: ROS levels assessed by DCFDA fluorescence in control and RING1B, BMI-1 or RING1A-deficient mEFs. Bar charts show mean±s.d.. p values were calculated using unpaired, two-tailed Student's t-test. (**D**) Western blotting analysis performed with control and RING1B-mutant neurospheres extracts, treated (+NAC), or not (-), with antioxidant. In Western blotting analysis, alpha-tubulin was used as loading control.

It would be possible that RING1B and BMI-1 also exerted reciprocal and specific effect on each other levels. We thus analyzed BMI-1 constitutively knocked-out mEFs. BMI-1 absence significantly affected RING1A, but only marginally RING1B levels (Fig.R17A, right), reinforcing the idea of RING1B specific control over BMI-1.

To determine if this effect was directly related to RING1B function ubiquitylating H2A, we reintroduced a wild type or an E3 ligase mutant form of RING1B by means of doxycycline-inducible lentiviral transduction. As shown in Fig.R17B, doxycycline treatment clearly induced the expression of RING1B-WT or RING1B-E3 mutant in transduced mEFs and compensated for endogenous RING1B protein loss after 4'-OHT treatment. Both WT or E3-mutant RING1B were able to stabilize BMI-1 and restore RING1A to control levels, indicating that BMI-1 and RING1A homeostasis are directly controlled by RING1B, independently of its E3-ligase activity.

To understand if RING1B loss affected proliferation and/or oxidative stress response in mEFs, as seen in NSCs, we performed EdU-incorporation assay and DCFDA (ROS)-analysis. We also analyzed mEFs derived from Bmi-1 and Ring1A KO embryos. As can be seen in Fig.R17C (left bar chart), *Ring1B*$^{\Delta/\Delta}$, and also *Bmi-1*$^{-/-}$, but not *Ring1A*$^{-/-}$ mEFs displayed a proliferation defect. However, only a modest increase in ROS levels was found after RING1B or RING1A loss (1.5-fold increase), whereas BMI-1 loss increased ROS up to 3-fold compared to control mEFs (Fig.R17C, right). This suggests a principal role of BMI-1 in redox homeostasis and that RING1B depletion-elicited phenotype might be due to BMI-1 downregulation, that even increased RING1A levels cannot counterbalance. The data also imply the crucial importance of RING1B integrity to assure BMI-1 pool.

In NSCs, it has been proposed that BMI-1 protein levels decrease could be a consequence of oxidative stress through activation of p38 MAPK pathway and AKT inhibition, with subsequent degradation of BMI-1 (Kim & Wong, 2009). We wondered if BMI-1 degradation observed in RING1B-deficient NSCs could be related to the presence of higher levels of ROS, and not the other way round as above hypothesized. Treatment with NAC (that rescued proliferation defect and DNA damage in Ring1B deficient NSCs) did not restore BMI-1 levels (Fig.R17D), despite the fact that AKT remained active, as indicated by maintained levels of phosphorylated, p-AKT. Altogether, the results show that BMI-1 stability is strictly dependent on the presence of RING1B in both NSCs and mEFs, probably to assure an efficient response to oxidative stress.

6.1. Partial rescue of RING1B-deficient NSCs proliferation defect by overexpression of BMI-1

To determine if the phenotype observed after RING1B loss in NSCs was due, at least in part, to BMI-1 degradation, we transduced NSCs with a doxycycline-inducible lentiviral vector to

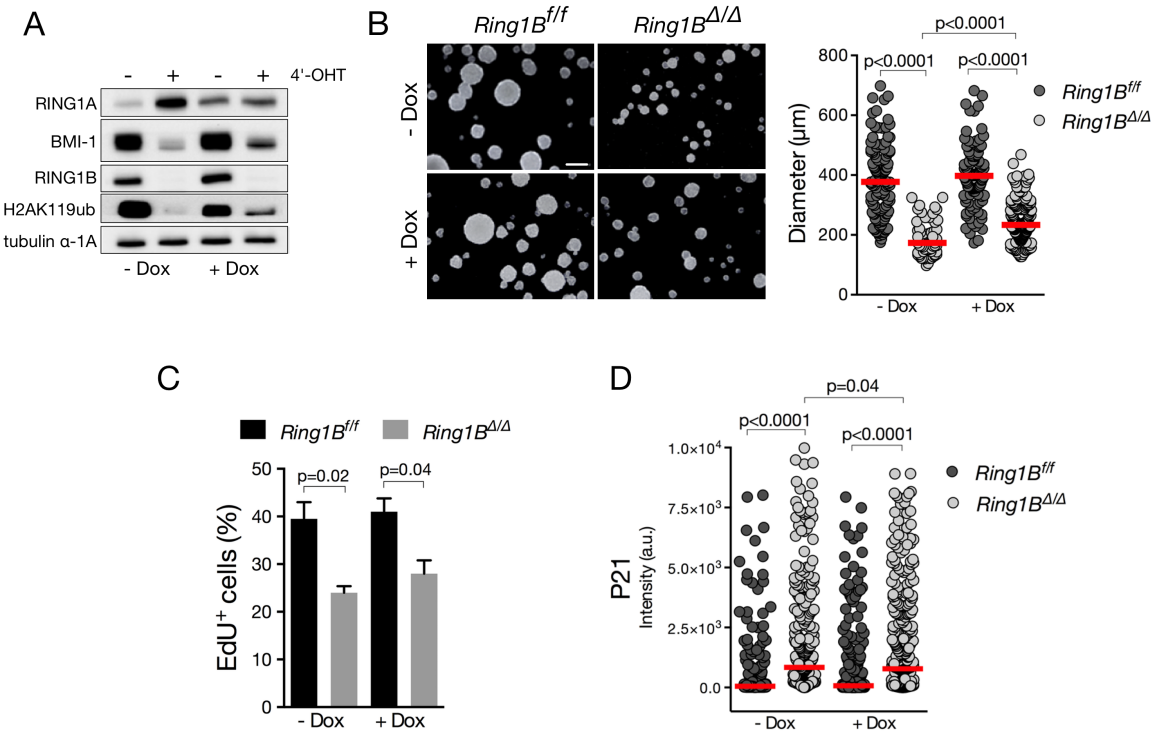

Figure R18. Overexpression of BMI-1 in RING1B-mutant neural stem cells partially rescued proliferation defect. **(A)** Western blotting analysis performed with neural stem cells transduced with a doxycycline-inducible lentiviral vector expressing BMI-1 (-/+ Dox) and selected with puromycin treatment for 4 days. RIPA protein extracts were performed at day +4 after EtOH/4'-OHT treatment to induced *Ring1B* recombination. **(B)** Representative photographs of *Ring1B$^{f/f}$* or *Ring1B$^{Δ/Δ}$* neurosphere cultures transduced with doxycycline-inducible lentiviral vector expressing BMI-1, cultured in presence (+) or not (-) of doxycycline, Right: Scatter plot of neurospheres diameters showing that BMI-1 overexpression (+Dox) partially restore RING1B-mutant neurospheres diameters. At least 200 neurosphere diameters were analyzed in each experiment (n=2). Red bars show median values. Scale bar=400 microns. **(C)** Proliferation rates: percentage of EdU-positive cells after a pulse of 10 minutes, 96 hours after addition of EtOH/4'-OHT (n=2) of monolayer cultures previously transduced with doxycycline-inducible lentiviral vector expressing BMI-1 (-/+ Dox). Bar charts show mean±s.d.. **(D)** Scatter plot of p21 fluorescent intensity in control or mutant cells previously transduced with doxycycline-inducible lentiviral vector expressing BMI-1 (-/+ Dox). p values were calculated using unpaired, two-tailed

express BMI-1 (gain-of-function assay).

We found that exogenous BMI-1 stability was compromised in RING1B-deficient NSCs to a similar extent as the endogenous protein (Fig.R18A). However, BMI-1 levels increased in both *Ring1B$^{f/f}$* and *Ring1B$^{\Delta/\Delta}$* cells cultured in the presence of doxycycline almost twice as, much endogenous levels in untreated control and mutant cells. As expected, H2AK119ub levels increased after BMI-1 over-expression and RING1A levels were comparable to those in control cells. We observed a modest, but only partial, recovery of proliferation measured as neurospheres diameters (Fig.R18B) and EdU-incorporation (Fig.R18D). Nonetheless, a statistically significant difference was still present between *Ring1B$^{f/f}$* and *Ring1B$^{\Delta/\Delta}$* NSCs, despite BMI-1 over-expression. As could be expected according to impaired proliferation, p21/CDKN1A levels remained higher in RING1B-mutant cells also even though BMI-1 amount was partially recovered (Fig.R18C).

Altogether, the data suggest that RING1B assures, at least in part, redox homeostasis and proliferation of NSCs by stabilizing its co-factor BMI-1.

Discussion

In this work we find that the major cause of proliferation arrest of RING1B-depleted NSCs is caused by a DNA damage response, in turn triggered by an accumulation of ROS products. The proposed chain of events, leading to proliferation arrest in RING1B-deficient NSCs, starts with an imbalance of ROS products, a condition favorable to DNA damage, enhanced perhaps by defective repair in the absence of RING1B, which triggers the well known ATM-P53-p21/CDKN1A pathway activated under stress conditions. Considering the possible involvement of BMI-1 in the regulation of ROS homeostasis in NSCs, RING1B function in ROS homeostasis appears inexorably linked to that of BMI-1 because of its destabilization in the absence of RING1B. Differentiation towards a neuronal pathway associated to RING1B depletion, however, is independent of RING1B-dependent proliferation status. Thus, levels of heterodimeric E3 ligase RING1-BMI-1 are critical to prevent DNA damage hindering NSCs expansion. In this function RING1B appears in a dominant position within its epistatic relationship with BMI-1.

1. RING1B role in proliferation, an indirect consequence of the activation of ATM/P53/p21 DNA damage response pathway.

Our experiments show that P21/CDKN1A, but not p16-INK4a, is the main CDKI that mediates the proliferative defect of RING1B-deficient NSCs. KO of *Cdkn2a/Ink4a*, a well-known Polycomb target locus, (Bracken et al., 2007; Calés et al., 2008; Jacobs et al., 1999; Maertens et al., 2009) is insufficient to rescue the proliferation defect in RING1B-deficient NSCs. This p16-INK4a-independent RING1B function is reminiscent of what happens in other settings, e.g lethality of RING1B-deficient embryos not rescued in *Cdkn2a/Ink4a* KO mice (Voncken et al., 2003) or the cooperation between mutations in *Ring1B* and *Cdkn2a/Ink4a* in myeloid progenitors expansion (Calés et al., 2008).

Upregulation of CDK inhibitor p21/CDKN1A, concomitant to RING1B inactivation, had been observed by us and others in different cell systems (Bravo et al., 2015; Koike et al., 2014). Knockdown of *Bmi-1* also induces p21/CDKN1A upregulation in NSCs (Fasano et al., 2007) thus indicating a clear relationship between RING1B/BMI-1 and p21/CDKN1A. Such a correspondence, however, is incomplete because in our cultures of *Ring1B* KO NSCs

we have not detected the increased apoptotic rates associated to NSCs *Bmi-1* knock down (Fasano et al., 2007).

Upregulation of p21/CDKN1A could be interpreted as the consequence of the removal of a transcriptional repression exerted by PRC1. However, chromatin immunoprecipitation experiments from our lab did not show RING1B association to *p21/Cdkn1a* promoter proximal regions (Román-Trufero et al., 2009), making difficult to sustain a repressive function being relieved in the absence of RING1B. Instead, we found that it is the activation of P53, a quintessential positive regulator of *p21/Cdkn1a* the influence responsible for its upregulation. In agreement with this, other targets of P53 (*Trp53inp*, *Bid*) were also found upregulated in RING1B-deficient NSCs (Román-Trufero et al., 2009),

P53 activation, in turn, is the consequence of NSCs cells triggering DDR. Following RING1B deficiency, foci of phosphorylated of histone H2AX and 53BP1, two well established markers of of DSBs (Balajee & Geard, 2004; Wang et al., 2002)) accumulate in mutant cells. These changes at places of DSB, activate a complex pathway for DNA repair and, as stated above, relay on the activation of ATM kinase, which among its many substrates (S139 of H2AX phosphorylation only one of them) has P53, again one of the steps leading to its activation as transcriptional regulator (Lakin & Jackson, 1999; Maréchal & Zou, 2013; Sulli, Di Micco, & di Fagagna, 2012)

Indeed, inhibition of ATM activity (ATM inhibitor treatment) in mutant NSCs blocks, P53 and H2AX phosphorylation, p21/CDKN1A decreases to basal levels and proliferation arrest of RING1B-deficient NSCs does not occur. The results are coherent with the rescue of proliferation arrest of mutant NSCs bearing null alleles of *p21/Cdkn1a* or *Tp53* genes. The close relationship between p21/CDKN1A and P53 in stressed NSCs is clear and had already been shown with irradiated NSCs which, if deficient in P53, cannot express p21/CDKN1A (Armesilla-Diaz et al., 2009). Altogether, we believe that proliferation arrest, a quick response to RING1B depletion, is the consequence of a DDR-related pathway which does not involve possible functions in transcriptional repression, at later stages in a senescent state, of genes encoding other cell cycle regulators may be derepressed.

1.1. Is DDR impaired in the absence of RING1B?

Increased signs of DNA damage (γH2AX and 53BP1 foci, marking DSBs) in RING1B-deficient NSCs relates clearly to oxidative stress. However, the persistence of DSBs foci may also be a signal of impairment of DNA repair functions. This may come as no surprise given the large body of evidence implying both RING1B and BMI-1 in the repair of irradiation-induced DNA breaks (Bergink et al., 2006; Ginjala et al., 2011; H. Ismail et al., 2010; Pan, Peng, Hungs, & Lin, 2011; Vissers Joseph H. A., 2012).A difference, though, is that in our system DNA damage arises spontaneously, without exogenous perturbation. DNA damage related to oxidative stress is thought to derive from replication of DNA structures altered by oxidation leading, perhaps, to replication blocks (Burhans & Weinberger, 2007; Lindahl, 1993; Woodbine et al., 2011). Our data fit this interpretation as the accumulation of DSB foci correlates with the ability of mutant cells to incorporate EdU. At this stage, DNA damage secondary to oxidative stress would be equivalent to the breaks induced upon irradiation, a situation in which contributions of RING1B and BMI-1 have been probed necessary ((Ginjala et al., 2011; Ismail et al., 2010; Pan et al., 2011; Ui et al., 2015). The participation of Polycomb E3 ligases in DSB repair using its activity to monoubiquitylate histones H2A and H2AX has been inferred from radiation-induced DNA breaks, many of which would take place on G1, i.e. non replicating cells (Ginjala et al., 2011; I. H. Ismail et al., 2012). It could be assumed that histone H2A modifications may also be required for DSB appearing during S-phase and therefore, the very low E3 ligase activity of mutant cells, despite their increased levels in RING1A, would imply that a similar DNA repair functionality is missing in RING1B-deficient NSCs. This in an assumption ease to subject to experimental test by ectopic expression of a E3 ligase inert form of RING1B.

1.2. RING1B management of oxidative stress

Why loss of RING1B could end up in DNA damage? We and others have appreciated a function of RING1B (particularly together with RING1A) during DNA replication (Bravo et al., 2015; Piunti et al., 2014), preventing fork stalling and associated accumulation of DSB. We have not attempted to get direct evidence of replicative stress on DNA fibers (molecular combing experiments) on the basis that such a replication defect is associated to the combined inactivation of both RING1A and RING1B and, therefore, we consider it a less likely possibility. The possibility of an alternative source of DNA damage, that triggered by

an accumulation of ROS was not as clear as it might have appeared from initial reports on *Bmi-1* KO-hematopoietic cells. Instead, in NSCs and neurons oxidative stress occurs both under gain-of and loss-of BMI-1 function (Acquati et al., 2013; Chatoo et al., 2009). Oxidative stress comes as an imbalance between ROS and cellular anti-oxidant defenses (Lombard et al., 2005)). ROS can cause lipid peroxidation, protein damage, and several types of DNA lesions: single- and double-strand breaks, adducts (as 8-oxoguanine (8-oxoG)) and cross-links (Lindahl, 1993; RichardWagner, 2013). SSBs or DSBs normally are thought to occur arise when replicative (and also transcription) machinery encounters endogenous ROS-induced lesions (Burhans & Weinberger, 2007; Lindahl, 1993; Woodbine et al., 2011).

Our observation of increased ROS products in *Ring1B*-mutant NSCs, however, suggested that, after all, it was possible that as a consequence of their accumulation some DNA damage might occur. Indeed, the addition of a ROS scavenger, such as NAC to the cultures, prevented the development of DSB foci and proliferation arrest, thus linking alterations in ROS homeostasis with proliferation status in NSCs depleted of RING1B. However, when considering the anti-proliferative consequences of ROS accumulation, we stand on our conclusion that the major player involved is p21/CDK21A, despite precedents linking p16-INK4a upregulation to ROS-induced activation of p38-MAPK. Reports on hematopoietic and skin cells showed a clear antiproliferative response associated to increased ROS (Jenkins et al., 2011; K. Sato et al., 2008; Shao et al., 2011) but in our system p38-MAPK inhibition failed to rescue RING1B-induced senescence.

How RING1B may participate in ROS homeostasis is not clear. A very first idea, that the expression of genes encoding anti-oxidant products was affected was ruled out from our analysis showing no evidence of altered levels of mRNAs encoding products with a role in ROS homeostasis (Román-Trufero et al., 2009). Although loss-of-BMI-1 function in NSCs also failed to show alterations in these mRNAs (Fasano et al., 2007), of known this contrasts with deregulation of some of these products in *Bmi-1* KO neurons and thymocytes ((Chatoo et al., 2009; Liu et al., 2009)). In this regard, our *Bmi-1* KO mEFs also showed ROS accumulation.

2. RING1B-BMI-1 stabilization

The inability of RING1A to substitute for RING1B and act as an E3 ligase in mutant NSCs could be due to the downregulation of BMI-1. In vitro, RING1B and RING1A show E3 ligase activity on nucleosomal substrates upon heterodimerization with any of the members of the PCGF family (Taherbhoy et al., 2015). Therefore it could have been expected that any of the other of the PCGF members in NSCs could substitute for BMI-1. However, proteomic analysis of neural progenitors suggest that it is BMI-1 the major PCGF that associates to RING1B (Kloet et al., 2016) perhaps because either levels of other PCGFs are low or their hypothetical association to RING1A in vivo differs from what is observed in vitro. One way or another we determined that the outcome is one in which global levels of H2AUb are very low in *Ring1B* mutant NSCs.

Downregulation of BMI-1 in the absence of RING1B is also seen in ES cells ((Leeb & Wutz, 2007)) and at a much lower extent in mEFs. It is possible then that the mechanisms involved in the positive regulation of BMI-1 by RING1B are cell type-specific. In NSCs, at least, such mechanism(s) are unrelated to transcriptional control because decreased protein level is not accompanied by a reduction in *BMI-1* mRNA (Román-Trufero et al., 2009). It is likely that events related to ubiquitylation of BMI-1, by other protein ligases than RING1B are involved (Ben-Saadon et al, 2006) and that RING1B, perhaps by forming a complex with BMI-1 interferes with such a destructive modification. Another example of PCGF stabilization by RING1B was seen in the co-transfection of plasmids expressing PCGF1 together with increasing amounts of a plasmid expressing RING1B (Sánchez et al., 2007). Whether a reciprocal effect, that the PCGF partner, i.e. BMI-1 has a positive effect on RING1B (or RING1A) stability is another possibility implied by the notion of a reinforced steadiness linked to their association. In agree with this, we observed a partial decrease of RING1B, and clear downregulation of RING1A, in *Bmi-1* KO mEFs.

An alternative possibility to regulate Polycomb RING finger proteins is through the activity of deubiquitinases such as USP7 (Maertens et al., 2010). USP7 associates with RING1B-containing complexes (Sánchez et al., 2007) and binds directly to BMI-1 (and MEL18) (Maertens et al., 2010). It is not clear how the regulatory hierarchy is, whether USP7 function can take place independently of RING1B or not. If a direct contact with BMI-1 would be everything that was necessary for its USP7-dependent stabilization then it might not be affected by RING1B depletion. However, being parallel, the depletion of both RING1B and BMI-1 in *Ring1B*$^{-/-}$ NSCs, it would appear more likely that perhaps the USP7-

BMI-1 contact was dependent on the heterodimer (with RING1B) and that not being in place, UPS7 fails to deubiquitylate BMI-1.

3. In NSCs, RING1B independently regulates self-renewal/differentiation balance and proliferation.

NSCs proliferate while maintaining their undifferentiated state thanks to signalling pathways that mediate the actions of growth factors FGF and EGF. The transcriptional program responsible for the maintenance of this cell state depends, in part, of chromatin regulators such as Polycomb RING1B. Following its inactivation, NSCs become conducive to senescence and neuronal differentiation which together lead to severe loss of its original self-renewal capacity. Thus, in RING1B-depleted NSCs, a possible link between ROS-induced DNA-damage, subsequent proliferative arrest, self-renewal loss and differentiation could be established. In fact, in other cell types such as skin or hematopoietic cells, the relationship between differentiation and DNA damage is clear (Santos et al., 2014; Sherman et al., 2011; Tedeschi & Di Giovanni, 2009). However, our data indicate that such links are rather cell type/context-specific, because neuronal differentiation, in our system, can be uncoupled from the DNA-damage response triggered by ROS accumulation. The manipulation of ROS levels in our system, using NAC, leads to an amelioration of the symptoms of self-renewal but once differentiation is set in motion it seems clear that no remedy related to ROS will prevent self-renewal capacity from being lost in the absence of RING1B.

Thus, although proliferation arrest can only imply self-renewal loss (certainly, not renewing in the absence of proliferation) the truly underlying cause appears more a consequence of ROS-independent differentiation.

As a way of summary, the cartoon in Fig.D1 shows a simplified representation of pathways regulated by RING1B (and BMI-1) in NSCs with an emphasis in proliferation control and the effects of the DDR activated by oxidative stress when cells are depleted of RING1B.

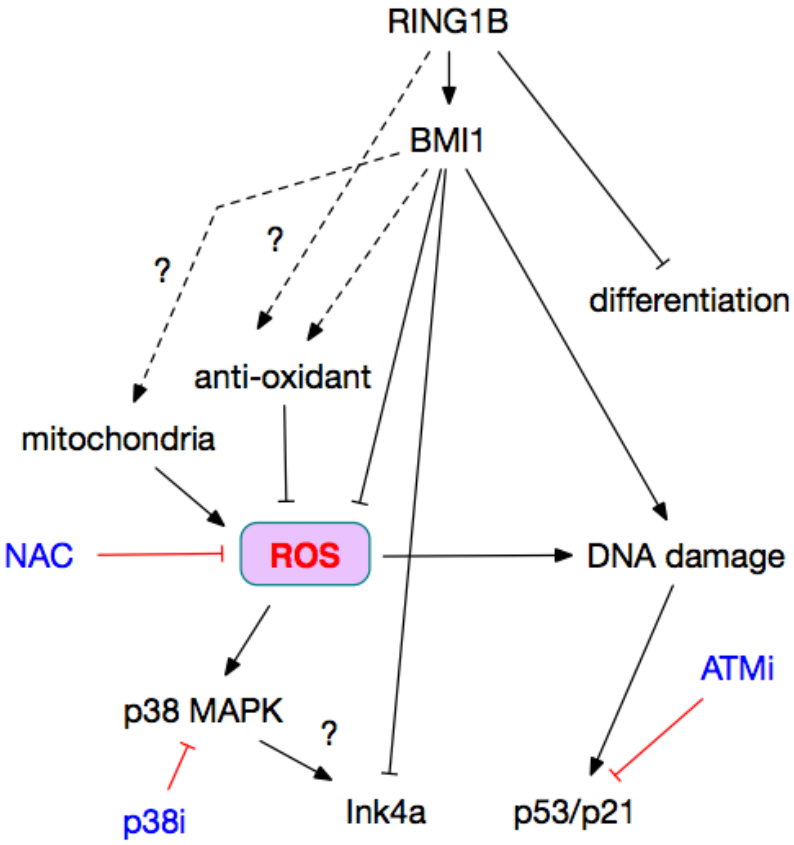

Figure D1. The model highlights pathways regulated by RING1B (and BMI-1) in NSCs

Conclusions

Conclusions

1) RING1B deficiency induces a drastic proliferation defect in neural stem cells mediated by upregulation of cell cycle inhibitor p21/CDKN1A

2) Loss of RING1B results in an accumulation of endogenous DSBs that activate a DNA damage response (DDR) involving ATM activation, P53 phosphorylation and p21/CDKN1A upregulation

3) RING1B participates in redox homeostasis. High levels of ROS damage DNA and activate DDR in RING1B-deficient neural stem cells

4) RING1B role in self-renewal and differentiation balance is independent from proliferation and cell cycle progression

5) RING1B assures BMI-1 stability in neural stem cells. In mEFs, RING1B stabilizing effect on BMI-1 is independent of the E3 ligase activity.

Conclusiones

Conclusiones

1) La ausencia de RING1B produce un drástico arresto proliferativo como consecuencia de una upregulación de p21/CDKN1A en células madres neurales

2) La falta de RING1B provoca una acumulación de roturas a doble cadenas endógenas que activan una respuesta a daño a DNA mediado por ATM, que induce la fosforilación de P53 y la upregulación de p21/CDKN1A

3) RING1B participa en la homeostasis oxidativa en cuanto, en ausencia de RING1B, se acumulan elevados niveles de Especie Reactiva del Oxigeno que dañan al ADN y activan una respuesta de daño a ADN.

4) El papel de RING1B en el balance entre autorenovacción y diferenciación es independiente de la proliferación y de la progresión del ciclo celular

5) RING1B garantiza la estabilidad de su cofactor BMI-1 en células madre neurales. En los fibroblastos embrionario de ratón el efecto estabilizador sobre BMI-1 es independiente de su actividad E3 ligasa

Bibliography

Abbas, T., & Dutta, A. (2009). P21 in Cancer: Intricate Networks and Multiple Activities. *Nature Reviews Cancer*, *9*(6), 400–414. https://doi.org/10.1038/nrc2657

Abraham, R. T. (2001). cell cycle checkpoint signaling therough the ATM an ATR kinases.pdf. *Genes & Development*, *15*, 2177–2196. https://doi.org/10.1101/gad.914401.DNA

Acquati, S., Greco, A., Licastro, D., Bhagat, H., Ceric, D., Rossini, Z., … Marino, S. (2013). Epigenetic regulation of survivin by Bmi1 is cell type specific during corticogenesis and in gliomas. *Stem Cells*, *31*(1), 190–202. https://doi.org/10.1002/stem.1274

Adams, B. R., Golding, S. E., Rao, R. R., & Valerie, K. (2010). Dynamic dependence on ATR and ATM for double-Strand break repair in human embryonic stem cells and neural descendants. *PLoS ONE*, *5*(4). https://doi.org/10.1371/journal.pone.0010001

Alabert, C., & Groth, A. (2012). Chromatin replication and epigenome maintenance. *Nature Rev MCB*, *13*(3), 153–167. https://doi.org/10.1038/nrm3288

Aranda, S., Mas, G., & Di Croce, L. (2015). Regulation of gene transcription by Polycomb proteins. *Science Advances*, *1*(11), e1500737. https://doi.org/10.1126/sciadv.1500737

Armesilla-Diaz, A., Bragado, P., del Valle, I., Cuevas, E., Lazaro, I., Martin, C., … Silva, A. (2009). P53 Regulates the Self-Renewal and Differentiation of Neural Precursors. *Neuroscience*, *158*(4), 1378–1389. https://doi.org/10.1016/j.neuroscience.2008.10.052

Arnold, S. J., Huang, G., Cheung, A. F. P., Era, T., Nishikawa, S., Bikoff, E. K., … Groszer, M. (2008). The T-box transcription factor Eomes / Tbr2 regulates neurogenesis in the cortical subventricular zone The T-box transcription factor Eomes / Tbr2 regulates neurogenesis in the cortical subventricular zone. *Genes Dev*, *22*(18), 2479–2484. https://doi.org/10.1101/gad.475408

Azuara, V., Perry, P., Sauer, S., Spivakov, M., Jørgensen, H. F., John, R. M., … Fisher, A. G. (2006). Chromatin signatures of pluripotent cell lines. *Nature Cell Biology*, *8*(5), 532–8. https://doi.org/10.1038/ncb1403

Balajee, A. S., & Geard, C. R. (2004). Replication protein a and ??-H2AX foci assembly is triggered by cellular response to DNA double-strand breaks. *Experimental Cell Research*, *300*(2), 320–334. https://doi.org/10.1016/j.yexcr.2004.07.022

Banerjee Mustafi, S., Aznar, N., Dwivedi, S. K. D., Chakraborty, P. K., Basak, R., Mukherjee, P., … Bhattacharya, R. (2016). Mitochondrial BMI1 maintains bioenergetic homeostasis in cells. *The FASEB Journal*, *30*(14), 4042–4055. https://doi.org/10.1096/fj.201600321R

Ben-Saadon, R., Zaaroor, D., Ziv, T., & Ciechanover, A. (2006). The Polycomb Protein Ring1B Generates Self Atypical Mixed Ubiquitin Chains Required for Its In Vitro Histone H2A Ligase Activity. *Molecular Cell*, *24*(5), 701–711.

https://doi.org/10.1016/j.molcel.2006.10.022

Bergink, S., Salomons, F. A., Hoogstraten, D., Groothuis, T. A. M., De Waard, H., Wu, J., … Dantuma, N. P. (2006). DNA damage triggers nucleotide excision repair-dependent monoubiquitylation of histone H2A. *Genes and Development*, *20*(10), 1343–1352. https://doi.org/10.1101/gad.373706

Bernstein, B. E., Mikkelsen, T. S., Xie, X., Kamal, M., Huebert, D. J., Cuff, J., … Lander, E. S. (2006). A Bivalent Chromatin Structure Marks Key Developmental Genes in Embryonic Stem Cells. *Cell*, *125*(2), 315–326. https://doi.org/10.1016/j.cell.2006.02.041

Bertoli, C., Skotheim, J. M., & de Bruin, R. A. M. (2013). Control of cell cycle transcription during G1 and S phases. *Nature Reviews. Molecular Cell Biology*, *14*(8), 518–28. https://doi.org/10.1038/nrm3629

Blackledge, N. P., Farcas, A. M., Kondo, T., King, H. W., McGouran, J. F., Hanssen, L. L. P., … Klose, R. J. (2014). Variant PRC1 complex-dependent H2A ubiquitylation drives PRC2 recruitment and polycomb domain formation. *Cell*, *157*(6), 1445–1459. https://doi.org/10.1016/j.cell.2014.05.004

Boutin, C., Hardt, O., de Chevigny, A., Coré, N., Goebbels, S., Seidenfaden, R., … Cremer, H. (2010). NeuroD1 induces terminal neuronal differentiation in olfactory neurogenesis. *Proceedings of the National Academy of Sciences of the United States of America*, *107*(3), 1201–1206. https://doi.org/10.1073/pnas.0909015107

Boyer, L. A., Plath, K., Zeitlinger, J., Brambrink, T., Medeiros, L. A., Lee, T. I., … Jaenisch, R. (2006). Polycomb complexes repress developmental regulators in murine embryonic stem cells. *Nature*, *441*(7091), 349–53. https://doi.org/10.1038/nature04733

Bracken, A. P., Dietrich, N., Pasini, D., Hansen, K. H., & Helin, K. (2006). Genome-wide mapping of polycomb target genes unravels their roles in cell fate transitions. *Genes and Development*, *20*(9), 1123–1136. https://doi.org/10.1101/gad.381706

Bracken, A. P., Kleine-kohlbrecher, D., Dietrich, N., Bracken, A. P., Kleine-kohlbrecher, D., Dietrich, N., … Hansen, K. H. (2007). The Polycomb group proteins bind throughout the INK4A-ARF locus and are disassociated in senescent cells The Polycomb group proteins bind throughout the INK4A-ARF locus and are disassociated in senescent cells, 525–530. https://doi.org/10.1101/gad.415507

Branzei, D., & Foiani, M. (2010). Maintaining genome stability at the replication fork. *Nature Reviews. Molecular Cell Biology*, *11*(3), 208–19. https://doi.org/10.1038/nrm2852

Bravo, M., Nicolini, F., Starowicz, K., Barroso, S., Calés, C., Aguilera, A., & Vidal, M. (2015). Polycomb RING1A/RING1B-dependent histone H2A monoubiquitylation at pericentromeric regions promotes S phase progression. *Journal of Cell Science*, jcs.173021-. https://doi.org/10.1242/jcs.173021

Brugarolas, J., Chandrasekaran, C., Gordon, J. I., Beach, D., Jacks, T., & Hannon, G. J. (1995). Radiation-induced cell cycle arrest compromised by p21 deficiency. *Nature*. https://doi.org/10.1038/377552a0

Bruggeman, S. W. M., Valk-Lingbeek, M. E., Van Der Stoop, P. P. M., Jacobs, J. J. L., Kieboom, K., Tanger, E., … Van Lohuizen, M. (2005). Ink4a and Arf differentially affect cell proliferation and neural stem cell self-renewal in Bmi1-deficient mice. *Genes and Development*, *19*(12), 1438–1443. https://doi.org/10.1101/gad.1299305

Bruggeman, S. W. M., & Van Lohuizen, M. (2006). Controling Stem Cell Proliferation: CKI at work. *Cell Cycle*, *5:12*(June), 1281–1285.

Burhans, W. C., & Weinberger, M. (2007). DNA replication stress, genome instability and aging. *Nucleic Acids Research*, *35*(22), 7545–7556. https://doi.org/10.1093/nar/gkm1059

Calés, C., Román-Trufero, M., Pavón, L., Serrano, I., Melgar, T., Endoh, M., … Vidal, M. (2008). Inactivation of the polycomb group protein Ring1B unveils an antiproliferative role in hematopoietic cell expansion and cooperation with tumorigenesis associated with Ink4a deletion. *Molecular and Cellular Biology*, *28*(3), 1018–1028. https://doi.org/10.1128/MCB.01136-07

Cao, R., Tsukada, Y., & Zhang, Y. (2005). Supplemental Data Role of Bmi-1 and Ring1A in H2A Ubiquitylation and Hox Gene Silencing Table S1 mHox, *20*, 1–4. https://doi.org/10.1016/j.molcel.2005.12.002

Cazzalini, O., Donà, F., Savio, M., Tillhon, M., Maccario, C., Perucca, P., … Prosperi, E. (2010). p21CDKN1A participates in base excision repair by regulating the activity of poly(ADP-ribose) polymerase-1. *DNA Repair*, *9*(6), 627–635. https://doi.org/10.1016/j.dnarep.2010.02.011

Chan, C. S., Rastelli, L., & Pirrotta, V. (1994). A Polycomb response element in the Ubx gene that determines an epigenetically inherited state of repression. *The EMBO Journal*, *13*(11), 2553–2564.

Chatoo, W., Abdouh, M., David, J., Champagne, M.-P., Ferreira, J., Rodier, F., & Bernier, G. (2009). The Polycomb Group Gene Bmi1 Regulates Antioxidant Defenses in Neurons by Repressing p53 Pro-Oxidant Activity. *Journal of Neuroscience*, *29*(2), 529–542. https://doi.org/10.1523/JNEUROSCI.5303-08.2009

Chou, D. M., Adamson, B., Dephoure, N. E., Tan, X., Nottke, A. C., Hurov, K. E., … Elledge, S. J. (2010). A chromatin localization screen reveals poly (ADP ribose)-regulated recruitment of the repressive polycomb and NuRD complexes to sites of DNA damage. *Proceedings of the National Academy of Sciences of the United States of America*, *107*(43), 18475–18480. https://doi.org/10.1073/pnas.1012946107

Ciccia, A., & Elledge, S. J. (2010). The DNA Damage Response: Making It Safe to Play with Knives. *Molecular Cell*, *40*(2), 179–204. https://doi.org/10.1016/j.molcel.2010.09.019

Cui, K., Zang, C., Roh, T. Y., Schones, D. E., Childs, R. W., Peng, W., & Zhao, K. (2009). Chromatin Signatures in Multipotent Human Hematopoietic Stem Cells Indicate the Fate of Bivalent Genes during Differentiation. *Cell Stem Cell*, *4*(1), 80–93. https://doi.org/10.1016/j.stem.2008.11.011

de Napoles, M., Mermoud, J. E., Wakao, R., Tang, Y. A., Endoh, M., Appanah, R., … Brockdorff, N. (2004). Polycomb group proteins ring1A/B link ubiquitylation of histone H2A to heritable gene silencing and X inactivation. *Developmental Cell*, *7*(5), 663–676. https://doi.org/10.1016/j.devcel.2004.10.005

del Mar Lorente, M., Marcos-Gutiérrez, C., Pérez, C., Schoorlemmer, J., Ramírez, A., Magin, T., & Vidal, M. (2000). Loss- and gain-of-function mutations show a polycomb group function for Ring1A in mice. *Development (Cambridge, England)*, *127*(23), 5093–5100. Retrieved from http://eutils.ncbi.nlm.nih.gov/entrez/eutils/elink.fcgi?dbfrom=pubmed&id=11060235&retmode=ref&cmd=prlinks%5Cnpapers2://publication/uuid/CF8CD765-87FD-441D-B312-47F508E338F9

Di Croce, L., & Helin, K. (2013). Transcriptional regulation by Polycomb group proteins. *Nature Publishing Group*, *20*(10), 1–4. https://doi.org/10.1038/nsmb.2669

Ditch, S., & Paull, T. T. (2012). The ATM protein kinase and cellular redox signaling: Beyond the DNA damage response. *Trends in Biochemical Sciences*, *37*(1), 15–22. https://doi.org/10.1016/j.tibs.2011.10.002

Endoh, M., Endo, T. A., Endoh, T., Fujimura, Y., Ohara, O., Toyoda, T., … Koseki, H. (2008). Polycomb group proteins Ring1A/B are functionally linked to the core transcriptional regulatory circuitry to maintain ES cell identity. *Development*, *135*(8), 1513–1524. https://doi.org/10.1242/dev.014340

Endoh, M., Endo, T. A., Endoh, T., Isono, K. ichi, Sharif, J., Ohara, O., … Koseki, H. (2012). Histone H2A mono-ubiquitination is a crucial step to mediate PRC1-dependent repression of developmental genes to maintain ES cell identity. *PLoS Genetics*, *8*(7), 1–10. https://doi.org/10.1371/journal.pgen.1002774

Entrevan, M., Schuettengruber, B., & Cavalli, G. (2016). Regulation of Genome Architecture and Function by Polycomb Proteins. *Trends in Cell Biology*, *26*(7), 511–525. https://doi.org/10.1016/j.tcb.2016.04.009

Eskeland, R., Leeb, M., Grimes, G. R., Kress, C., Boyle, S., Sproul, D., … Bickmore, W. A. (2010). Ring1B Compacts Chromatin Structure and Represses Gene Expression Independent of Histone Ubiquitination. *Molecular Cell*, *38*(3), 452–464. https://doi.org/10.1016/j.molcel.2010.02.032

Facchino, S., Abdouh, M., Chatoo, W., & Bernier, G. (2010). BMI1 confers radioresistance to normal and cancerous neural stem cells through recruitment of the DNA damage

response machinery. *The Journal of Neuroscience*, *30*(30), 10096–10111. https://doi.org/10.1523/JNEUROSCI.1634-10.2010

Farcas, A. M., Blackledge, N. P., Sudbery, I., Long, H. K., McGouran, J. F., Rose, N. R., … Klose, R. J. (2012). KDM2B links the polycomb repressive complex 1 (PRC1) to recognition of CpG islands. *eLife*, *2012*(1), 1–26. https://doi.org/10.7554/eLife.00205

Fasano, C. A., Dimos, J. T., Ivanova, N. B., Lowry, N., Lemischka, I. R., & Temple, S. (2007). shRNA Knockdown of Bmi-1 Reveals a Critical Role for p21-Rb Pathway in NSC Self-Renewal during Development. *Cell Stem Cell*, *1*(1), 87–99. https://doi.org/10.1016/j.stem.2007.04.001

Fernandez-Capetillo, O., Lee, A., Nussenzweig, M., & Nussenzweig, A. (2004). H2AX: The histone guardian of the genome. *DNA Repair*, *3*(8–9), 959–967. https://doi.org/10.1016/j.dnarep.2004.03.024

Fischle, W., Wang, Y., & Allis, C. D. (2003). Histone and chromatin cross-talk. *Current Opinion in Cell Biology*, *15*(2), 172–183. https://doi.org/10.1016/S0955-0674(03)00013-9

Francis, N. J., Saurin, A. J., Shao, Z., & Kingston, R. E. (2001). Reconstitution of a functional core polycomb repressive complex. *Molecular Cell*, *8*(3), 545–556. https://doi.org/10.1016/S1097-2765(01)00316-1

Fritsch, C., Beuchle, D., & Müller, J. (2003). Molecular and genetic analysis of the Polycomb group gene Sex combs extra/Ring in Drosophila. *Mechanisms of Development*, *120*(8), 949–954. https://doi.org/10.1016/S0925-4773(03)00083-2

Gao, Z., Zhang, J., Bonasio, R., Strino, F., Sawai, A., Parisi, F., … Reinberg, D. (2012). PCGF Homologs, CBX Proteins, and RYBP Define Functionally Distinct PRC1 Family Complexes. *Molecular Cell*, *45*(3), 344–356. https://doi.org/10.1016/j.molcel.2012.01.002

Garcia, E., Marcos-Gutiérrez, C., Del Mar Lorente, M., Moreno, J. C., & Vidal, M. (1999). RYBP, a new repressor protein that interacts with components of the mammalian Polycomb complex, and with the transcription factor YY1. *EMBO Journal*, *18*(12), 3404–3418. https://doi.org/10.1093/emboj/18.12.3404

Gérard, C., & Goldbeter, A. (2012). From quiescence to proliferation: Cdk oscillations drive the mammalian cell cycle. *Frontiers in Physiology*, *3 NOV*(November), 1–18. https://doi.org/10.3389/fphys.2012.00413

Giacinti, C., & Giordano, a. (2006). RB and cell cycle progression. *Oncogene*, *25*(38), 5220–7. https://doi.org/10.1038/sj.onc.1209615

Ginjala, V., Nacerddine, K., Kulkarni, A., Oza, J., Hill, S. J., Yao, M., … Ganesan, S. (2011). BMI1 is recruited to DNA breaks and contributes to DNA damage-induced H2A ubiquitination and repair. *Molecular and Cellular Biology*, *31*(10), 1972–82. https://doi.org/10.1128/MCB.00981-10

Gorfinkiel, N., Fanti, L., Melgar, T., García, E., Pimpinelli, S., Guerrero, I., & Vidal, M. (2004). The Drosophila Polycomb group gene Sex combs extra encodes the ortholog of mammalian Ring1 proteins. *Mechanisms of Development*, *121*(5), 449–462. https://doi.org/10.1016/j.mod.2004.03.019

Götz, M., & Huttner, W. B. (2005). The cell biology of neurogenesis. *Nat Rev Mol Cell Biol*, *6*(10), 777–788. https://doi.org/10.1038/nrm1739

Guillemot, F. (2007). Spatial and temporal specification of neural fates by transcription factor codes. *Development*, *134*(21), 3771–3780. https://doi.org/10.1242/dev.006379

Guo, W., Patzlaff, N. E., Jobe, E. M., & Zhao, X. (2012). Isolation of multipotent neural stem or progenitor cells from both the dentate gyrus and subventricular zone of a single adult mouse. *Nature Protocols*, *7*(11), 2005–12. https://doi.org/10.1038/nprot.2012.123

Guo, Z., Deshpande, R., & Paull, T. T. (2010). ATM activation in the presence of oxidative stress. *Cell Cycle*, *9*(24), 4805–4811. https://doi.org/10.4161/cc.9.24.14323

He, J., Kallin, E. M., Tsukada, Y., Zhang, Y., Comprehensive, L., Hill, C., … Hill, C. (2009). HHS Public Access, *15*(11), 1169–1175. https://doi.org/10.1038/nsmb.1499.The

He, J., Shen, L., Wan, M., Taranova, O., Wu, H., & Zhang, Y. (2013). Kdm2b maintains murine embryonic stem cell status by recruiting PRC1 complex to CpG islands of developmental genes. *Nature Cell Biology*, *15*(4), 373–84. https://doi.org/10.1038/ncb2702

Hickson, I., Zhao, Y., Richardson, C. J., Green, S. J., Martin, N. M. B., Orr, A. I., … Smith, G. C. M. (2004). Identification and Characterization of a Novel and Specific Inhibitor of the Ataxia-Telangiectasia Mutated Kinase ATM Identification and Characterization of a Novel and Specific Inhibitor of the Ataxia-Telangiectasia Mutated Kinase ATM. *Cancer Research*, *64*(24), 9152–9159. https://doi.org/10.1158/0008-5472.CAN-04-2727

Hoeijmakers, J. H. J. (2009). DNA damage, aging, and cancer. *The New England Journal of Medicine*, *361*(15), 1475–85. https://doi.org/10.1056/NEJMra0804615

Illingworth, R. S., Moffat, M., Mann, A. R., Read, D., Hunter, C. J., Pradeepa, M. M., … Bickmore, W. A. (2015). The E3 ubiquitin ligase activity of RING1B is not essential for early mouse development1. Illingworth, R. S. et al. The E3 ubiquitin ligase activity of RING1B is not essential for early mouse development. Genes Dev. 1897–1902 (2015). doi:10.1101/gad.26815. *Genes and Development*, 1897–1902. https://doi.org/10.1101/gad.268151.115.

Ismail, H., Andrin, C., McDonald, D., & Hendzel, M. J. (2010). BMI1-mediated histone ubiquitylation promotes DNA double-strand break repair. *Journal of Cell Biology*, *191*(1), 45–60. https://doi.org/10.1083/jcb.201003034

Ismail, I. H., Gagné, J. P., Caron, M. C., McDonald, D., Xu, Z., Masson, J. Y., … Hendzel,

M. J. (2012). CBX4-mediated SUMO modification regulates BMI1 recruitment at sites of DNA damage. *Nucleic Acids Research*, *40*(12), 5497–5510. https://doi.org/10.1093/nar/gks222

Isono, K., Mizutani-Koseki, Y., Komori, T., Schmidt-Zachmann, M. S., & Koseki, H. (2005). Mammalian Polycomb-mediated repression of Hox genes requires the essential spliceosomal protein Sf3b1. *Genes and Development*, *19*(5), 536–541. https://doi.org/10.1101/gad.1284605

Iwama, A., Oguro, H., Negishi, M., Kato, Y., Morita, Y., Tsukui, H., … Nakauchi, H. (2004). Enhanced self-renewal of hematopoietic stem cells mediated by the polycomb gene product Bmi-1. *Immunity*, *21*(6), 843–851. https://doi.org/10.1016/j.immuni.2004.11.004

Jacks, T., Remington, L., Williams, B. O., Schmitt, E. M., Halachmi, S., Bronson, R. T., & Weinberg, R. A. (1994). Tumor spectrum analysis in p53-mutant mice. *Current Biology*, *4*(1), 1–7. https://doi.org/10.1016/S0960-9822(00)00002-6

Jacobs, J. J., Kieboom, K., Marino, S., DePinho, R. a, & van Lohuizen, M. (1999). The oncogene and Polycomb-group gene bmi-1 regulates cell proliferation and senescence through the ink4a locus. *Nature*, *397*(6715), 164–168. https://doi.org/10.1038/16476

Jazayeri, A., Falck, J., Lukas, C., Bartek, J., Smith, G., Lukas, J., & Jackson, S. P. (2006). ATM- and cell cycle-dependent regulation of ATR in response to DNA double-strand breaks. *Nature Cell Biology*, *8*(1), 37–45. https://doi.org/10.1038/ncb1337

Jenkins, N. C., Liu, T., Cassidy, P., Leachman, S. a, Boucher, K. M., Goodson, a G., … Grossman, D. (2011). The p16(INK4A) tumor suppressor regulates cellular oxidative stress. *Oncogene*, *30*(3), 265–274. https://doi.org/10.1158/1538-7445.AM10-4390

Kalb, R., Latwiel, S., Baymaz, H. I., Jansen, P. W. T. C., Müller, C. W., Vermeulen, M., & Müller, J. (2014). Histone H2A monoubiquitination promotes histone H3 methylation in Polycomb repression. *Nature Structural & Molecular Biology*, *21*(6), 569–71. https://doi.org/10.1038/nsmb.2833

Karimian, A., Ahmadi, Y., & Yousefi, B. (2016). Multiple functions of p21 in cell cycle, apoptosis and transcriptional regulation after DNA damage. *DNA Repair*, *42*, 63–71. https://doi.org/10.1016/j.dnarep.2016.04.008

Kim, J., & Wong, P. K. Y. (2009). Loss of ATM impairs proliferation of neural stem cells through oxidative stress-mediated p38 MAPK signaling. *Stem Cells*, *27*(8), 1987–1998. https://doi.org/10.1002/stem.125

King, I. F. G., Emmons, R. B., Francis, N. J., Wild, B., Müller, J., Kingston, R. E., & Wu, C.-T. (2005). Analysis of a polycomb group protein defines regions that link repressive activity on nucleosomal templates to in vivo function. *Molecular and Cellular Biology*, *25*(15), 6578–6591. https://doi.org/10.1128/MCB.25.15.6578-6591.2005

Kloet, S. L., Makowski, M. M., Baymaz, H. I., van Voorthuijsen, L., Karemaker, I. D., Santanach, A., … Vermeulen, M. (2016). The dynamic interactome and genomic targets of Polycomb complexes during stem-cell differentiation. *Nature Structural & Molecular Biology*, *23*(7), 682–690. https://doi.org/10.1038/nsmb.3248

Klose, R. J., Cooper, S., Farcas, A. M., Blackledge, N. P., & Brockdorff, N. (2013). Chromatin Sampling-An Emerging Perspective on Targeting Polycomb Repressor Proteins. *PLoS Genetics*, *9*(8). https://doi.org/10.1371/journal.pgen.1003717

Kohlmaier, A., Savarese, F., Lachner, M., Martens, J., Jenuwein, T., & Wutz, A. (2004). A chromosomal memory triggered by Xist regulates histone methylation in X inactivation. *PLoS Biology*, *2*(7). https://doi.org/10.1371/journal.pbio.0020171

Koike, H., Ueno, Y., Naito, T., Shiina, T., Nakata, S., Ouchi, R., … Taniguchi, H. (2014). Ring1B promotes hepatic stem/progenitor cell expansion through simultaneous suppression of Cdkn1a and Cdkn2a in mice. *Hepatology*, *60*(1), 323–333. https://doi.org/10.1002/hep.27046

Kracikova, M., Akiri, G., George, A., Sachidanandam, R., & Aaronson, S. A. (2013). A threshold mechanism mediates p53 cell fate decision between growth arrest and apoptosis. *Cell Death and Differentiation*, *20*(4), 576–88. https://doi.org/10.1038/cdd.2012.155

Ku, M., Koche, R. P., Rheinbay, E., Mendenhall, E. M., Endoh, M., Mikkelsen, T. S., … Bernstein, B. E. (2008). Genomewide analysis of PRC1 and PRC2 occupancy identifies two classes of bivalent domains. *PLoS Genetics*, *4*(10). https://doi.org/10.1371/journal.pgen.1000242

Lakin, N. D., & Jackson, S. P. (1999). Regulation of p53 in response to DNA damage. *Oncogene*, *18*(53), 7644–7655. https://doi.org/10.1038/sj.onc.1203015

Lanzuolo, C., & Orlando, V. (2012). Memories from the polycomb group proteins. *Annual Review of Genetics*, *46*, 561–89. https://doi.org/10.1146/annurev-genet-110711-155603

Lee, H.-S., Lee, S.-A., Hur, S.-K., Seo, J.-W., & Kwon, J. (2014). Stabilization and targeting of INO80 to replication forks by BAP1 during normal DNA synthesis. *Nature Communications*, *5*(May), 5128. https://doi.org/10.1038/ncomms6128

Lee, T. I., Jenner, R. G., Boyer, L. A., Guenther, M. G., Levine, S. S., Kumar, R. M., … Young, R. A. (2006). Control of Developmental Regulators by Polycomb in Human Embryonic Stem Cells. *Cell*, *125*(2), 301–313. https://doi.org/10.1016/j.cell.2006.02.043

Leeb, M., & Wutz, A. (2007). Ring1B is crucial for the regulation of developmental control genes and PRC1 proteins but not X inactivation in embryonic cells. *Journal of Cell Biology*, *178*(2), 219–229. https://doi.org/10.1083/jcb.200612127

Lessard, J., & Sauvageau, G. (2003). Bmi-1 determines the proliferative capacity of normal

and leukaemic stem cells. *Nature*, *423*(6937), 255–260. https://doi.org/10.1038/nature01572

Levine, S. S., Weiss, A., Erdjument-Bromage, H., Shao, Z., Tempst, P., & Kingston, R. E. (2002). The core of the polycomb repressive complex is compositionally and functionally conserved in flies and humans. *Molecular and Cellular Biology*, *22*(17), 6070–6078. https://doi.org/10.1128/MCB.22.17.6070-6078.2002

Lewis, E. (1978). A gene complex controlling segmentation in Drosophila. *Nature*, *276*(5688), 565–70.

Lewis, Z. A. (2017). Polycomb Group Systems in Fungi: New Models for Understanding Polycomb Repressive Complex 2. *Trends in Genetics*, *xx*, 1–12. https://doi.org/10.1016/j.tig.2017.01.006

Lindahl, T. (1993). Instability and decay of the primary structure of DNA. *Nature*, *362*. https://doi.org/10.1038/362709a0

Liu, J., Cao, L., Chen, J., Song, S., Lee, I. H., Quijano, C., … Finkel, T. (2009). Bmi1 regulates mitochondrial function and the DNA damage response pathway. *Nature*, *459*(7245), 387–392. https://doi.org/10.1038/nature08040

Lombard, D. B., Chua, K. F., Mostoslavsky, R., Franco, S., Gostissa, M., & Alt, F. W. (2005). DNA repair, genome stability, and aging. *Cell*, *120*(4), 497–512. https://doi.org/10.1016/j.cell.2005.01.028

Lovering, R., Hanson, I. M., Borden, K. L., Martin, S., O'Reilly, N. J., Evan, G. I., … Freemont, P. S. (1993). Identification and preliminary characterization of a protein motif related to the zinc finger. *Proceedings of the National Academy of Sciences of the United States of America*, *90*(6), 2112–2116. https://doi.org/10.1073/pnas.90.6.2112

Lukas, J., Lukas, C., & Bartek, J. (2011). More than just a focus: The chromatin response to DNA damage and its role in genome integrity maintenance. *Nature Cell Biology*, *13*(10), 1161–9. https://doi.org/10.1038/ncb2344

Maertens, G. N., El Messaoudi-Aubert, S., Elderkin, S., Hiom, K., & Peters, G. (2010). Ubiquitin-specific proteases 7 and 11 modulate Polycomb regulation of the INK4a tumour suppressor. *The EMBO Journal*, *29*(15), 2553–2565. https://doi.org/10.1038/emboj.2010.129

Maertens, G. N., El Messaoudi-Aubert, S., Racek, J. K., Nicholls, J., Rodriguez-Niedenführ, M., Gil, J., & Peters, G. (2009). Several distinct polycomb complexes regulate and co-localize on the INK4a tumor suppressor locus. *PLoS ONE*, *4*(7). https://doi.org/10.1371/journal.pone.0006380

Maréchal, A., & Zou, L. (2013). DNA damage sensing by the ATM and ATR kinases. *Cold Spring Harbor Perspectives in Biology*, *5*(9), 1–17. https://doi.org/10.1101/cshperspect.a012716

Margueron, R., Li, G., Sarma, K., Blais, A., Zavadil, J., Woodcock, C. L., … Reinberg, D. (2008). Ezh1 and Ezh2 Maintain Repressive Chromatin through Different Mechanisms. *Molecular Cell*, *32*(4), 503–518. https://doi.org/10.1016/j.molcel.2008.11.004

Margueron, R., & Reinberg, D. (2011). The Polycomb complex PRC2 and its mark in life. *Nature*, *469*(7330), 343–9. https://doi.org/10.1038/nature09784

McGinty, R. K., Henrici, R. C., & Tan, S. (2014). Crystal structure of the PRC1 ubiquitylation module bound to the nucleosome. *Nature*, *514*(7524), 591–6. https://doi.org/10.1038/nature13890

McKenzie Duncan, I. (1982). Polycomblike: A gene that appears to be required for the normal expression of the bithorax and antennapedia gene complexes of Drosophila melanogaster. *Genetics*, *102*(1), 49–70.

Mendrysa, S. M., Ghassemifar, S., & Malek, R. (2011). p53 in the CNS: Perspectives on Development, Stem Cells, and Cancer. *Genes & Cancer*, *2*(4), 431–442. https://doi.org/10.1177/1947601911409736

Meter, M. Van, Simon, M., Tombline, G., Bohr, V. A., Gorbunova, V., Seluanov, A., … Seluanov, A. (2016). JNK Phosphorylates SIRT6 to Stimulate DNA Double- Strand Break Repair in Response to Oxidative Stress by Recruiting PARP1 to DNA Breaks Article JNK Phosphorylates SIRT6 to Stimulate DNA Double-Strand Break Repair in Response to Oxidative Stress by Recruit. *CellReports*, *16*(10), 1–10. https://doi.org/10.1016/j.celrep.2016.08.006

Mihaly, J., Mishra, R., & Karch, F. (1998). A conserved sequence motif in polycomb-response elements. *Molecular Cell*, *1*, 1065–1066. https://doi.org/10.1016/S1097-2765(00)80107-0

Mijimolle, N., Velasco, J., Dubus, P., Guerra, C., Weinbaum, C. A., Casey, P. J., … Barbacid, M. (2005). Protein farnesyltransferase in embryogenesis, adult homeostasis, and tumor development. *Cancer Cell*, *7*(4), 313–324. https://doi.org/10.1016/j.ccr.2005.03.004

Mikkelsen, T. S., Ku, M., Jaffe, D. B., Issac, B., Lieberman, E., Giannoukos, G., … Bernstein, B. E. (2007). Genome-wide maps of chromatin state in pluripotent and lineage-committed cells. *Nature*, *448*(7153), 553–560. https://doi.org/10.1038/nature06008

Molofsky, A. V, He, S., & Pardal, R. (2005). BMI-1 promotes neural stem cell self-renewal and neural development but not mouse growth and survival by repressing the p16Ink4a and p19Arf senescence pathways. *Genes & Development*, 1432–1437. https://doi.org/10.1101/gad.1299505.vageau

Molofsky, A. V, Pardal, R., Iwashita, T., Park, I., Clarke, M. F., & Morrison, S. J. (2003).

Bmi-1 dependence distinguishes neural stem cell self-renewal from progenitor proliferation. *October*, *425*(6961), 962–967. https://doi.org/10.1038/nature02060.Bmi-1

Pan, M. R., Peng, G., Hungs, W. C., & Lin, S. Y. (2011). Monoubiquitination of H2AX protein regulates DNA damage response signaling. *Journal of Biological Chemistry*, *286*(32), 28599–28607. https://doi.org/10.1074/jbc.M111.256297

Park, I., Qian, D., Kiel, M., Becker, M. W., Pihalja, M., Weissman, I. L., … Clarke, M. F. (2003). Bmi-1 is required for maintenance of adult self-renewing haematopoietic stem cells. *Nature*, *423*(6937), 302–305. https://doi.org/10.1038/nature01587

Pasini, D., Bracken, A. P., Hansen, J. B., Capillo, M., & Helin, K. (2007). The polycomb group protein Suz12 is required for embryonic stem cell differentiation. *Molecular and Cellular Biology*, *27*(10), 3769–79. https://doi.org/10.1128/MCB.01432-06

Pateras, I. S., Apostolopoulou, K., Niforou, K., Kotsinas, A., & Gorgoulis, V. G. (2009). p57KIP2: "Kip"ing the cell under control. *Mol Cancer Res*, *7*(12), 1902–1919. https://doi.org/10.1158/1541-7786.MCR-09-0317

Pinto, L., & Götz, M. (2007). Radial glial cell heterogeneity-The source of diverse progeny in the CNS. *Progress in Neurobiology*, *83*(1), 2–23. https://doi.org/10.1016/j.pneurobio.2007.02.010

Piunti, A., Rossi, A., Cerutti, A., Albert, M., Jammula, S., Scelfo, A., … Pasini, D. (2014). Polycomb proteins control proliferation and transformation independently of cell cycle checkpoints by regulating DNA replication. *Nat Commun*, *5*, 3649. https://doi.org/10.1038/ncomms4649

Porter, A. C. (2008). Preventing DNA over-replication: a Cdk perspective. *Cell Division*, *3*(1), 3. https://doi.org/10.1186/1747-1028-3-3

Posfai, E., Kunzmann, R., Brochard, V., Salvaing, J., Cabuy, E., Roloff, T. C., … Peters, A. H. F. M. (2012). Polycomb function during oogenesis is required for mouse embryonic development. *Genes and Development*, *26*(9), 920–932. https://doi.org/10.1101/aad.188094.112

Reynolds, B. A., & Rietze, R. L. (2005). Neural stem cells and neurospheres--re-evaluating the relationship. *Nat Methods*, *2*(5), 333–336. https://doi.org/10.1038/nmeth758

Reynolds, B. A., & Weiss, S. (1996). Clonal and population analyses demonstrate that an EGF-responsive mammalian embryonic CNS precursor is a stem cell. *Developmental Biology*, *175*(1), 1–13. https://doi.org/10.1006/dbio.1996.0090

Reynolds, N., O'Shaughnessy, A., & Hendrich, B. (2013). Transcriptional repressors: multifaceted regulators of gene expression. *Development (Cambridge, England)*, *140*, 505–512. https://doi.org/10.1242/dev.083105

RichardWagner, J. C. and. (2013). DNA Base Damage by Reactive Oxygen Species ,. *Cold*

Spring Harb Perspect Biol, *5*, 1–18. https://doi.org/10.1101/cshperspect.a012559

Ringrose, L., & Paro, R. (2004). Epigenetic regulation of cellular memory by the Polycomb group and trithorax group proteins. *Annu. Rev. Genet.*, *38*, 413–443. https://doi.org/10.1146/annurev.genet.38.072902.091907

Román-Trufero, M., Méndez-Gómez, H. R., Pérez, C., Hijikata, A., Fujimura, Y. I., Endo, T., … Vidal, M. (2009). Maintenance of undifferentiated state and self-renewal of embryonic neural stem cells by polycomb protein Ring1B. *Stem Cells*, *27*(7), 1559–1570. https://doi.org/10.1002/stem.82

Sancar, A., Lindsey-Boltz, L. A., Unsal-Kacmaz, K., & Linn, S. (2004). Molecular mechanisms of mammalian DNA repair and the DNA damage checkpoints. *Annu.Rev.Biochem.*, *73*(0066–4154 (Print) LA–eng PT–Journal Article PT–Review RN–0 (Cross–Linking Reagents) RN–9007–49–2 (DNA) SB–IM), 39–85. https://doi.org/10.1146/annurev.biochem.73.011303.073723

Sanchez-Pulido, L., Devos, D., Sung, Z., & Calonje, M. (2008). RAWUL: A new ubiquitin-like domain in PRC1 Ring finger proteins that unveils putative plant and worm PRC1 orthologs. *BMC Genomics*, *9*(1), 308. https://doi.org/10.1186/1471-2164-9-308

Sánchez, C., Sánchez, I., Demmers, J. A. A., Rodriguez, P., Strouboulis, J., & Vidal, M. (2007). Proteomics analysis of Ring1B/Rnf2 interactors identifies a novel complex with the Fbxl10/Jhdm1B histone demethylase and the Bcl6 interacting corepressor. *Molecular & Cellular Proteomics*, *6*(5), 820–34. https://doi.org/10.1074/mcp.M600275-MCP200

Santos, M. A., Faryabi, R. B., Ergen, A. V, Day, A. M., Malhowski, A., Canela, A., … Nussenzweig, A. (2014). DNA-damage-induced differentiation of leukaemic cells as an anti-cancer barrier. *Nature*, *514*(7520), 107–111. https://doi.org/10.1038/nature13483

Sato, K., Hamanoue, M., & Takamatsu, K. (2008). Inhibitors of p38 mitogen-activated protein kinase enhance proliferation of mouse neural stem cells. *Journal of Neuroscience Research*, *86*(10), 2179–2189. https://doi.org/10.1002/jnr.21668

Sato, T., & Denell, R. E. (1985). Homoeosis in Drosophila: Anterior and posterior transformations of Polycomb lethal embryos. *Developmental Biology*, *110*(1), 53–64. https://doi.org/10.1016/0012-1606(85)90063-6

Schoorlemmer, J., Marcos-Gutiérrez, C., Were, F., Martinez, R., Garcia, E., Satijn, D. P. E., … Vidal, M. (1997). Ring1A is a transcriptional repressor that interacts with the Polycomb-M33 protein and is expressed at rhombomere boundaries in the mouse hindbrain. *EMBO Journal*, *16*(19), 5930–5942. https://doi.org/10.1093/emboj/16.19.5930

Schwartz, Y. B., & Pirrotta, V. (2007). Polycomb silencing mechanisms and the management of genomic programmes. *Nature Reviews Genetics*, *8*(1), 9–22.

https://doi.org/10.1038/nrg1981

Seibler, J., Zevnik, B., K??ter-Luks, B., Andreas, S., Kern, H., Hennek, T., … Schwenk, F. (2003). Rapid generation of inducible mouse mutants. *Nucleic Acids Research*, *31*(4), e12. https://doi.org/10.1093/nar/gng012

Serrano, M., Lee, H. W., Chin, L., Cordon-Cardo, C., Beach, D., & DePinho, R. A. (1996). Role of the INK4a locus in tumor suppression and cell mortality. *Cell*, *85*(1), 27–37. https://doi.org/10.1016/S0092-8674(00)81079-X

Shao, L., Hongliang, L., Pazhanisamy, S. K., Meng, A., Wang, Y., Zhou, D., & Li, H. (2011). Reactive oxygen species and hematopoietic stem cell senescence. *Int J Hematol*, *94*(1), 24–32. https://doi.org/10.1007/s12185-011-0872-1.Reactive

Shen, X., Liu, Y., Hsu, Y. J., Fujiwara, Y., Kim, J., Mao, X., … Orkin, S. H. (2008). EZH1 Mediates Methylation on Histone H3 Lysine 27 and Complements EZH2 in Maintaining Stem Cell Identity and Executing Pluripotency. *Molecular Cell*, *32*(4), 491–502. https://doi.org/10.1016/j.molcel.2008.10.016

Sherman, M. H., Bassing, C. H., & Teitell, M. a. (2011a). DNA damage response regulates cell differentiation. *Trends in Cell Biology*, *21*(5), 312–319. https://doi.org/10.1016/j.tcb.2011.01.004.DNA

Sherman, M. H., Bassing, C. H., & Teitell, M. A. (2011b). Regulation of cell differentiation by the DNA damage response. *Trends in Cell Biology*, *21*(5), 312–319. https://doi.org/10.1016/j.tcb.2011.01.004

Shieh, S. Y., Ikeda, M., Taya, Y., & Prives, C. (1997). DNA damage-induced phosphorylation of p53 alleviates inhibition by MDM2. *Cell*, *91*(3), 325–334. https://doi.org/10.1016/S0092-8674(00)80416-X

Shiloh, Y., & Ziv, Y. (2013). The ATM protein kinase: regulating the cellular response to genotoxic stress, and more. *Nature Reviews. Molecular Cell Biology*, *14*(4), 197–210. https://doi.org/10.1038/nrm3546

Simon, J. a, & Kingston, R. E. (2009). Mechanisms of polycomb gene silencing: knowns and unknowns. *Nature Reviews. Molecular Cell Biology*, *10*(10), 697–708. https://doi.org/10.1038/nrm2763

Smith, J., Mun Tho, L., Xu, N., & A. Gillespie, D. (2010). *The ATM-Chk2 and ATR-Chk1 pathways in DNA damage signaling and cancer*. *Advances in Cancer Research* (1st ed., Vol. 108). Elsevier Inc. https://doi.org/10.1016/B978-0-12-380888-2.00003-0

Stock, J. K., Giadrossi, S., Casanova, M., Brookes, E., Vidal, M., Koseki, H., … Pombo, A. (2007). Ring1-mediated ubiquitination of H2A restrains poised RNA polymerase II at bivalent genes in mouse ES cells. *Nature Cell Biology*, *9*(12), 1428–1435. https://doi.org/10.1038/ncb1663

Sulli, G., Di Micco, R., & di Fagagna, F. d'Adda. (2012). Crosstalk between chromatin state

and DNA damage response in cellular senescence and cancer. *Nature Reviews Cancer*, *12*(10), 709–720. https://doi.org/10.1038/nrc3344

Taherbhoy, A. M., Huang, O. W., & Cochran, A. G. (2015). BMI1–RING1B is an autoinhibited RING E3 ubiquitin ligase. *Nature Communications*, *6*(May), 7621. https://doi.org/10.1038/ncomms8621

Tavares, L., Dimitrova, E., Oxley, D., Webster, J., Poot, R., Demmers, J., … Brockdorff, N. (2012). RYBP-PRC1 complexes mediate H2A ubiquitylation at polycomb target sites independently of PRC2 and H3K27me3. *Cell*, *148*(4), 664–678. https://doi.org/10.1016/j.cell.2011.12.029

Tedeschi, A., & Di Giovanni, S. (2009). The non-apoptotic role of p53 in neuronal biology: enlightening the dark side of the moon. *EMBO Reports*, *10*(6), 576–583. https://doi.org/10.1038/embor.2009.89

Temple, S. (2001). The development of neural stem cells. *Nature*, *414*(6859), 112–117. https://doi.org/10.1038/35102174

Tillib, S., Petruk, S., Sedkov, Y., Kuzin, a, Fujioka, M., Goto, T., & Mazo, a. (1999). Trithorax- and Polycomb-group response elements within an Ultrabithorax transcription maintenance unit consist of closely situated but separable sequences. *Molecular and Cellular Biology*, *19*(7), 5189–5202. https://doi.org/10.1128/MCB.19.7.5189

Toledo, L. I., Murga, M., Zur, R., Soria, R., Rodriguez, A., Martinez, S., … Fernandez-Capetillo, O. (2011). A cell-based screen identifies ATR inhibitors with synthetic lethal properties for cancer-associated mutations. *Nature Structural & Molecular Biology*, *18*(6), 721–727. https://doi.org/10.1038/nsmb.2076

Ui, A., Nagaura, Y., & Yasui, A. (2015). Transcriptional elongation factor ENL phosphorylated by ATM recruits polycomb and switches off transcription for DSB repair. *Molecular Cell*, *58*(3), 468–482. https://doi.org/10.1016/j.molcel.2015.03.023

Vergaño-Vera, E., Yusta-boyo, M. J., Castro, F. De, Bernad, A., Pablo, F. De, Vicario-abejón, C., … de Pablo, F. (2006). Generation of GABAergic and dopaminergic interneurons from endogenous embryonic olfactory bulb precursor cells. *Development (Cambridge, England)*, *133*(21), 4367–79. https://doi.org/10.1242/dev.02601

Vicario-Abejon, C., Yusta-Boyo, M. J., Fernandez-Moreno, C., de Pablo, F., Vicario-abejo, C., Yusta-boyo, J., … Pablo, F. De. (2003). Locally born olfactory bulb stem cells proliferate in response to insulin-related factors and require endogenous insulin-like growth factor-I for differentiation into neurons and glia. *J Neurosci*, *23*(3), 895–906. https://doi.org/23/3/895 [pii]

Vissers Joseph H. A., van L. M. and C. E. (2012). The emerging role of Polycomb repressors in the response to DNA damage. *Journal of Cell Science*, *125*, 3939–3948.

https://doi.org/0.1242/jcs.107375

Voncken, J. W., Roelen, B. A. J., Roefs, M., de Vries, S., Verhoeven, E., Marino, S., … van Lohuizen, M. (2003). Rnf2 (Ring1b) deficiency causes gastrulation arrest and cell cycle inhibition. *Proceedings of the National Academy of Sciences of the United States of America*, *100*(5), 2468–73. https://doi.org/10.1073/pnas.0434312100

Wang, B., Matsuoka, S., Carpenter, P. B., & Elledge, S. J. (2002). 53BP1, a mediator of the DNA damage checkpoint. *Science (New York, N.Y.)*, *298*(5597), 1435–8. https://doi.org/10.1126/science.1076182

Weiss, C. N., & Ito, K. (2015). DNA damage: A sensible mediator of the differentiation decision in hematopoietic stem cells and in leukemia. *International Journal of Molecular Sciences*, *16*(3), 6183–6201. https://doi.org/10.3390/ijms16036183

Whitcomb, S. J., Basu, A., Allis, C. D., & Bernstein, E. (2007). Polycomb Group proteins: an evolutionary perspective. *Trends in Genetics*, *23*(10), 494–502. https://doi.org/10.1016/j.tig.2007.08.006

Woodbine, L., Brunton, H., Goodarzi, A. A., Shibata, A., & Jeggo, P. A. (2011). Endogenously induced DNA double strand breaks arise in heterochromatic DNA regions and require ataxia telangiectasia mutated and Artemis for their repair. *Nucleic Acids Research*, *39*(16), 6986–6997. https://doi.org/10.1093/nar/gkr331

Wu, X., Johansen, J. V., & Helin, K. (2013). Fbxl10/Kdm2b Recruits Polycomb Repressive Complex 1 to CpG Islands and Regulates H2A Ubiquitylation. *Molecular Cell*, *49*(6), 1134–1146. https://doi.org/10.1016/j.molcel.2013.01.016

Zou, L., & Elledge, S. J. (2003). Sensing DNA damage through ATRIP recognition of RPA-ssDNA complexes. *Science (New York, N.Y.)*, *300*(June), 1542–1548. https://doi.org/10.1126/science.1083430